iScience

CellPress
OPEN ACCESS

Review

Bioengineered human arterial equivalent and its applications from vascular graft to *in vitro* disease modeling

Xi Luo,[1,6] Zherui Pang,[1,6] Jinhua Li,[1,2,3,*] Minjun Anh,[4] Byoung Soo Kim,[4,5,*] and Ge Gao[1,2,*]

SUMMARY

Arterial disorders such as atherosclerosis, thrombosis, and aneurysm pose significant health risks, necessitating advanced interventions. Despite progress in artificial blood vessels and animal models aimed at understanding pathogenesis and developing therapies, limitations in graft functionality and species discrepancies restrict their clinical and research utility. Addressing these issues, bioengineered arterial equivalents (AEs) with enhanced vascular functions have been developed, incorporating innovative technologies that improve clinical outcomes and enhance disease progression modeling. This review offers a comprehensive overview of recent advancements in bioengineered AEs, systematically summarizing the bioengineered technologies used to construct these AEs, and discussing their implications for clinical application and pathogenesis understanding. Highlighting current breakthroughs and future perspectives, this review aims to inform and inspire ongoing research in the field, potentially transforming vascular medicine and offering new avenues for preclinical and clinical advances.

INTRODUCTION

The artery serves as an essential component of the human vascular system, responsible for the delivery of oxygen-rich blood from the heart to various tissues throughout the body.[1] Despite their critical role, arteries are susceptible to a range of disorders, including atherosclerosis (AS), aneurysms, stenosis, and dissection, which can significantly compromise their function and lead to life-threatening diseases.[2,3] For instance, AS is the pathological basis of cardiovascular diseases (CVDs), such as heart attack and stroke,[4] which account for approximately 17 million global deaths annually, representing the leading cause of mortality worldwide.[5] In clinical settings where saving a patient's life is paramount, the restoration of arterial function often involves the bypassing or replacement of the affected arteries with either autologous or synthetic vessels.[6] Besides, the pathogenesis of arterial diseases remains not fully understood, impeding the advancement of innovative therapeutic strategies and effective medication.[7] Therefore, there is a pressing need for reliable tools that can accurately mimic both the physiological functions and pathological responses of human arteries for clinical and research purposes.

Currently, artificial grafts used in clinical practices for artery replacement are primarily composed of synthetic polymers, such as expanded polytetrafluoroethylene and polyester (Dacron).[8] These grafts are particularly effective for replacing large-diameter arteries such as the aorta and abdominal artery, where blood flow is rapid and occurs in a laminar fashion.[9] Nevertheless, their application in smaller-diameter vessels is problematic due to the increased risk of thrombosis, attributable to slower and more turbulent blood flow which facilitates clot formation.[10] Moreover, the inherent mechanical compliance mismatch between synthetic materials and the natural vascular tissue can lead to significant stress at the interface of the artery and the implant, potentially resulting in graft failure or neointimal hyperplasia.[11] Additionally, these grafts produced from synthetic polymers may lack the capacity for adequate integration with the host's tissues, manifesting deficiencies in crucial processes such as reendothelialization, muscularization, and extracellular matrix (ECM) remodeling, ultimately limiting their ability to transition from a foreign substance to a regenerated tissue. To address these challenges, there is a growing preference for living arterial equivalents (AEs) with biomimetic dimensions, structures, and physiological functions over rigid plastic conduits.

The concept of bioengineered blood vessels was first proposed by Weinberg and Bell in the 1980s,[12] marking a significant milestone in the development of AEs as alternatives to conventional synthetic vascular grafts. With the advent of innovative biomaterials and flexible biofabrication techniques, the field of bioengineered AEs has seen considerable advancements. These biologically derived conduits are poised to transform clinical applications by closely replicating the mechanical and biological properties of native arteries.[13] Not only do they facilitate

[1]School of Medical Technology, Beijing Institute of Technology, Beijing 100081, China
[2]School of Medical Technology, Beijing Institute of Technology, Zhengzhou Academy of Intelligent Technology, Zhengzhou 450000, China
[3]Beijing Institute of Technology, Zhuhai, Beijing Institute of Technology, Zhuhai 519088, China
[4]Medical Research Institute, Pusan National University, Yangsan 50612, Republic of Korea
[5]School of Biomedical Convergence Engineering, Pusan National University, Yangsan 50612, Republic of Korea
[6]These authors contributed equally
*Correspondence: lijinhua@bit.edu.cn (J.L.), bskim7@pusan.ac.kr (B.S.K.), gaoge@bit.edu.cn (G.G.)
https://doi.org/10.1016/j.isci.2024.111215

the implantation process, but they also mitigate the adverse effects typically associated with synthetic products, such as clotting and stenosis,[14] while promoting integration with the host through the incorporation of functional tissues such as endothelium and smooth muscles.[15,16] Despite these achievements, consistent performance and long-term durability of these grafts continue to be a formidable challenge.

Given their high physiological relevance to human arteries, AEs also hold the potential for elucidating the pathogenesis of arterial diseases, serving as an alternative to traditional animal and 2D cell culture models. While *in vivo* and *ex vivo* models using experimental animals have provided invaluable insights into complex signaling pathways involved in arterial disease initiation and progression,[17] discrepancies between species inevitably limit the applicability of these findings to human conditions.[18] AEs, developed using human or patient-specific cells, are capable of precisely reflecting cellular responses to various stimuli, thus overcoming the limitations of animal experiments. Unlike 2D cultures, AEs offer a tissue-specific 3D microenvironment that supports controlled cell distribution, alignment, and dynamic biochemical and mechanical signals essential for promoting cellular functions and interactions.[19,20] Furthermore, through thoughtful design, bioengineered AEs can be seamlessly integrated with cutting-edge techniques such as real-time biomedical imaging and artificial intelligence (AI) to conduct multifactorial analyses for accurate disease diagnosis and prognosis.[21,22] However, constructing reliable and controllable AEs as *in vitro* models for studying arterial diseases under standardized and tunable blood flow conditions remains a critical research priority.

This review provides a comprehensive overview of the recent advances in bioengineered AEs and their applications in clinical practice and disease modeling (Figure 1). It begins by detailing the physiological features and functions of arteries, alongside prevalent pathogenic theories of arterial diseases, including AS, stenosis, aneurysm, and dissection. Subsequent sections systematically summarize the bioengineered technologies used to construct AEs, categorized into scaffold-based, cell-based, and dynamic devices, emphasizing their implications for clinical applications, and understanding of pathogenesis. Finally, it concludes by discussing current breakthroughs, challenges, and future perspectives in this rapidly evolving field.

Physiological function and pathological feature of the artery

To develop biomimetic artificial tissues/organs, it is crucial to understand the fundamental characteristics of their natural counterparts thoroughly. This section delves into the anatomy, structure, composition, function, and mechanical properties of human arteries crucial for bioengineered AEs (Figure 2). It also emphasizes the significance of comprehending pathogenesis and replicating pathological microenvironments for accurately modeling arterial diseases.

Anatomy and function of the artery

A detailed understanding of arterial anatomy and physiological functions is critical for the structural design, and selection of appropriate biomaterials, cells, and bioengineered techniques. Human arteries are composed of three distinct layers: the tunica intima, tunica media, and tunica adventitia.[23] Each layer contains specialized vascular tissues, cells, and complex ECM components essential for performing specific physiological functions.[24]

The tunica intima includes an elastic layer composed of elastic fibers and an endothelial tissue made up of a single layer of endothelial cells (ECs).[25] The primary function of the elastic layer is to provide elasticity and flexibility to the vessel wall, enabling it to adapt to dynamic pressure changes caused by blood flow.[26] ECs are optimally arranged along the direction of blood flow to reduce blood flow resistance and maintain the stability of the vascular internal environment. These cells form a selectively permeable barrier through tight junctions, adherence junctions, and gap junctions, restricting nonspecific transendothelial migration of large molecules and cells.[27] In addition, ECs maintain blood fluidity and prevent blood coagulation by releasing anticoagulant factors such as nitric oxide (NO), prostacyclin, and tissue plasminogen activator, and by expressing thrombomodulin to inhibit platelet aggregation and fibrin formation.[28,29] Besides, under inflammatory conditions, ECs upregulate the expression of intercellular adhesion molecules, selectins, and vascular cell adhesion molecules to promote the interaction between immune cells and ECs, guiding immune cells to migrate from the bloodstream to sites of inflammation or infection.[30] Furthermore, under flow conditions, the EC initiates a signal to recruit SMCs and pericytes, contributing to the mechanical properties of the arterial wall that allow it to withstand high vascular pressures.[31] The functional endothelium on the luminal surface is a critical component in the human artery and plays a significant role in the development of dependable bioengineered AEs.

The tunica media is the middle layer of the arterial wall, primarily composed of smooth muscle cells (SMCs) and ECM (e.g., collagen, elastin) fibers. ECM fibers provide the main structural support for the tunica media, offering stability and elasticity to the vessel wall. SMCs can contract and relax, controlling the dilation and constriction of the aorta by this characteristic, thereby regulating the vessel's internal diameter and resistance.[32,33] Notably, SMCs exhibit different phenotypes based on their physiological or pathological states, primarily contractile and synthetic.[34] While, the contractile SMCs are mainly responsible for vascular contraction, playing a crucial role in maintaining vascular tone and regulating blood pressure, the synthetic SMCs are involved in the synthesis of ECM proteins and regulating cell growth, especially during the repair and remodeling process after vascular injury.[35–37] Therefore, the transformation of SMCs to the synthetic phenotype is a significant factor in the development of CVDs.[38] Inhibition or reversal of this phenotypic transformation can slow down or even halt the process of cardiovascular remodeling, which is essential for constructing bioengineered AEs with long-term stability and functionality.

The tunica adventitia, the outermost layer, is composed of connective tissue that includes collagen and elastic fibers, vasa vasorum, adrenergic nerves, and lymphatic vessels.[39] It provides structural support and elasticity, enabling the artery to withstand external pressures and protect the blood vessels. The adventitia houses various cell types, including fibroblasts, progenitor cells, and immune cells such as macrophages, T cells, B cells, and dendritic cells.[40] These cells collaborate in the repair, remodeling, and tone regulation of blood vessels. In response to injury and stress, fibroblasts from the adventitia proliferate, differentiate into myofibroblasts, and migrate to the intima.[41]

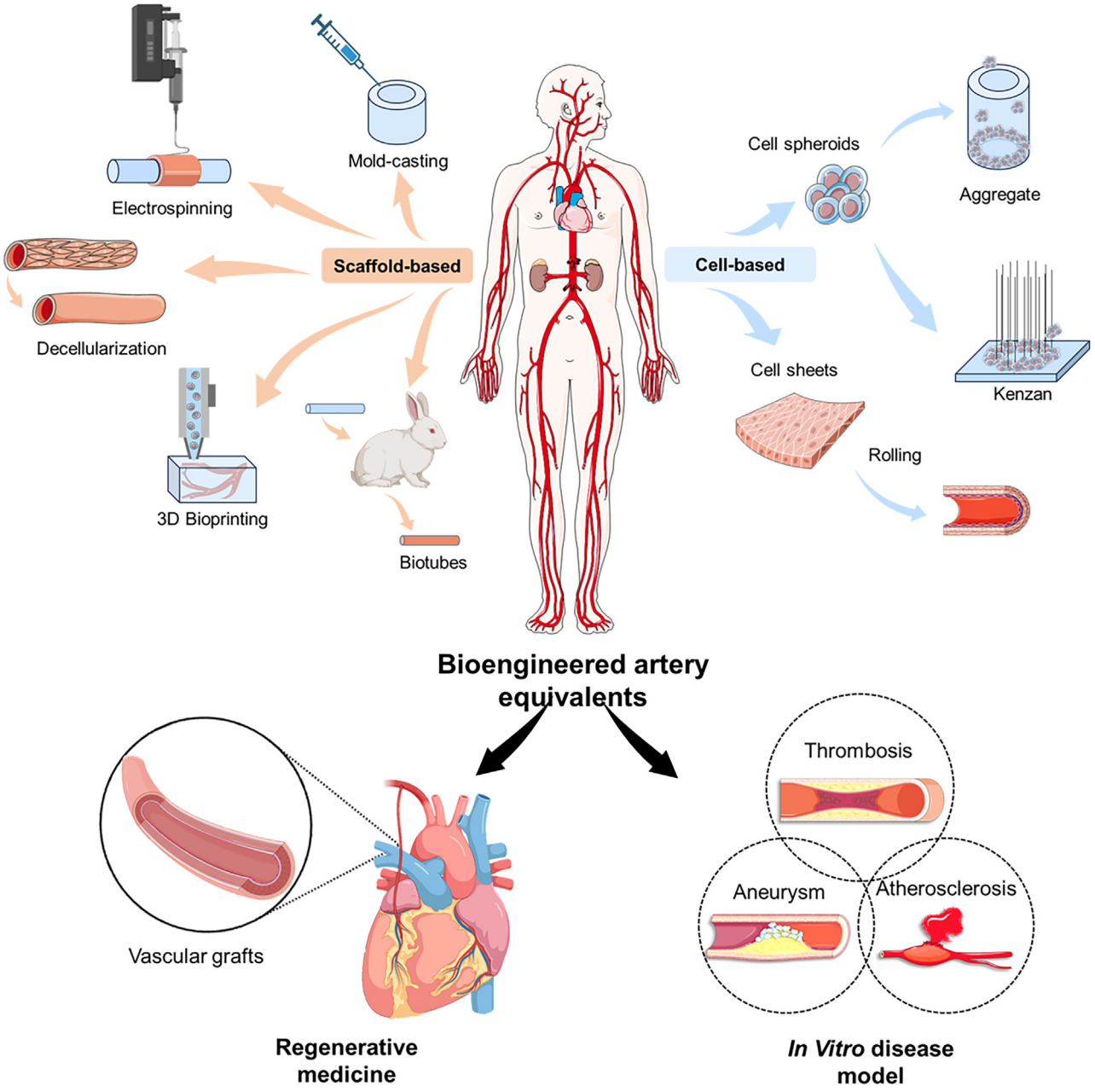

Figure 1. Overview schematic of this review
This figure was created using materials from BioRender.

They secrete factors that regulate the growth of ECs and VSMCs and recruit inflammatory and progenitor cells to the vessel wall.[42] These processes are crucial for vascular repair and remodeling. In a majority of cases, the reconstruction of the adventitial layer is overlooked in the design and construction of bioengineered AEs. However, this layer not only provides necessary structural support and protection but also plays a crucial role in function, particularly in immune regulation, tissue remodeling, and integration, which is essential for reducing rejection reactions and enhancing the long-term stability and functionality of the implant.

Mechanical property and stimulation

Mechanical property. The natural arteries, endowed with densely packed and organized elastic and collagen fibers in the tunica media and adventitia, exhibit robust mechanical properties. Elastic fibers, with their excellent elasticity and recovery capabilities, are primarily responsible for the tissue's extension and rebound after being subjected to force. In contrast, collagen fibers provide structural stability and tensile

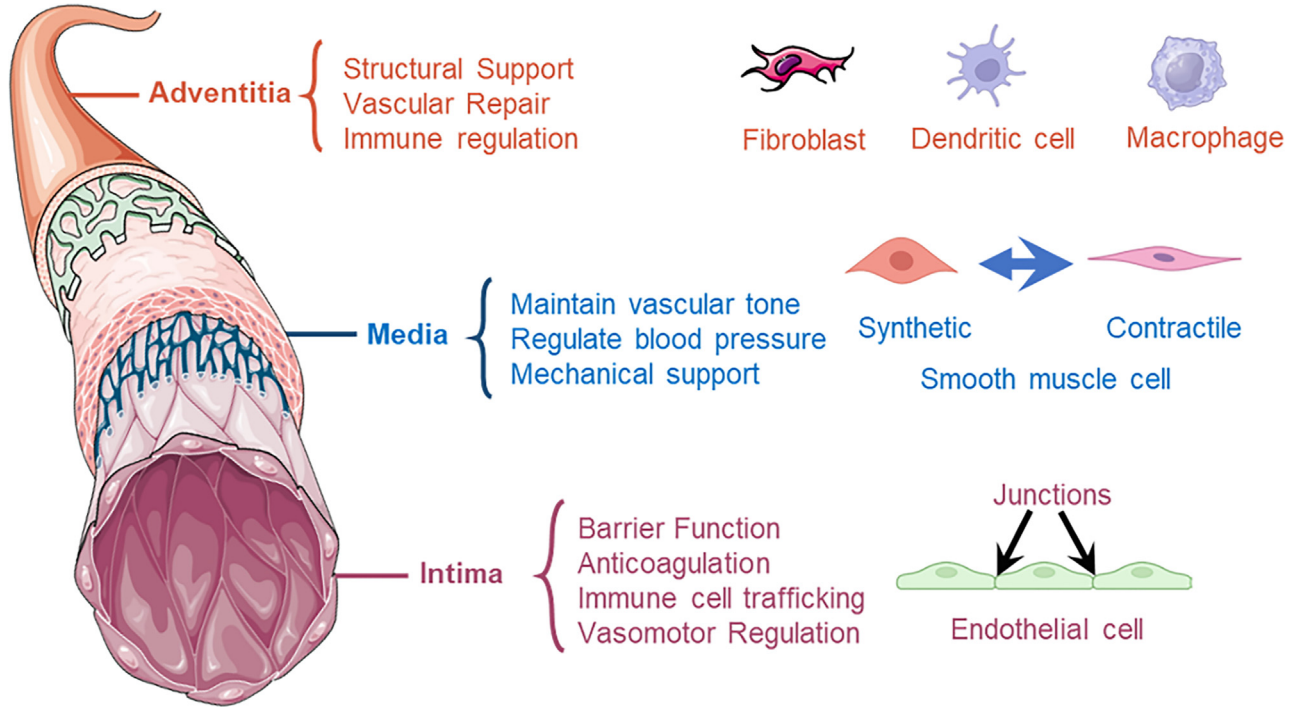

Figure 2. Structure and composition of the human arterial wall

strength. Through stratification, directional arrangement, interweaving, spiral alignment, and guidance by ECM, these fibers form a complex network that can withstand pressure and maintain the structural integrity of the tissue. To prevent deformation and rupture from circulating blood flow, AEs should emulate key mechanical properties such as burst pressure, ultimate tensile strength, suture tension, and compliance.

Resembling the burst rupture of an inflating balloon, the burst pressure refers to the maximum pressure that a vascular vessel can withstand before an acute leak occurs and fails, depending mainly on the characteristics and arrangement of elastic and collagen fibers.[43] The average burst pressure of small-diameter arteries (e.g., coronary artery) is 1681.6 $\pm$ 446.4 mmHg.[44] To improve the burst pressure of the bioengineered AE, it is important to precisely control the strength and arrangement of ECM or ECM-mimicking fibers in the matrix.

Similar to burst pressure, the ultimate tensile strength measures an arterial vessel's capacity to withstand tensile forces. This strength is enhanced by the orderly arrangement and proper cross-linking of extracellular matrix (ECM) fibers, which distribute stresses evenly and prevent the formation of local weak spots. For instance, the ultimate tensile strength ranges from 0.5–3 MPa in coronary arteries to 1.5–4 MPa in the radial, mammary, and saphenous veins, with strain values for natural blood vessels between 40 and 100%.[11] Evaluating vascular tissue's tensile strength can be performed through circumferential and longitudinal tensile strength tests.[45]

Suture tension, the maximum tension that arterial vessels can withstand during suturing, is a critical parameter in surgical procedures, especially in vascular anastomosis.[46] Proper suture tension is essential for ensuring the stability of the anastomosis, promoting healing, preventing tissue damage, maintaining blood flow, and reducing postoperative complications. For example, a common femoral artery anastomosis usually requires a 5-0 Prolene suture, while a tibial artery may require a 6-0 or 7-0 Prolene suture.[47,48] Inferior suture tension may lead to serious problems, including anastomosis narrowing, graft twisting, and angulation, which can affect the patency and dynamics of blood flow.[49,50]

Compliance in vascular grafts refers to the capacity for dimensional change in response to variations in intraluminal pressure.[51] A mismatch between the compliance of a host artery and a graft can disrupt the hemodynamic flow and concentrate stress at the anastomosis, potentially leading to intimal hyperplasia and thrombosis.[52,53] Arterial compliance, a key measure of elasticity, is commonly assessed in the central aorta, with an estimated compliance of 1.23 $\pm$ 0.48 mL/mmHg using the pulse pressure method.[54] Dynamic radial compliance testing is an effective method to evaluate the compliance of grafts.[55,56]

A bioengineered AE, particularly for implantable grafts, should have mechanical performance similar to those of human arteries, ensuring that the graft can effectively mimic the function of natural arteries under physiological conditions and maintain structural and functional integrity after long-term implantation. Bioreactors are powerful tools for studying the effects of mechanical stimuli on the extracellular matrix structure and mechanical properties of engineered blood vessels, enabling optimal chemical biomechanical culture conditions.[57]

Hemodynamics. The association mechanism between hemodynamic conditions and vascular tissue is critical to mediate vascular physiopathology. Regulating flow signaling is crucial for developing arterial endothelium with physiological and pathological capabilities, and

biomechanical analysis can identify patients prone to rapid plaque progression and destabilization.[58] In general, the key mechanical stimulations caused by the blood flow involve shear stress, flow pattern, and wall pressure.

Shear stress is defined as the frictional force exerted by blood flow on ECs, with its magnitude being related to blood flow velocity, vascular diameter, and blood viscosity. Within the human arterial system, the normal range of shear stress values is approximately 10–70 dyne/cm^2. The shear stress not only dictates cell alignment but also promotes the release of cytokines or biochemical factors from ECs.[59,60] While physiological levels of shear stress can induce the release of NO from ECs, contributing to the regulation of vascular tone and offering beneficial effects such as inhibiting platelet aggregation, anti-inflammation, and anti-oxidation, excessively high shear stress may cause endothelial damage.[61] In contrast, low oscillating shear stress may promote the formation of vascular diseases, such as AS.[62]

Flow pattern also plays a decisive role in regulating cell fates. In human arteries, the normal laminar flow pattern, characterized by orderly fluid layers parallel to the vessel wall, applies stable shear stress to ECs, promoting an anti-inflammatory and anti-thrombotic phenotype expression, which helps maintain the stability of the vascular internal environment.[63] However, at arterial bends or bifurcations, the flow pattern may shift to turbulent or transitional flow, leading to ECs dysfunction and an increased risk of AS.[64] This shift in flow pattern is accompanied by the generation of abnormal shear stress, which activates signaling pathways within ECs, causing significant changes in cell morphology and function, including cytoskeletal rearrangement and adjustments in intercellular junctions, ultimately promoting arterial wall remodeling and the progression of aneurysms.

Wall pressure is determined by the interplay of cardiac output and peripheral vascular resistance, which is influenced by factors such as vascular geometry, compliance, and blood viscosity. The normal arterial blood pressure range for healthy adults is approximately a systolic pressure of 90–120 mmHg and a diastolic pressure of 60–80 mmHg.[65] Wall pressure affects vascular function by ensuring blood flow, inducing vascular remodeling in response to chronic hypertension, regulating the release of endothelium-derived vasoactive substances, and deteriorating the degenerative progress of arterial walls in relevant diseases such as aneurysm and dissection.[66,67]

Pathogenesis of human arterial diseases

Atherosclerosis. Atherosclerosis is a chronic inflammatory vascular disease, which is also related to the mechanisms of age-related diseases.[68] The characterized by lipid deposition, inflammatory responses, and fibrosis within the arterial wall, leading to atherosclerotic plaque formation.[69] These plaques can narrow arteries, disrupt blood flow, and increase the risk of heart disease and stroke.[70]

Among various hypotheses for explaining the pathogenesis of AS, the endothelial dysfunction theory is widely regarded as the central and dominant theory (Figure 3A).[71] Accordingly, endothelial dysfunction is considered the initial trigger, where ECs are injured by abnormal hemodynamics, hyperlipidemia, and inflammatory stimulation, resulting in the decreased synthesis of NO and the increased expression of adhesion molecules (e.g., ICAM-1, VCAM-1, selectins), facilitating the recruitment of monocytes and T cells.[72,73] Meanwhile, lipids, particularly Ox-LDL, accumulate in the arterial intima, are taken up by macrophages, and transformed into lipid-rich foam cells. These cells, along with the ECM proliferation of SMCs, form plaques that can grow and cause arterial lumen stenosis.[74]

For *in vitro* modeling of AS, precise definition and control of the pathogenic microenvironment and condition is necessary. Key early events in the model must include endothelial dysfunction, marked by reduced NO production and increased adhesion molecule expression. The simulations that help to initiate AS include the introduction of inflammatory factors such as tumor necrosis factor-alpha (TNF-α), IL-1β, and IL-6, essential drivers of the inflammatory cascade at high concentrations in lesions.[68] Another central is Ox-LDL, alongside the recruitment and activation of immune cells such as monocytes and lymphocytes.[75] Additionally, hemodynamic changes such as alterations in shear stress and mechanical stress on vascular walls are crucial.

Thrombosis. Atherosclerosis not only thickens and hardens arterial walls but also exposes blood when its unstable plaques rupture, triggering thrombosis and heightening the risk of cardiovascular events. Thrombosis involves abnormal blood clotting within vessels, potentially leading to severe health issues such as stroke, heart attack, and deep vein thrombosis, collectively responsible for approximately 25% of global deaths.

Thrombosis is a complex physiological process that includes vascular endothelial cell injury, platelet adhesion and activation, activation of the coagulation cascade, and hemodynamic interactions (Figure 3B).[76] Increased intracellular reactive oxygen species (ROS) levels activate calcium channels, resulting in red blood cell (RBC) damage and reduced deformability, thereby increasing blood viscosity.[77] Elevated ROS levels and increased blood viscosity promote the activation of platelets responsible for hemostasis and thrombosis. Oxidative stress also induces the expression of adhesion molecules (e.g., ICAM-1, VCAM-1) and inflammatory factors (TNF-α, IL-6, and MCP-1), enhancing the adhesion of platelets and ECs and promoting leukocyte migration to ECs, which further elevates the risk of thrombosis.[78] Additionally, the shear rate of blood flow significantly influences platelet aggregation and activation; low shear rates favor aggregation, whereas high shear rates may enhance platelet activation.

Given the intricate nature of thrombosis, encompassing cell adhesion, platelet signaling, and the precise timing and location of clot formation, conventional research methods may struggle to accurately replicate this process. This challenge underscores the growing demand for advanced *in vitro* models.

Aneurysm. Different from AS which is associated with a process of arterial wall thickening and hardening, the aneurysm represents the tissue degenerative pathological process. An aneurysm is the result of localized abnormal dilation of the arterial wall, primarily due to structural

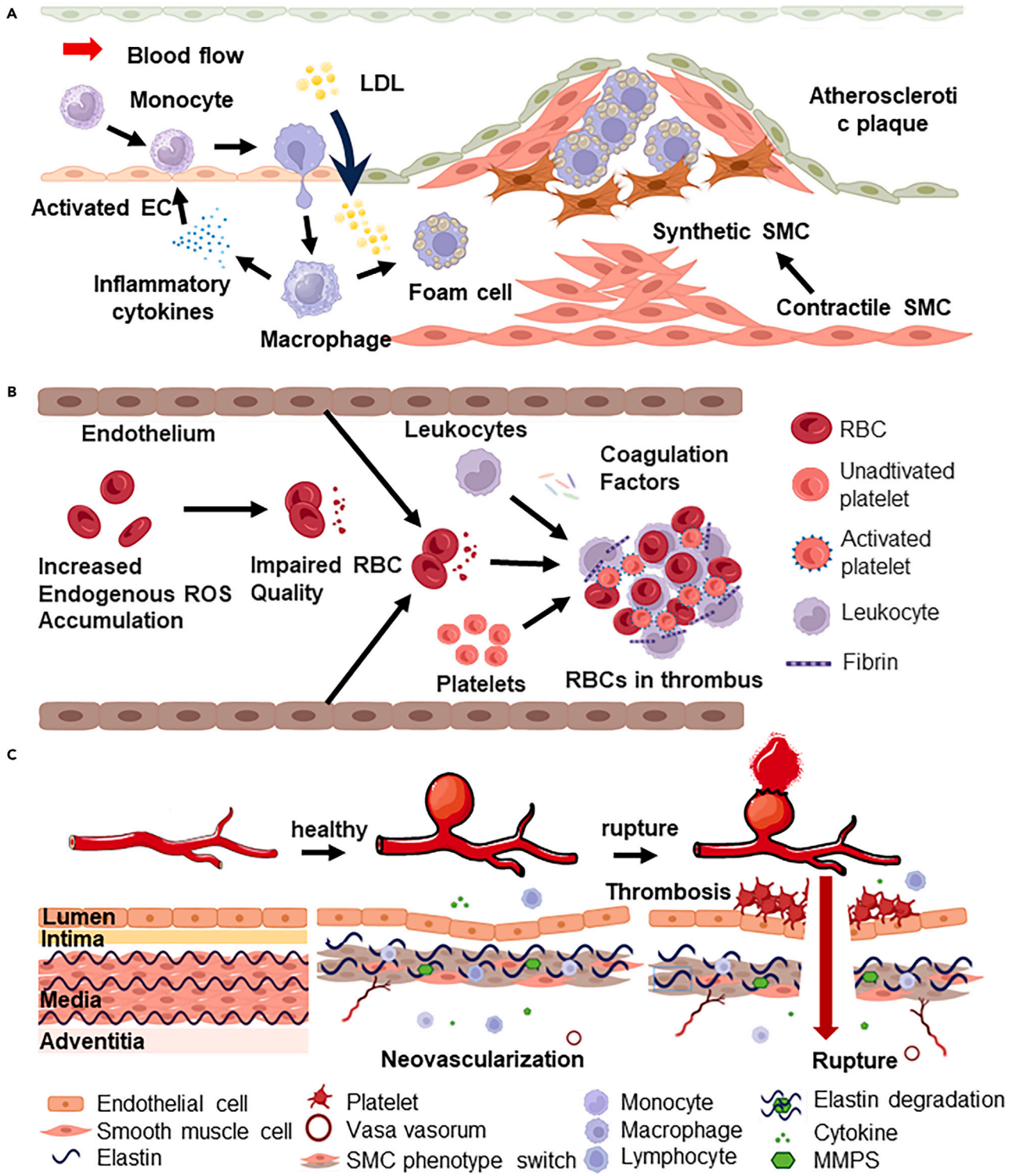

Figure 3. Pathological processes of human arterial diseases

(A) Atherosclerosis.

(B) Thrombosis.

(C) Aneurysm.

weakening that renders it incapable of withstanding normal blood pressure, leading to permanent expansion, which is typically manifest in two forms: saccular (asymmetric outpouchings) or fusiform (circular dilation).[79]

Similar to the inflammatory mechanisms observed in AS, the formation and development of aneurysms are significantly influenced by inflammatory responses (Figure 3C). Inflammation typically initiates within the dysfunctional endothelium, regulated by nuclear factor-kappa B, secrete pro-inflammatory cytokines TNF-α, IL-13, and MCP-1.[80] This induces the recruitment of immune cells (monocytes, macrophages, T-cells), altering VSMC phenotypes. SMCs, key matrix-synthetic cells, proliferate with a pro-inflammatory phenotype,[81] degrading the internal elastic lamina and promoting ECM remodeling.[82] Both involved immune cells and phenotypically switched SMCs can express MMPs (MMP-1, MMP-2, MMP-9) that gradually degrade arterial ECM. This cascade, in turn, recruits inflammatory cells, upregulates proteolytic enzymes, and reduces contractile gene/protein expression, such as myosin heavy chain and α-actin). Ultimately, these changes diminish collagen synthesis, exacerbate VSMC loss, and weaken the arterial wall, predisposing it to aneurysm rupture.

In the development of *in vitro* models of aneurysms, precise design of geometric morphology and hemodynamic conditions is pivotal. Aneurysms exhibit diverse and complex shapes, and accurately replicating these features is crucial for recreating the complexity of the hemodynamics signals within the local lesions, such as blood flow velocity, pressure distribution, and fluid shear forces. Besides, as the inflammation cascade is another critical pathogenic factor of the aneurysm, it is indispensable to establish biomimetic vascular tissue analogs that are responsive to relevant stimuli for the recapitulation of the tissue degenerative process.

PREVAILING TECHNOLOGIES FOR BIOENGINEERED ARTERIAL EQUIVALENTS

Scaffold-based technologies

Mold-casting

Mold-casting is a straightforward engineering technique used to create AEs by casting a solution of biomaterials and cells into an annular mold, which then crosslinks to form the designed 3D structures.[83] The first bioengineered blood vessel, constructed using such a method, was 7.5 cm long with a 6-millimeter inner diameter (Figure 4A).[12] It comprised layers designed to mimic natural blood vessels, using collagen with SMCs, an additional wrapped dacron mesh, and an endothelial lining created by seeding ECs on the luminal surface. However, even with the reinforcement of a polyester mesh, its burst pressure only reaches 40 to 70 mmHg which is vulnerable to implantation. The inherent softness of natural polymers such as fibrin,[84,85] gelatin,[86] and elastin[87] pose challenges in load-bearing applications despite the biological advantages.

Efforts to enhance the mechanical properties of natural hydrogels have involved modifying the crosslinking methods.[90] For instance, chemical crosslinking, which creates strong covalent bonds between molecules, can significantly improve the mechanical strength of collagen compared to thermally induced self-assembly.[91] This method also promotes a uniform network that distributes stress evenly, enhances resistance to enzymatic degradation, and improves stability.[92] For instance, using Type I bovine collagen gel with transglutaminase-mediated crosslinking, which forms covalent amide bonds between protein fibers, significantly increases the burst pressure (71 $\pm$ 4 mmHg vs. 46 $\pm$ 3 mmHg). To reinforce the mechanical strength of hydrogels, other methods such as small molecule crosslinkers (e.g., glutaraldehyde,[93] catechol compounds,[94] genipin,[95] and tannic acid[96]), photoinitiated crosslinking (ultraviolet[97] or visible light[98]), and non-enzymatic glycation[99] techniques have been applied, though some conditions may compromise cell viability.

Alternatively, interpenetrating network hydrogel paves a way to reinforce the mechanical properties of materials by integrating the merits of multiple components. For instance, an alginate/acrylamide double-crosslinked hydrogel exhibits excellent mechanical properties, in which the reversible crosslinking alginate offers elasticity while the acrylamide provides robust frames (Figure 4B). The elongation rate can optimally reach 196%, and the hydrogel tube, even after sewing, retains the shape perfectly before stretching, after stretching, and after perfusion. The small diameter graft (inner diameter: 0.2–1.2 mm) built with this material was implanted into a rabbit model for 28 days, demonstrating good patency.[88] In addition, mold-casting based on 3D molds provides a new idea for the preparation of bioengineered arteries.

Besides improving the strength of biomaterials, the application of mechanical stimulation through bioreactors stimulates cells to synthesize and organize the matrix composition, thereby improving the mechanical properties of the construct.[100–102] This process aids in forming tissue with an elastic modulus similar to that of natural tissue and promotes effective ECM production by cells.[103] In a representative study, fibroblasts-laden fibrin tubes were mounted on a bioreactor that supplies pulsatile flow (pulse frequency: 0.5 Hz, peak circumferential strain: 7.3 $\pm$ 1.9%) to train the cell via cyclical distension and transmural flow (Figure 4C).[89] Upon such dynamic cultures for 2–9 weeks, the vascular grafts were extensively remodeled by cells, encompassing circumferentially aligned collagen and other ECM component fibers, achieving mechanical anisotropy comparable to natural arteries, with burst pressures in the range of 1400–1600 mmHg and compliance similar to native arteries.

While traditional molding techniques face limitations in precisely controlling the microstructural organization, leading to suboptimal mechanical performance for clinical use, they are valuable as preclinical *in vitro* models to test drug efficacy, study disease mechanisms, and guide treatments.[104,105]

Electrospinning

Electrospinning is a technique that utilizes a high-voltage field to eject a polymer solution or melt, generating a polymer jet to produce polymer fibers.[106] This method can replicate the microstructure of ECM,[107] providing a wide range of fiber diameters and pore sizes (from nanometers to microns),[108] a high surface area-to-volume ratio, and porosity structures that effectively promote tissue formation after cell seeding.

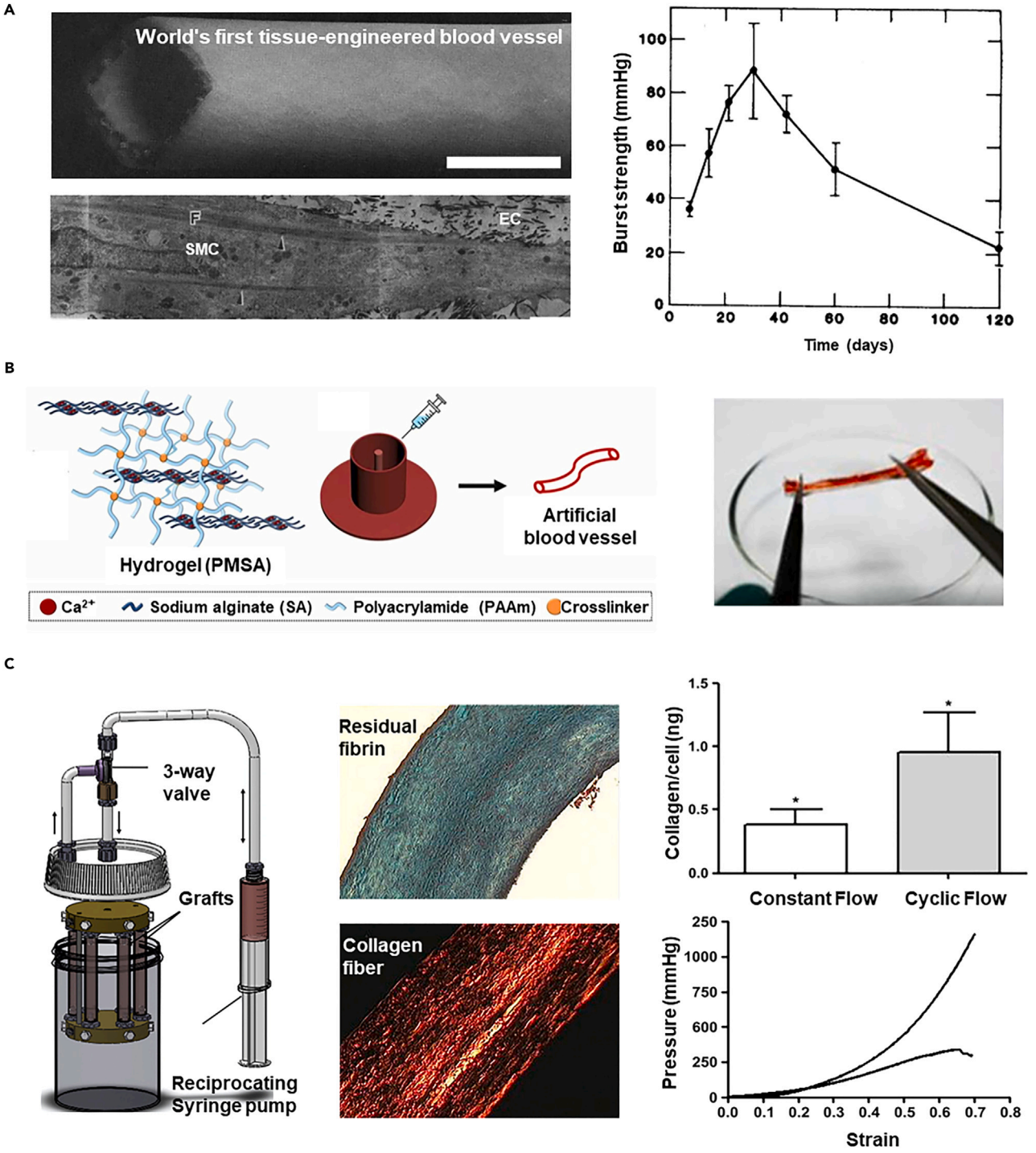

Figure 4. Representative AEs constructed by mold-casting technology

(A) The panoramic view of the first three-layered vascular graft by mold-casting, the structure of its wall, and the burst strength (scale bar 5 mm). Copyright 1986, Royal Society of Chemistry, Reproduced with permission.[12]

(B) Mold cast vascular grafts using an interpenetrating network hydrogel model crosslinked with sodium alginate and acrylamide to enhance its mechanical properties. Copyright 2023, Elsevier, Reproduced with permission.[88]

(C) In the bioreactor, cells within the vascular grafts are conditioned to acquire enhanced mechanical properties. Copyright 2011, Elsevier, Reproduced with permission.[89]

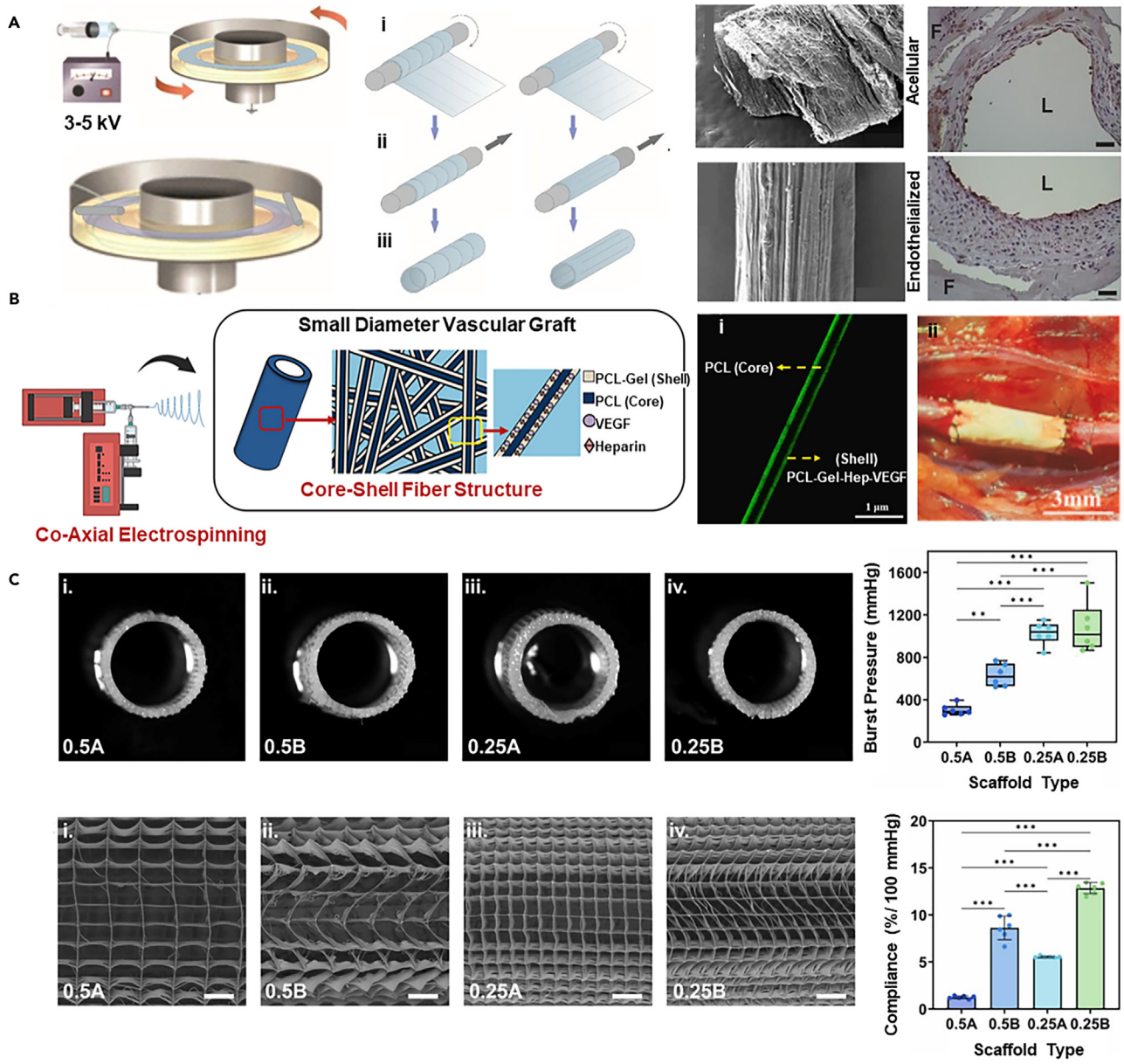

Figure 5. Representative AEs constructed by electrospinning

(A) Electrospinning achieves controlled microstructures with circumferential and longitudinal alignment, guiding ECs to converge and form an endothelial layer (scale bar 30 μm). Copyright 2019, National Academy of Sciences, Reproduced with permission.[113]

(B) Coaxial electrospun vascular grafts with heparin-VEGF and polycaprolactone/gelatin demonstrate 100% patency and complete endothelialization in rats after four months (scale bar i: 1 μm, ii: 3 mm). Copyright 2024, Elsevier, Reproduced with permission.[114]

(C) The MEW technology regulates the fiber arrangement of the stent, mimicking the arrangement of collagen fibers to achieve a vascular graft with a wavy circumferential ultra-fine fiber arrangement, exhibiting good biomechanical compliance (scale bar 500 μm). Copyright 2023, IOP Publishing, Reproduced with permission.[115]

By using a rotating drum for fiber deposition, it is easy to construct vessel-like constructs with tunable microstructures.[109] With the increased concentration of electrospun polymer solutions, the fiber diameter, pore size, porosity, and pore interconnectivity significantly increase.[110] Adjustments to collector rotational speed or the use of metal plates can improve fiber orientation.[111,112] For example, electrospun fibrin fibers can be wrapped around a mandrel forming a controlled microstructure with circumferential and longitudinal alignment (Figure 5A).[113] The controlled surface morphology of the hollow fibrin ultrafine fiber tubes guides the formation of confluent ECs both *in vitro* and *in vivo*. Within 3-4 days *in vitro*, the cells immediately and controllably adhere to form confluent endothelial layers, while generating stable endothelialization can be observed after 4 weeks' implantation, representing a promising approach for arterial bypass surgery.

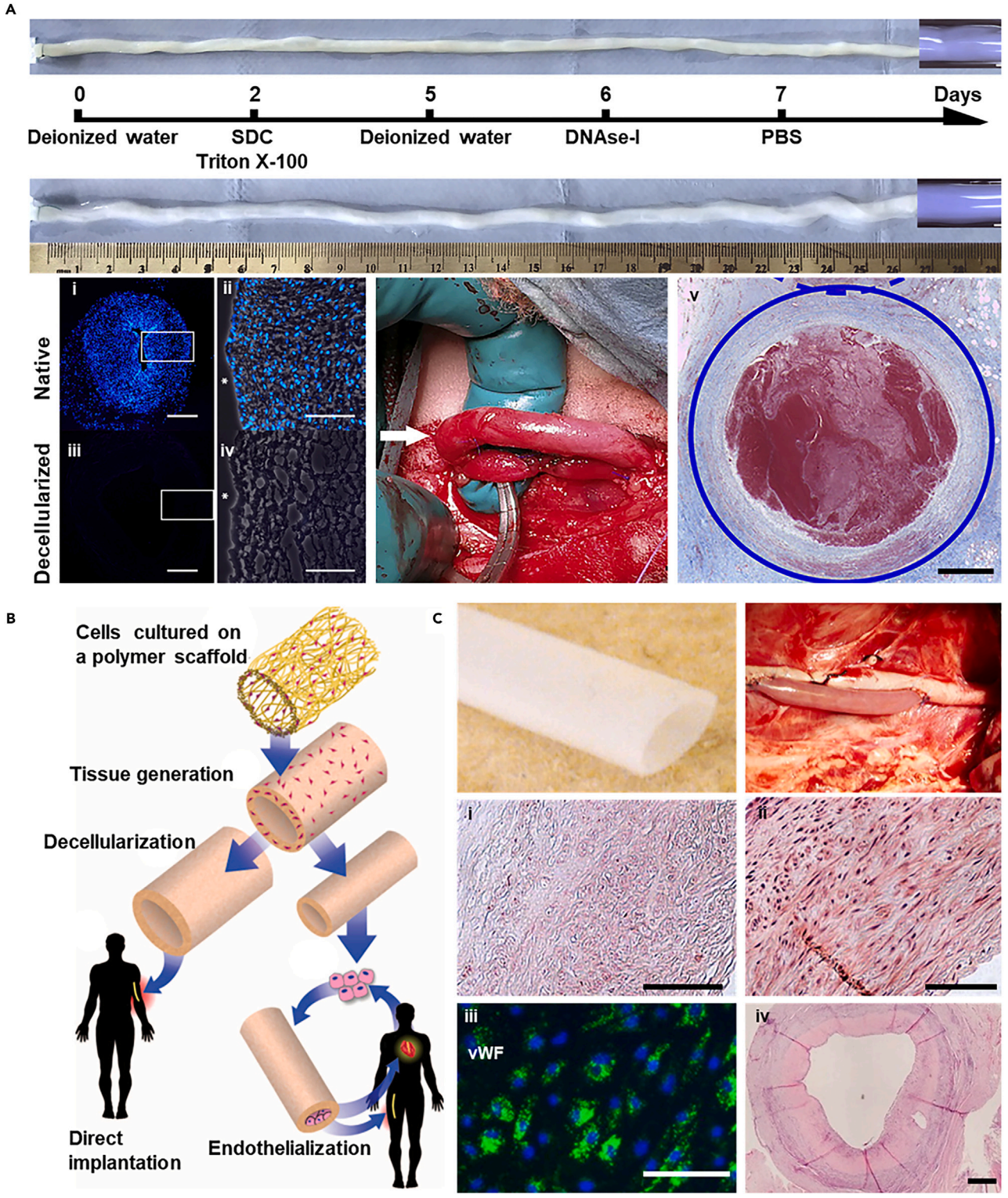

Figure 6. Representative AEs constructed by decellularized arterial tissue

(A) Decellularized HUA were tested in a sheep carotid artery bypass model, demonstrating initial compatibility with arterial pressures but ultimately occluding on the seventh day (scale bar i, iii: 500 μm, ii, iv: 100 μm, v: 1 mm). Copyright 2020, Elsevier, Reproduced with permission.[143]

Figure 6. *Continued*

(B) Strategy for producing tissue-engineered vascular grafts. Copyright 2011, American Association for the Advancement of Science, Reproduced with permission.[144]

(C) A tissue-engineered vascular graft with a robust ECM was obtained by culturing aortic SMCs on a biodegradable PGA mesh scaffold, followed by decellularization, which was evaluated in a porcine model (scale bar i-iii: 100 μm, iv: 500 μm). Copyright 2011, National Academy of Sciences, Reproduced with permission.[135]

Electrospinning offers strong adaptability in materials, enabling the combination of natural polymer (e.g., collagen,[116] gelatin,[117] fibrin,[118] alginate[119]) with synthetic polymers (e.g., polylactic acid (PLA),[120–122] polycaprolactone (PCL),[120,123–125] poly(lactic-co-glycolic acid)[126–128]) for co-spinning to optimize both bioactivity and mechanical properties. In constructing electrospun multilayer scaffolds for arterial grafts, varying materials, pore sizes, and fiber orientations allow for a flexible definition of each layer's properties (mechanical, topological, biological), effectively mimicking the structure of native arteries.[129] For instance, the technology to fabricate scaffolds from bovine gelatin and PCL involves sequential electrospinning and co-electrospinning.[130] The sequential approach enables layer-by-layer structure development, whereas co-electrospinning achieves better fiber alignment and a more optimal pore area ratio. The resulting structure exhibits a yield strain of 38.72 $\pm$ 3.23% and a tensile strength of 3.46 $\pm$ 0.088 MPa. Furthermore, the mesh membrane produced by co-electrospinning enhances NIH3T3 fibroblasts' adhesion and proliferation, demonstrating excellent biocompatibility.

Another advantage of electrospinning lies in the incorporation of various bioactive factors for co-manufacturing, thereby enhancing bioactivity or anticoagulation. The fabrication of vascular grafts through the use of coaxial electrospinning involves the incorporation of heparin-VEGF and PCL (as the core) as well as a shell composed of a blend of PCL and gelatin (Figure 5B).[114] The shell structure undergoes degradation to release heparin-VEGF, while the core provides mechanical strength. Upon implantation into the aorta of rats for a period of four months, they demonstrate smooth muscle cell regeneration and complete endothelialization, with a patency rate of 100%. The introduction of bioactive molecules provides an alternative option for small-diameter peripheral or arterial vascular remodeling and repair.

Electrospun vascular grafts, while beneficial, still exhibit several limitations that affect their clinical effectiveness and need addressing. First, the degradation of synthetic polymers can release by-products that potentially alter pH levels, disrupt cellular functions and growth, and may trigger local inflammatory responses.[131,132] Second, controlling the degradation rate, which involves both hydrolytic and enzymatic processes, remains a challenge. Additionally, a critical issue is the mismatch of radial mechanical compliance at the anastomotic site, which can lead to intimal hyperplasia and ultimately graft failure.[133,134] To overcome these issues, it is crucial to optimize the scaffold structure for uniform morphology and mechanical properties. Using melt electrospinning writing (MEW) provides superior control over the scaffold's morphological structure. For instance, scaffolds with a wavy circumferential microfiber arrangement mimic natural collagen fiber alignment and exhibit physiological compliance (12.9 $\pm$ 0.6% per 100 mmHg),[115] enhancing their potential for successful integration and function in clinical applications (Figure 5C).

Decellularized arterial tissue

Decellularized arterial tissue represents a significant advancement in replicating the natural ECM microenvironment, overcoming the limitations of artificial structures made from biomaterials. This technique, which involves removing cellular components while preserving essential ECM features such as microstructures and protein compositions, is critical for promoting cell adhesion, differentiation, and proliferation. It has been successfully applied to various tissues including blood vessels,[135] skin,[136] heart,[137] lungs,[138] liver,[139] and kidneys.[140,141]

The process for decellularizing blood vessels typically combines physical (freeze-thaw cycles and agitation), chemical (detergents, chelating agents), and biological (enzymes) treatments.[142] An example is the human umbilical artery (HUA), which, after decellularization, has been tested in sheep models for carotid artery bypass, showing initial success but also challenges such as immunological mismatch leading to occlusion (Figure 6A).[143]

Human vascular tissues, such as saphenous vein,[145] human umbilical vein,[146] and human common femoral artery,[147] are ideal for creating decellularized grafts, though sourcing human tissues for large-scale production presents challenges. Alternatively, animal tissues (e.g., pig,[148] bovine,[149] ovine[150]) are considered, ensuring minimal immunogenicity and safety. The effectiveness of decellularization is leveled by the absence of nuclear material and dsDNA content below 50 ng/mg ECM (dry weight).[142,151] Additionally, any toxic biochemical reagents (e.g., SDS,[152,153] Triton X-100,[154] and so forth) used in the process must be thoroughly removed to avoid adverse effects.

Commercially, decellularized vascular products from mammalian sources such as bovine carotid arteries are available, but these lack control over dimensions such as diameter, wall thickness, and length, limiting their use in personalized medicine. To address this, integrating decellularization with advanced bioengineered techniques has been explored (Figure 6B).[144] For instance, vascular grafts enhanced with multiple layers (15–20 layers) of SMCs have been developed using a biodegradable polyglycolic acid (PGA) mesh scaffold within a bioreactor, followed by decellularization, leaving a robust collagen ECM (Figure 6C).[135] These bioengineered vessels, seeded with recipient-specific ECs, showed reduced neointimal hyperplasia and proliferative cell activity.

Moreover, transforming decellularized tissues into tractable biomaterials such as hydrogels or powders expands their application potential. For example, dECM bioink derived from porcine aortic tissue has been used to 3D bioprint dual-layered vascular grafts with adjustable dimensions, offering enhanced support for ECs and SMCs, and leading to functional AEs suitable for *in vivo* studies.[155,156] This approach not only addresses dimensional limitations but also enhances the functionality and applicability of decellularized tissues in clinical settings.

3D bioprinting

3D bioprinting is a cutting-edge biofabrication technology that strategically places cells, biomaterials, and bioactive molecules in three-dimensional arrangements to reconstruct complex vascular structures *in vitro*.[157–159] This technology incorporates various biofabrication strategies for crafting artificial blood vessel grafts and models, each offering unique benefits and challenges.

One approach is the classical layer-by-layer deposition, which provides meticulous control over the vascular architecture, allowing for the emulation of natural blood vessel multilayered tissue. Utilizing a high-viscosity nano-engineered bioink made from gelatin methacryloyl, polyethylene glycol diacrylate, and nanosilicate, this method encapsulates SMCs and extrudes them to form cylindrical structures (Figure 7A).[160] ECs are subsequently seeded to complete the 3D bioprinted vessels. Despite its precision, this strategy typically relies on the use of high-viscosity bioinks to ensure stable material deposition and precise structure formation during the printing process. However, the viscous bioink can compromise cell viability due to the necessary high shear forces during printing.[161]

To address this problem by improving the printability of soft hydrogels, a suspension 3D bioprinting approach has been developed, which allows for the freeform deposition of low-viscosity bioinks into a supporting medium with shear-recovery properties.[164] Using gelatin, which does not negatively impact cellular integration and is thermally reversible, as a support bath material, rheological analysis indicates that the gelatin slurry behaves and remains a Bingham plastic at room temperature (Figure 7B).[162] Alginate hydrogel was used to print arterial tree structures (wall thickness: 1 mm, diameter: 1–3 mm) within this support bath, resulting in well-formed internal lumens and bifurcations.

An innovative method involves the sequentially suspended 3D bioprinting of different cell-laden bioinks to create multi-layered arterial models.[165,166] Such a strategy first employs microgel-based biphasic (MB) bioink as a supportive embedding medium for 3D bioprinting, which facilitates the creation of complex external geometries of natural vessels (Figure 7C).[163] Using sacrificial gelatin bioink enriched with human umbilical vein endothelial cells (HUVECs), embedded printing is performed into newly printed but uncrosslinked constructs. This process generates free-form vascular networks by leveraging the reversible self-healing behavior of the MB bioink. Following the photopolymerization of the suspension medium, the gelatin strands with HUVECs are liquefied at 37°C. The printed constructs are flipped, ensuring uniform adhesion of cells to the luminal surface, and post-cultivation results in the formation of a uniform, confluent endothelial layer. The sequentially suspended 3D bioprinting provides unmatched bioprinting capabilities to accelerate the replication of complex organ geometries and internal structures, facilitating the biomanufacturing of tissues and organs.

Coaxial 3D bioprinting, another impressive method, allows the simultaneous deposition of different cell types and bioinks, tailored for replicating the intricate, multi-layered vascular system.[167] This method necessitates meticulous technical control over bioink flow and intermixing to fabricate composite cell-layered vessels. Using vascular tissue-specific bioink containing HUVECs and human aortic smooth muscle cells (HAoSMCs), and a reservoir-assisted triple coaxial nozzle (18G/14G/10G) where the intermediate and shell needles contain Ca^{2+}-laden Pluronic F127, extrusion through the core nozzle supports vessel fabrication (Figure 7D).[15] This triple coaxial cell printing technique directly constructs biomimetic vascular grafts composed of a separate endothelial layer and muscle layer (inner diameter: 2 mm, wall thickness: 1 mm). The technology also permits customized adjustments to bio-ink properties, facilitating the design of vessels with tailored elasticity and cell-supportive characteristics, holding promise for advancing cardiovascular therapies and enabling more personalized and effective medical solutions.

In short, selecting the right 3D bioprinting strategy depends on the specific requirements and intended functions of the fabricated blood vessels. While each method has its applications and limitations, ongoing advancements in 3D bioprinting technology are expected to further enhance artificial blood vessel performance and open new avenues for treating CVDs.

In vivo bioengineered biotubes

In vivo bioengineered techniques leverage the interaction between host tissues and implants to construct AEs, known as biotubes, by subcutaneously embedding specially designed molds.[168] This process involves the immune system recognizing the implant as a foreign body, which stimulates the formation of fibrous capsules around the molds, ultimately forming biotubes. Additionally, the structure and size of the biotubes can be tailored according to the specifications of the implant.

This method has been used to create fully autologous vascular grafts directly within the body, eliminating issues such as immune mismatch or infection risks associated with *ex vivo* manufactured vascular structures. For example, a transparent nylon mold with a helical shell (inner diameter: 7 or 8 mm) and a core rod (outer diameter: 4 or 5 mm) was implanted in Beagle dogs' subcutaneous pouches for one or two months (Figure 8A).[169] This resulted in the formation of a tubular collagen tissue within the mold, and after its removal, a 25 cm biotube (inner diameter: 4 mm) was obtained. When used as an arterial graft in dogs, arterial reconstruction occurred three months post-transplantation. Despite good biocompatibility, endothelialization, and vascular regeneration, these grafts may lack sufficient mechanical strength (unit breaking force: 0.7 N/mm, burst pressure: 1500 mmHg), which can lead to post-transplant rupture and aneurysm formation.

To further improve its mechanical properties, integration of polymer melts spinning technology with *in vivo* bioengineered has been explored, resulting in heat-treated medium-fiber-angle poly(ε-caprolactone) fiber skeletons-reinforced biotubes (hMPBs). These enhanced biotubes maintain their shape and structure even after common surgical manipulations such as coiling, folding, twisting, and clamping (Figure 8B).[170] While polymer implants offer a simple, cost-effective solution with the potential for broad application, the bio-integration period for these grafts often spans several weeks, which may not suit acute surgical needs. Additionally, achieving the required lengths for procedures such as coronary artery bypass grafting may be challenging with *in situ* engineered vessels.

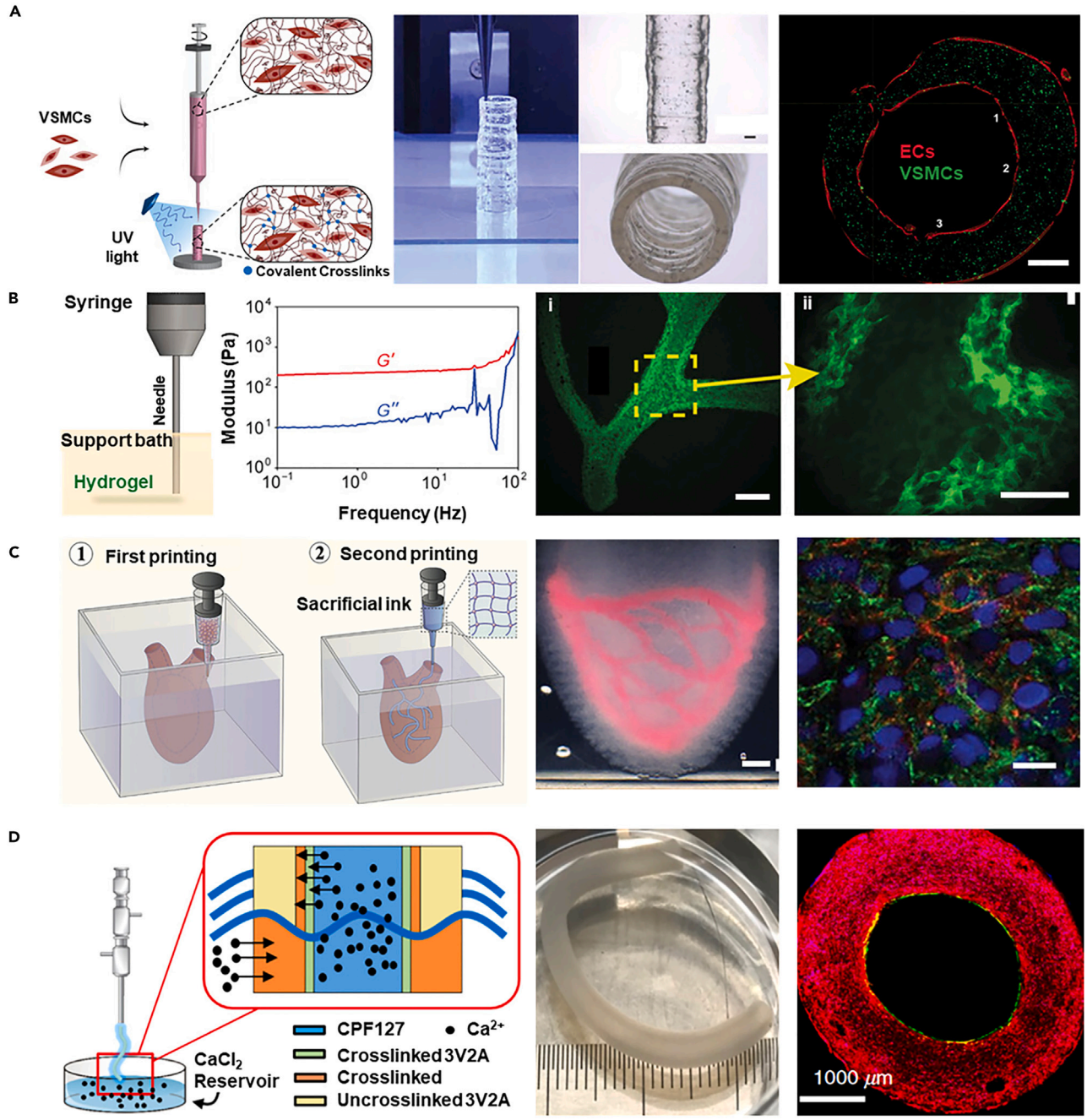

Figure 7. Representative AEs constructed by 3D bioprinting

(A) Utilizing a high-viscosity colloidal nanoengineered bioink encapsulating VSMCs, cylindrical blood vessels were printed using layer-by-layer 3D bioprinting technology, followed by seeding with ECs to form the vascular construct (scale bar 2.5 mm). Copyright 2021, Wiley, Reproduced with permission.[160]

(B) Gelatin, serving as a thermo-reversible support bath material that does not negatively impact cell integration, was rheologically analyzed to exhibit Bingham plastic properties, enabling the printing of an arterial tree structure with alginate hydrogel that features well-defined internal lumens and bifurcations (scale bar i: 2.5 mm, ii: 1 mm). Copyright 2015, American Association for the Advancement of Science, Reproduced with permission.[162]

(C) Sequential suspension 3D bioprinting technology employs MB bioink as a support matrix to facilitate the embedding printing of free-form vascular networks using a HUVECs-enriched sacrificial gelatin bioink (scale bar i: 2 mm, ii: 10 μm). Copyright 2023, Wiley Blackwell, Reproduced with permission.[163]

(D) Utilizing a bioink containing HUVECs and HAoSMCs, along with a triple coaxial 3D bioprinting, a biomimetic vascular graft with distinct endothelial and muscular layers is directly constructed (scale bar 1000 μm). Copyright 2019, AIP Publishing, Reproduced with permission.[15]

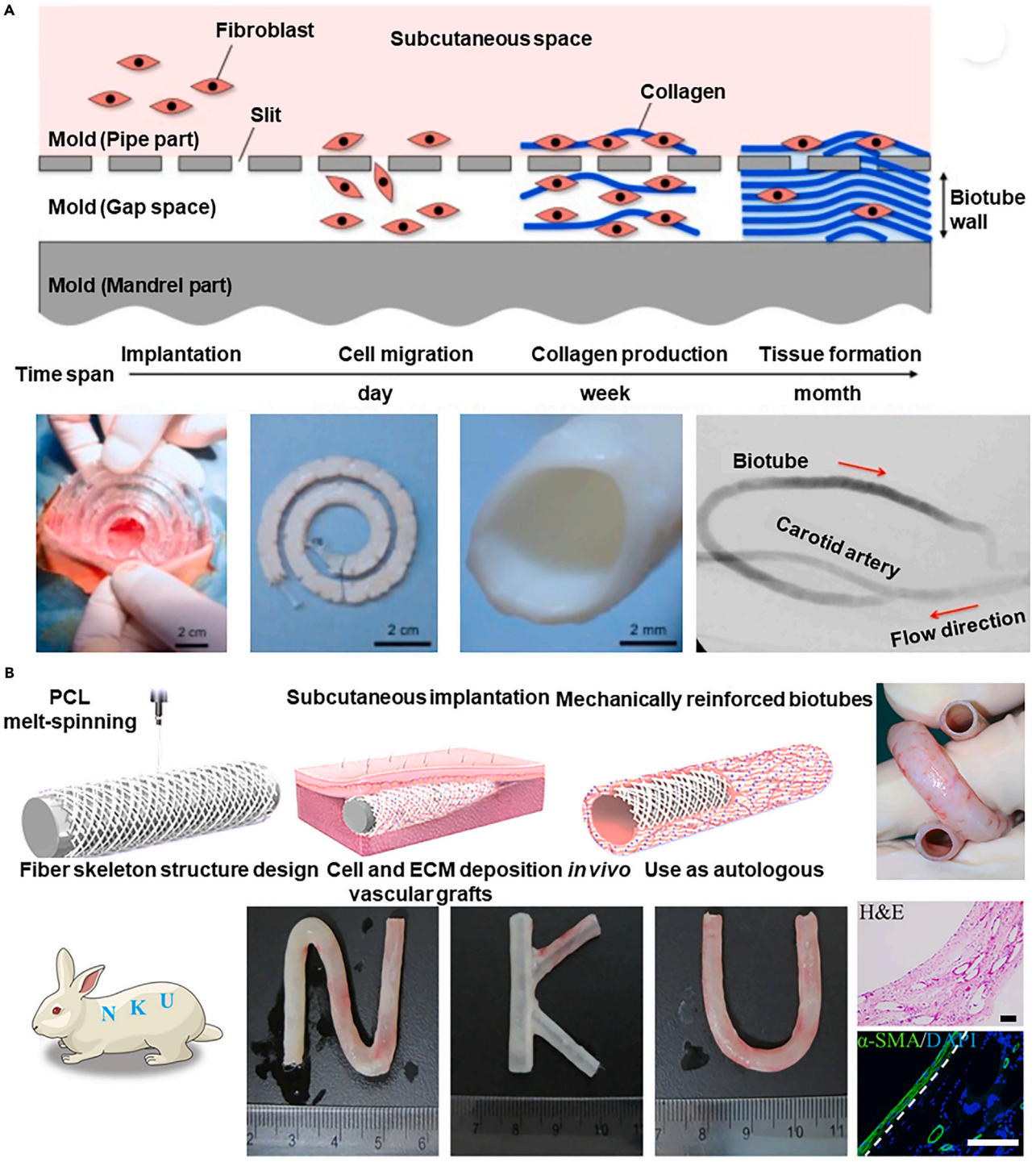

Figure 8. Representative AEs constructed by *in vivo* bioengineered

(A) Implanting transparent nylon molds subcutaneously in beagle dogs, tubular collagenous tissue is formed, which, after decellularization to acquire a biotube and allogeneic transplantation, successfully facilitates arterial reconstruction three months post-procedure. Copyright 2018, Elsevier, Reproduced with permission.[169]

(B) The integration of polymer melt spinning technology with *in vivo* engineering has enhanced the mechanical properties of hMPBs, ensuring their maintenance of original shape and structure post-surgical manipulations (scale bar 100 μm). Copyright 2022, American Association for the Advancement of Science, Reproduced with permission.[170]

Cell-based technologies

Cell-based technologies are advancing bioengineered by leveraging the natural tissue-forming capabilities of cells, bypassing the limitations of scaffolds-based techniques that can inhibit cell-cell interactions due to the presence of biomaterials.[171,172] These methods utilize spheroidal cell aggregates and cell sheets, allowing cells to self-organize without scaffold interference. This approach eliminates biomaterials, significantly enhances cell density, and fosters robust cell-cell interactions, crucial for developing functional tissues. This shift toward scaffold-free bioengineered aims to more naturally and efficiently replicate the complexity of natural arteries.

Cell spheroids assembly

Cell spheroids serve as the foundational units for cell-based biofabrication, produced through various techniques including hanging-drop,[173] low-adherence substrate,[174] microwells,[175] microfluidic.[176] The assembly of these spheroids forms cellular structures without scaffolds and promotes extensive cell interactions and ECM production. A key aspect of this method involves safely manipulating these "biobricks" to construct complex structures.

Introduced in 2010, the cell spheroid assembly technique utilized primary human arterial fibroblasts cultured in a 60-well plate, leading to the development of a bioreactor integrated with a ring-shaped mold that could hold 4000 to 5000 micro-tissues (Figure 9A).[177] After 14 days of flow and mechanical stimulation, fibroblasts reorganized along the vascular axis, forming small-diameter vessels (diameter: 3 mm, length: 5 mm, wall thickness: 1 mm).

The cell spheroid can also be magnetically assembled for the manufacturing of arterial grafts. In a representative study, magnetic nanoparticles were incorporated into the spheroids to facilitate the assembly and fusion of cellular aggregates, with thousands of magnetic cell spheroids assembled into a vascular tissue structure with a diameter of 5 mm (Figure 9B).[178] Despite concerns over the impact on cell viability, optimization of nanoparticle internalization has enhanced cell vitality and maintained phenotype in this report.

Further integration with 3D bioprinting technology has allowed for the precise construction of tubular structures (diameter: 900 μm, wall thickness: 300 μm) using multicellular spheroids containing SMCs and fibroblasts on a template built by agarose rods, which fuse over a period of 5–7 days to form branched, large blood vessel-like structures (Figure 9C).[179] By designing vessels of different shapes and using different cell types, intricate arterial structures are constructed in composition and architecture.

However, challenges remain in placing and stabilizing spheroids without supportive materials (e.g., agarose strands). To address this problem, an innovative assembly approach called the Kenzan method additionally uses a micro-needle array for precise 3D layering and stacking of spheroids, promoting three-dimensional organization and conferring specific tissue architecture and mechanical strength.[159,181,182] Upon the spheroids fusion and removal of needle arrays, such a 3D assembly method can manufacture tubular constructs as vascular grafts (Figure 9D).[180] The Kenzan approach has been successfully applied to reconstruct small-diameter blood vessels (diameter: 1.5 mm, length: 7 mm) using the spheroid of human dermal fibroblasts for the transplantation into an immunodeficient pig model, showing no immune rejection and maintaining structural integrity as a blood flow channel over three months.[183]

While promising for producing arterial grafts, the cell spheroid assembly method faces challenges in maintaining cell viability, enhancing mechanical strength, and scaling for industrial applications. Future research should focus on refining these techniques to improve the efficiency, cost-effectiveness, and clinical applicability of manufacturing arterial grafts.

Cell sheets assembly

Cell sheet technology differs from spheroid-based methods by cultivating cells into a paper-like structure that can be harvested intact without enzymes by simply adjusting the culture conditions.[184–186] This technique allows for the wrapping of cell sheets around a temporary mandrel to create bio-conduits easily.

L'Heureux et al.[187] pioneered a scaffold-free method for producing vascular grafts by cultivating layered sheets of ECs, SMCs, or other relevant cells, which are then rolled to form functional grafts. This cell sheet technique was used to assemble the first tissue-engineered blood vessel suitable for autologous small-diameter arterial reconstruction in adult patients.[188] Dermis fibroblasts cultured to enhance ECM protein production fused into a uniform tissue after about 10 weeks, creating multilayered vessels with burst pressures over 3,000 $mmHg^9$.

However, manually wrapping cell sheets may limit the development of artificial arteries with precise dimensions and cell alignment. Integrating technologies such as electrospinnig[189] and surface engineering[190] with cell sheets can produce size-tunable and morphology-controllable sheets. In a representative study, the stress-induced rolling membrane (SIRM) technique, which is based on the release of internal stress due to the stretching of the top layer, allows for the adhesion of two layers with different surface morphologies, resulting in the formation of a cohesive structure that can roll freely at one end, yielding a tube with controllable dimensions. Using the SIRM technology, vascular grafts with an inner diameter ranging from 10 μm to 2 mm can be fabricated (Figure 10A).[191] Concurrently, through the rolling process, simple patterns on a 2D membrane are transformed into complex patterns within a 3D tube. These tubes are capable of simulating the unique inner layer of HUVECs, the middle layer of SMCs, and the outer layer of NIH3T3 fibroblasts, replicating their natural arrangement within the body.

Additionally, to replicate the 3D helical and interwoven organization of SMCs in natural vessels, aligned human mesenchymal stem cells (HMSCs) sheets were prepared on nanogrates and wrapped around a mandrel layer-by-layer (Figure 10B).[192] After two weeks of maturation and removal from the mandrel, a tubular structure with circumferentially aligned HMSCs is formed, showing integration and uniform alignment after three weeks of perfusion maturation. Based on the cell sheet technology, the loss of scaffold-based mechanical

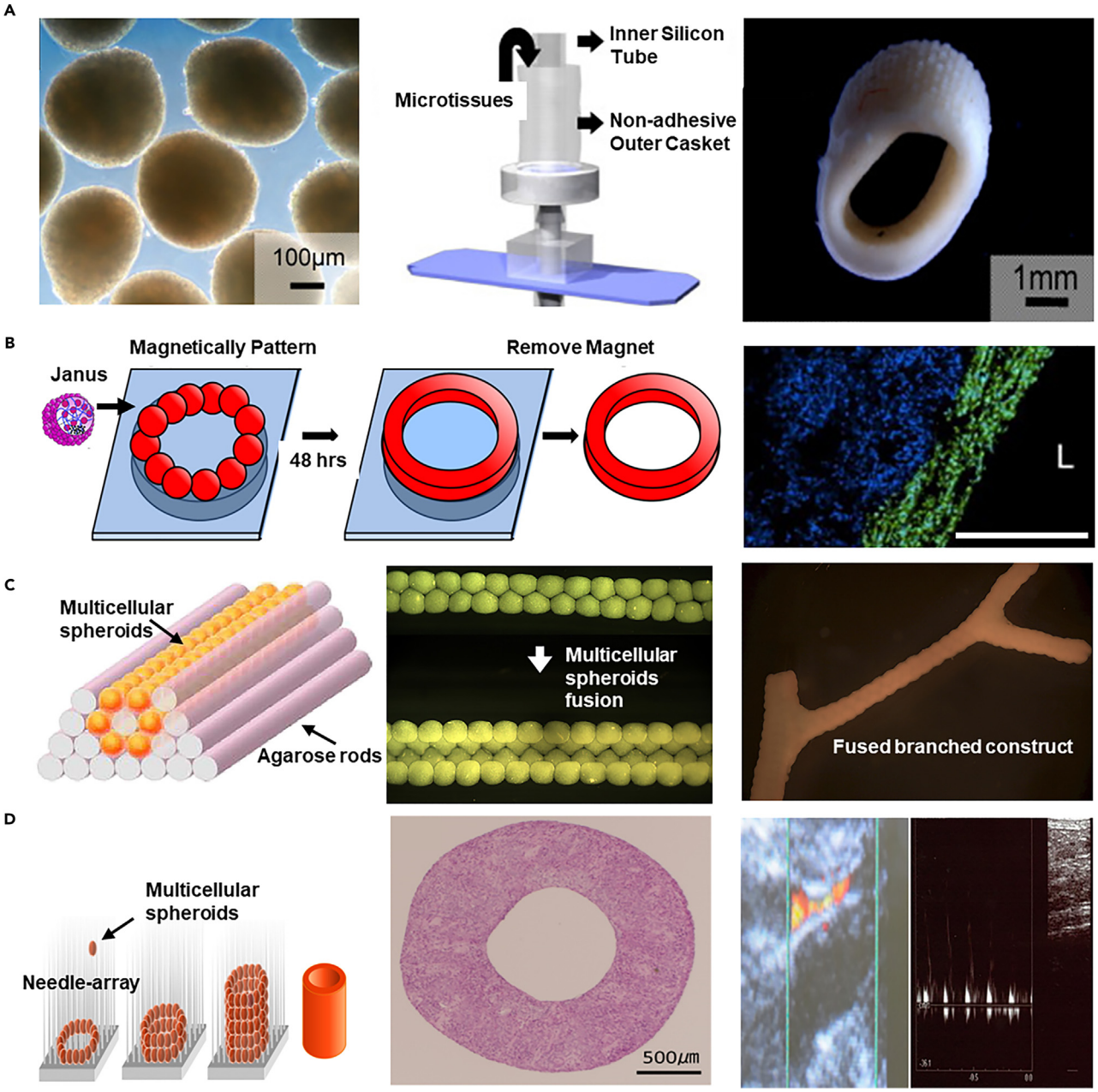

Figure 9. Representative AEs constructed by cell spheroids technology

(A) Primary human arterial fibroblast microtissues cultivated in 60-well plates are assembled using a mold integrated with a bioreactor, allowing the casting of microtissues, which after 14 days of flow and mechanical stimulation, reorganize along the vascular axis to form small-diameter blood vessels. Copyright 2010, Elsevier, Reproduced with permission.[177]

(B) Magnetic nanoparticles incorporated into cell spheroids facilitate the assembly of thousands of magnetic cell aggregates into vascular tissue constructs (scale bar 500 μm). Copyright 2014, Elsevier, Reproduced with permission.[178]

(C) Employing 3D bioprinting technology, multicellular spheroids are assembled onto a molded agarose rod template, resulting in the formation of branched, large vascular-like tubular structures within 5–7 days post-assembly. Copyright 2009, Elsevier, Reproduced with permission.[179]

(D) The Kenzan bioprinting method fabricates small-diameter vascular grafts by stacking cell spheroids onto a needle and integrating 3D bioprinting technology. Copyright 2015, Public Library of Science, Reproduced with permission.[180]

support is compensated for by employing additional cell layers and extended maturation periods to mitigate the adverse effects on *in vivo* applications. However, in the pursuit of these improvements, it is also necessary to consider the increased material consumption and time costs.

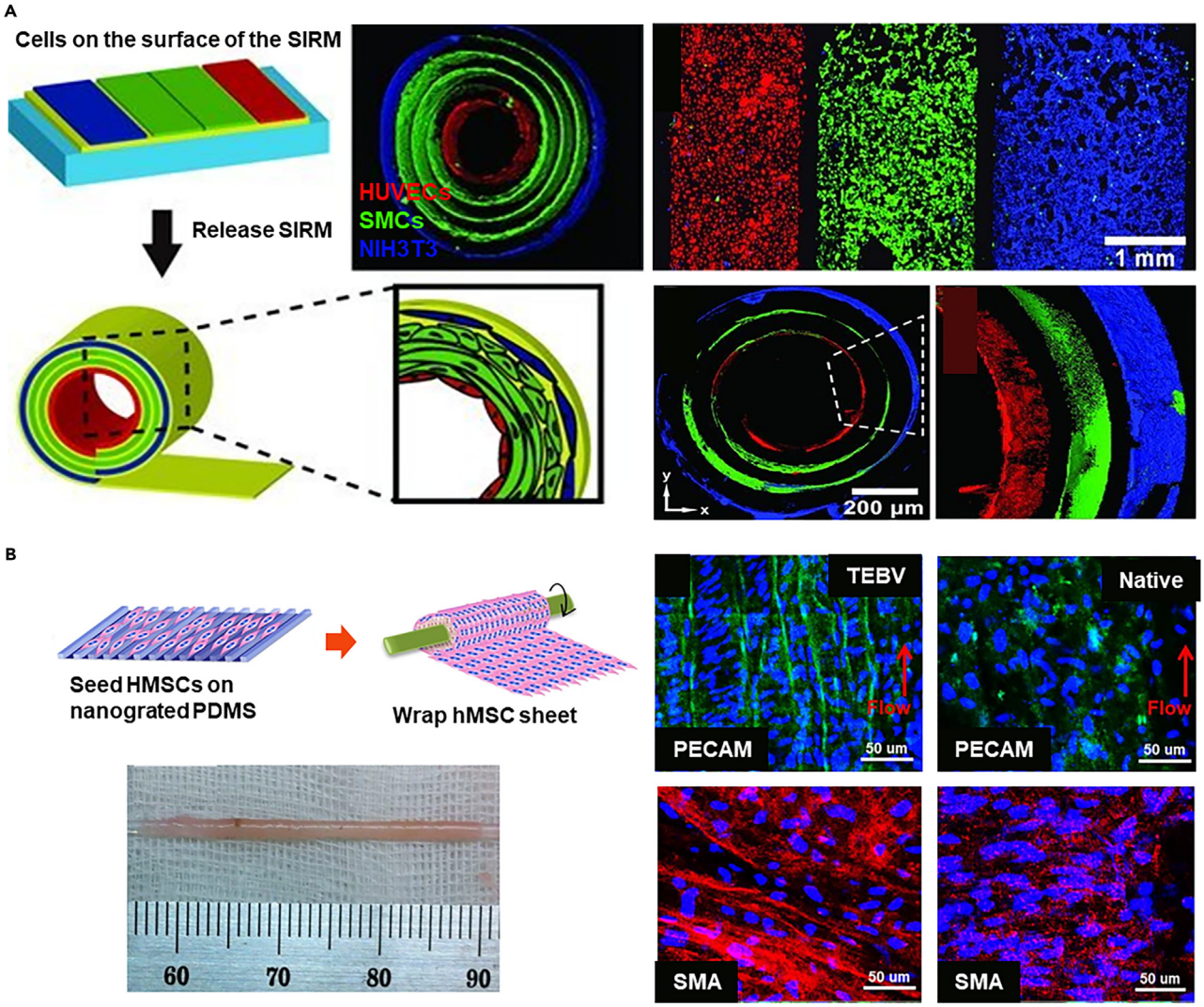

Figure 10. Representative AEs constructed by cell sheets

(A) The SIRM technique fabricates vascular grafts with an inner diameter ranging from 10μm to 2mm, replicating the complex patterns of HUVECs, SMCs, and NIH3T3 fibroblasts within 3D tubes through a rolling process, simulating their natural *in vivo* arrangement. Copyright 2012, Wiley-VCH, Reproduced with permission.[191]

(B) Employing nanogrid alignment and layer-by-layer wrapping techniques, a tubular construct with circumferentially aligned HMSCs is fabricated, achieving uniform integration and alignment of HMSCs through perfusion maturation. Copyright 2015, Springer Nature, Reproduced with permission.[192]

Despite the innovative approach, cell sheets technology faces challenges including high costs, complex processes, and total production cycles for clinical availability (an average of 7.5 months).[193–195] Issues such as inconsistent layer fusion due to individual variability, inadequate ECM formation in the short term, and difficulty in controlling graft geometry and mechanical properties during the rolling process affect the production consistency and quality of the grafts.

Bioengineered dynamic devices as arterial equivalents

Regular AEs, while dimensionally and structurally biomimetic, struggle with real-time imaging due to the thick arterial walls (>500μm) that reduce imaging quality and necessitate sectioning and staining. This complicates the observation of cellular responses and the integration of advanced technologies such as AI and big data, which could foster significant breakthroughs. Additionally, constructing these arterial models is both time-consuming and expensive, requiring vast quantities of cells and materials. Bioengineered dynamic devices, including organ-on-a-chip systems, are showing potential as tools for modeling human arteries. These devices may offer advantages over traditional isometric artery equivalents in certain aspects of pathological research and drug screening by providing more dynamic and physiologically relevant environments.

Using advanced bioengineered techniques, dynamic devices, such as vasculature-on-a-chip,[196] capture complex flow dynamics seen in blood vessels, including the unstable turbulent flows at bifurcations and curvatures that expose ECs to uneven shear forces, potentially triggering inflammation and AS.[197] Various specialized vascular structures have been engineered to replicate these conditions, including stenosis-integrated channel,[198] continues channel,[199] branching channels,[200] H-shaped channel,[201] T-shaped channel,[202] Y-shaped channel,[203] using techniques such as sacrificial molding,[204,205] self-assembled microfluidic approaches,[206,207] stereolithography, and 3D printing.[208] Yet, these models often feature only a single endothelial layer, limiting their ability to explore interactions under pathological conditions between ECs and SMCs, which failed to be categorized as AEs.

In contrast, the AE dynamic device (or artery on-a-chip) should recapitulate the key physiological features of the human artery. For instance, the chip should reconstruct the dual-layered structure that separately embeds ECs and SMCs, resembling the characteristics of an arterial wall.[209] Moreover, the device should be also able to provide physiological hemodynamic signals such as flow rate, flow pattern, and shear stress.

Various techniques are being explored to construct and shape rapidly perfused vascular-such as structures. Fabrication of biomimetic vascular structures via coaxial bioprinting techniques, utilizing a 3D-printed porous poly(ethylene glycol) diacrylate mold. SMCs are suspended within a bioink composed of a mixture of alginate, gelatin methacryloyl (GelMA), and fibronectin, and then coaxially printed to obtain cell-laden vascular constructs (Figure 11A).[210] After perfusion culture for seven days to allow for SMC stretching and migration to form a confluent layer on the luminal surface, HUVECs are seeded. Cultivation results in a multi-layered structure resembling that of a blood vessel.

To manufacture the *in silico* AEs with multi-layered structures and tunable geometries, 3D bioprinting has demonstrated its unique advantages. The construction of multi-layered arterial models with varying internal diameters and wall thicknesses was accomplished using sequentially suspended 3D bioprinting technique technology.[211] These models are capable of simulating the complex geometric structures of human arteries (Figure 11B). The models were utilized for the *in vitro* simulation of the pathophysiological processes initiating arterial diseases. Through co-culture and the simulation of fluid shear stress (FSS), the models mature into functionally competent vascular tissues. By simulating local turbulent flow, researchers observed the onset of EC dysfunction, which is a hallmark of arterial diseases.

Except for the cellular interaction and hemodynamics, another essential dynamic factor is the arterial vascular wall undergoing continuous contraction and relaxation. The mechanical stimulation of the model through isometric and isotonic forces is crucial for the pathophysiological functions of the vasculature. This can be simulated using mechanisms of elongation and contraction. Techniques such as using a Transwell elastic membrane[213] and vacuum control,[214] have been employed to induce deformation. In *in vitro* models of early AS (Figure 11C),[212] elastic membranes embedded in microfluidic devices can transmit non-uniform strain to VSMCs, ECs, and adhering monocytes. Stretchable microfluidic devices have been used to induce foam cell formation under low-density lipoproteins (LDL) and stretch treatments and to evaluate the efficacy of atorvastatin in inhibiting foam cell formation.

Overall, the integration of microfluidic and bioengineered technologies in dynamic AE devices offers a promising pathway for advancing the simulation of human vascular structures and diseases, combining the simplicity, usability, and cost-effectiveness of traditional models with enhanced physiological relevance.

BIOENGINEERED CLINICAL-LEVEL ARTERIAL EQUIVALENTS

Artificial blood vessels are imperative tools for clinical surgeries such as coronary artery bypass, treating peripheral artery disease, and establishing hemodialysis access. The implantation conditions, which involve exposure to strong blood pressure and a complex physiological microenvironment, require vascular grafts to meet stringent specifications. For successful implantation, these grafts must not only resist and facilitate effective blood flow but also maintain structural integrity post-implantation. They need to demonstrate essential mechanical properties such as ultimate tensile strength, suture retention, burst pressure, compliance, and long-term fatigue resistance qualities that are comparable to natural arteries to withstand physiological blood flow conditions, as detailed in section 2.2.1. Additionally, to ensure long-term success and integration with host tissue, the grafts must also mitigate risks such as acute thrombosis and stenosis and support cellular functions.[215] This involves incorporating anti-thrombogenic properties and promoting endothelialization to prevent immune rejection, ensuring the grafts perform effectively in clinical settings. This section highlights recent progress in bioengineered AEs that have brought these technologies closer to clinical application, marking significant advancements in the field.

Before progressing to clinical trials, vascular grafts require thorough preclinical evaluations using both small (e.g., mice,[216] rabbit[217,218]) and large animal models (e.g., dog,[170] pig,[219] sheep[169]). These evaluations primarily assess biocompatibility, mechanical properties, and initial biological responses to ensure the safety, efficacy, and functionality of the grafts. While many studies have reported on the *in vivo* performances of bioengineered AEs using animal models, the number of these products that advance to clinical trials remains limited. This discrepancy highlights the challenges in translating preclinical successes into clinically approved therapies.

The first bioengineered vascular graft used for the clinical trial was developed in 2001 using the cells from peripheral venous walls expanded and seeded onto biodegradable polymer conduits made from PCL and PLA copolymers, which was reinforced with woven PGA (diameter 10 mm, length 20 mm, thickness 1 mm). These scaffold-based tissue-engineered vascular grafts were implanted in a four-year-old patient with a single ventricle and pulmonary atresia,[220] successfully recanalizing an occluded pulmonary artery without postoperative complications. Subsequent checks showed full patency and no adverse changes seven months post-implantation.

As an innovative way for bioengineered vascular grafts, cell sheet technology has been used for autologous small-diameter arterial reconstruction in adults.[188] Fibroblasts isolated from patient's own body are cultured to deposit ECM, forming detachable viscous sheets. These

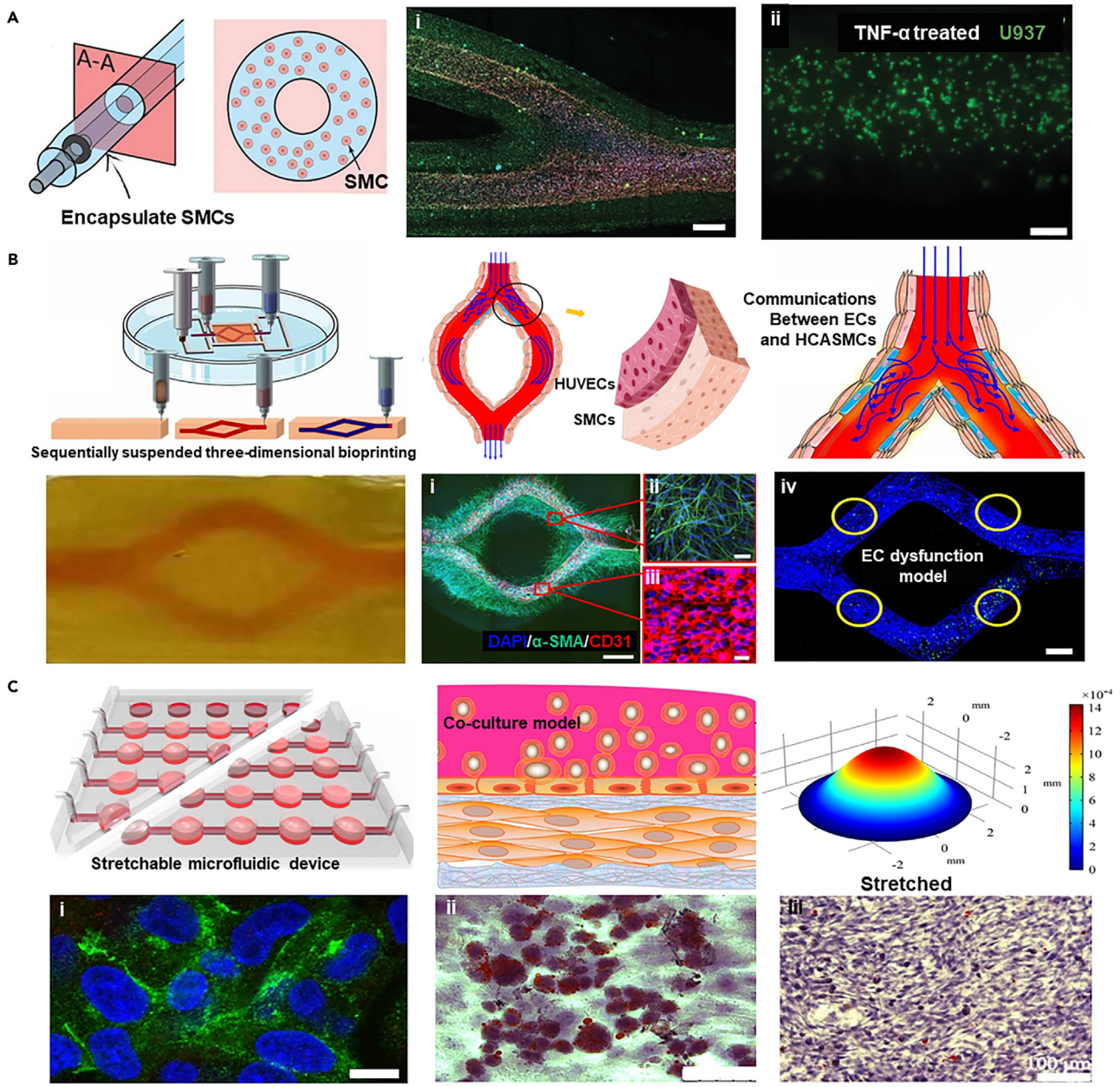

Figure 11. Representative bioengineered dynamic devices as AEs

(A) Utilizing 3D-printed porous PEGDA molds and coaxial bioprinting techniques, a biomimetic vascular construct loaded with SMCs and HUVECs is fabricated, which after perfusion culture forms a multi-layered structure, demonstrating potential in modeling pathophysiological conditions such as AS, upon TNF-α stimulation (scale bar i: 500 μm, ii: 100 μm). Copyright 2022, Wiley-VCH, Reproduced with permin.[210]

(B) Sequential suspension 3D-printed multi-layered arterial models, matured into functional vascular tissues through simulated blood flow and co-culture, are utilized for the observation of early arterial disease markers (scale bar i: 1 mm, ii, iii: 50 μm, iv: 500 μm). Copyright 2023, IOP Publishing, Reproduced with permission.[211]

(C) The elastic membrane within a microfluidic device transmits uneven strain to cells in an *ex vivo* AS model, assessing the efficacy of atorvastatin in inhibiting foam cell formation under LDL and strain conditions (scale bar i: 10 μm, ii: 50 μm, iii: 100 μm). Copyright 2019, Springer Nature, Reproduced with permission.[212]

sheets are layered to create three-dimensional tissues or organs, exhibiting physiological mechanical strength. A clinical trial involving 10 end-stage renal disease patients demonstrated these grafts could withstand arterial pressures for at least three months, with ongoing monitoring up to 13 months post-implantation. However, the lengthy production time of 7.5 months poses significant logistical and cost challenges.[221] Utilizing off-the-shelf allogeneic grafts that have been cryopreserved at −80°C post-production as an alternative can mitigate the potential

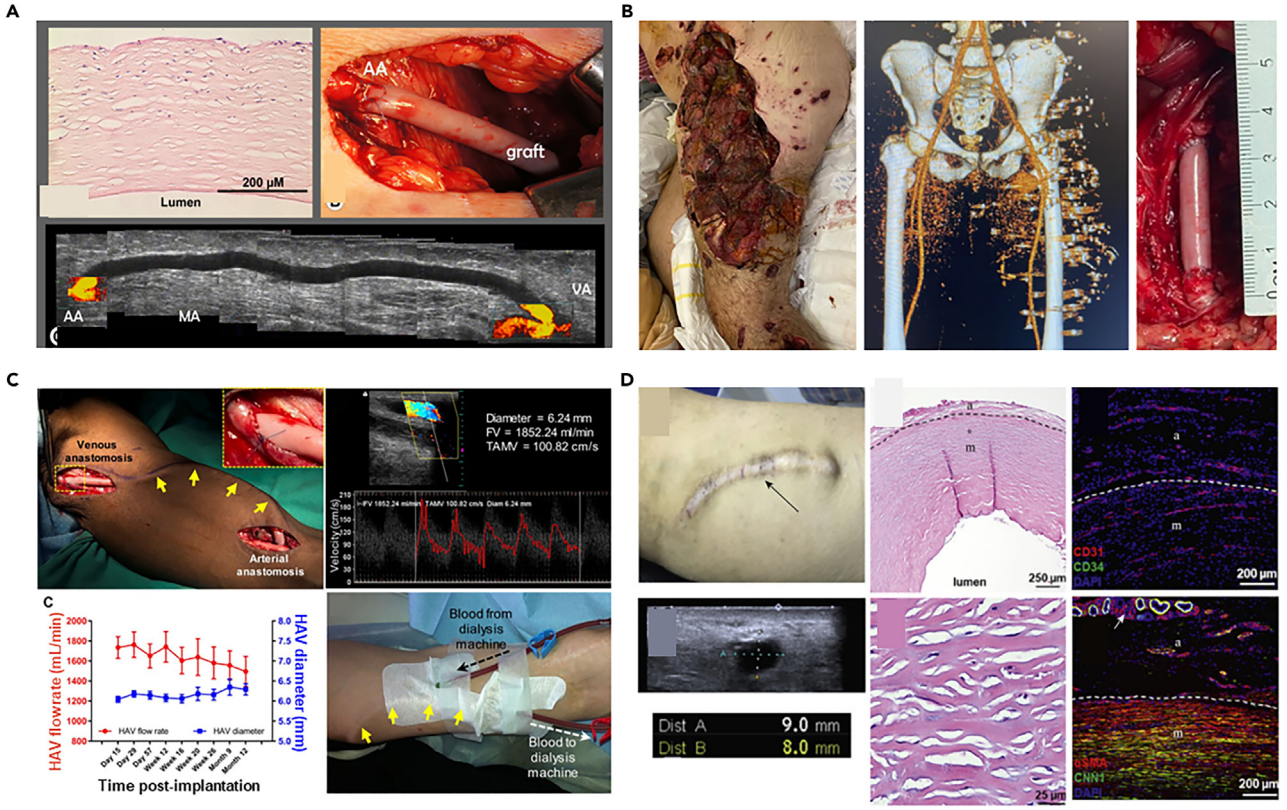

Figure 12. Blood vessel grafts for clinic trials

(A) An 80-year-old female patient with a history of glomerulonephritis and coronary artery disease underwent the implantation of an allogeneic tissue-engineered vascular graft for the first time, with post-transplant Doppler ultrasound showing stable blood flow, normal blood indices, and negative panel reactive antibody tests, indicating successful arteriovenous anastomosis. Copyright 2014, Mosby, Reproduced with permission.[193]

(B) A 29-year-old Ukrainian male combat casualty sustained a blast injury to the left leg, with pre-operative computed tomography (CT) scans revealing shrapnel in the vascular bundle adjacent to the inguinal ligament; subsequent repair of the left common femoral artery using HAVs was uncomplicated by infection during follow-up. Copyright 2023, Elsevier, Reproduced with permission.[222]

(C) Patients with end-stage renal disease successfully underwent the implantation of HAVs as an arteriovenous conduit, with postoperative monitoring showing no significant changes in vascular performance, and the HAVs proved suitable for repeated cannulation for hemodialysis. Copyright 2019, American Association for the Advancement of Science, Reproduced with permission.[223]

(D) A case study of six-year hemodialysis using a HAV demonstrates that despite a long-term puncture and catheter dilation, vascular ultrasound, and immunofluorescence staining indicate the preservation of structural and functional integrity of the HAVs. Copyright 2022, Elsevier, Reproduced with permission.[224]

risks associated with autologous tissue harvesting and processing, thereby demonstrating the feasibility and safety of transitioning to an allogeneic nonliving platform (Figure 12A).[193]

Another representative case for clinical application is the decellularized bioengineered biotubes. In particular, human VSMCs were seeded onto a PGA mesh scaffold within a bioreactor. Once the constructs have completed their *ex vivo* growth, they are decellularized to eliminate the potential for immunogenicity, thereby yielding human acellular vessels (HAVs) that possess compositional, biomechanical properties, and structural similarities to native vascular tissue. Currently, HAVs are undergoing clinical trials in adults for vascular trauma and end-stage renal disease (ESRD) requiring hemodialysis.[225] Thirteen patients lacking autologous venous repair have been treated with HAVs to repair various arteries, including the superficial femoral artery, common femoral artery (Figure 12B), popliteal artery, and brachial artery.[222] All HAVs maintained primary patency, with no reported infections or amputations of the affected limbs, and no reports of HAVs conduit infections or mechanical failures during a 7-month follow-up period. For ESRD patients unsuitable for fistulas, hemodialysis access grafts represent the optimal choice for chronic hemodialysis. HAV implantation in the arms of adults with ESRD for hemodialysis has been reported (Figure 12C).[223] After five years, one patient maintained primary patency, and ten patients maintained secondary patency (Figure 12D).[224] Considering deaths and dropouts, the secondary patency rate at five years was 58.2%, providing ESRD patients with a long-term, durable, and functional hemodialysis access.

Despite advances, bioengineered AEs as vascular grafts face challenges such as the need for faster production and increased availability. Issues with mechanical properties in small-caliber grafts also persist, necessitating further development of reinforced *in vivo* engineered

vessels. Moreover, graft infections remain a serious concern, requiring ongoing research to optimize treatment strategies. Epidemiologic studies, treatment evaluations, diagnostic imaging, and immunomodulatory approaches are crucial for addressing these challenges. Continued post-marketing clinical follow-up is essential to confirm the safety and efficacy of vascular grafts in clinical settings, enhancing therapeutic options for patients.

IN VITRO ARTERIAL DISEASE MODELS

Biomedical research is experiencing a significant shift toward human disease modeling, driven by the development of bioengineered tissue equivalents. These models circumvent the limitations posed by species differences in animal models and enable detailed studies of disease pathogenesis and the interactions of key factors by isolating the complex microenvironment of the disease sites.[226–228] This approach holds immense potential for advancing the understanding of arterial diseases and enhancing drug discovery efforts. This section will focus on the *in vitro* disease models of arterial diseases including AS, stenosis, and aneurysm.

In vitro atherosclerosis model

To study of atherosclerosis mechanisms, a prerequisite is to build a human artery model that can reveal the interplays between ECs, SMCs, and ECM. The bioengineered AE mimics the anatomy and structure of the arterial wall and thus can intrinsically contribute to recapitulating the cellular activities and responses during atherosclerosis. To monitor the dynamic changes that occurred in the relevant process, the models adaptable to real-time bioimaging are desired. In this regard, the artery-on-a-chip devices exhibited unparalleled advantages over other bioengineered AEs. A new microfluidic-based arterial wall on-a-chip simulates the intima-media interface of the artery by co-culturing ECs and SMCs, as well as precisely controlling the ECM microenvironment (Figure 13A).[229] This chip uses collagen and basement membrane matrix to simulate the sub-endothelial ECM layer and the 3D culture environment of SMCs in two hydrogel channels, respectively. Upon such a model, the study investigated the effects of vitamin D ($1,25(OH_)_2D_3$) and metformin in alleviating monocyte-endothelial cell adhesion and smooth muscle cell migration induced by cytokines.

Upon the construction of functional AE, the successful establishment of an atherosclerotic model relies on the recreation of core pathogenic signals to stimulate cells for the recapitulation of the downstream initiation and progression events. To achieve this, a viable method uses enzymatically modified low-density lipoprotein (eLDL) and TNF-α to mimic the atherosclerotic environment under physiological shear stress in tissue engineered blood vessels (Figure 13B).[105] This leads to the activation of ECs, accumulation of monocytes, formation of foam cells, and expression of pro-inflammatory cytokines. Enzymatically modified LDL is more effective in producing foam cells than oxidized LDL,[233] causing the upregulation of ICAM-1 and E-selectin in ECs, and readily inducing foam cell formation in SMCs[234] and macrophages.[233] The model also exhibits partial disease regression upon eLDL removal, demonstrating the potential for discovering effective therapies.

Besides the biochemical signals, the pathogenesis of AS is also significantly influenced by biomechanical stimuli, such as mechanical stress and hemodynamics that play critical roles in regulating cellular behaviors. The bioengineered AEs with regular geometries cultivated under laminar flows may face difficulties in providing these biomechanical signals. Therefore, the dynamic AE devices have gained attention. A stretchable microfluidic chip has been designed, integrating a microfluidic layer, an elastic PDMS membrane, and a pneumatic layer, which successfully constructed an early AS model capable of applying both FSS and cyclic stretch (Figure 13C).[230] By precisely controlling fluid flow and vacuum, this model simulated the mechanical hemodynamic signals presenting in arteries. Equipped with this design, the study demonstrated the unique advantages of this model over 2D culture conditions in drug evaluation and screening. The AE device facilitated the discovery of new evidence regarding the cytotoxicity of the clinical drug probucol underscores its indispensable role in drug evaluation and screening, which is conducive to the study of the pathological microenvironment on the early occurrence of atherosclerosis.

Another innovative *in vitro* atherosclerosis model has utilized a creative 3D suspended coaxial bioprinting technology to construct a three-layered AE with controllable geometry and dimensions (Figure 13D).[231] The model employed vascular tissue-derived decellularized extracellular matrix as a supportive bath for gel-embedded 3D bioprinting, as well as adjusting the printing path and speed to precisely control the inner diameter and wall thickness of the AE. This method overcame the limitations of traditional vascular models in terms of structural stability and geometric control. The direct construction of vascular models with adjustable geometries, including normal, stenotic, and tortuous shapes, simulated the complex hemodynamics in AS.

Currently, most of the established *in vitro* models focus on the early stage of atherosclerosis which only contributes to understanding the pathological mechanism of disease initiation (e.g., endothelial dysfunction, SMCs phenotype switch, foam cell formation). A few efforts attempted to construct the flatforms that are capable of recreating the build-up of atherosclerotic plaques composed of fibrose caps and necrotic cores, which are more significant to evaluate medications for the disease recovery.

Among the limited relevant reports, a three-dimensional human fibrous atherosclerotic plaque model that simulates late-stage atherosclerosis, marking an important step in the continuous study from lipid deposition and inflammatory responses in the early stages of the disease to plaque formation in the later stages (Figure 13E).[232] Using the suspension droplet technique, spherical cellular structures that include a fibrous cap and necrotic core can be created using myeloid cells, THP-1 cells, and human umbilical vein smooth muscle cells. These cell spheres form structures in three-dimensional space that are similar to atherosclerotic plaques, mimicking the inflammatory microenvironment in the vascular subendothelial space induced by cholesterol. Despite this, the model still has some shortcomings, such as the precise control of the composition, structure, and dimension of the plaques, as well as the consistent production, which limits their applications for high-throughput screening.

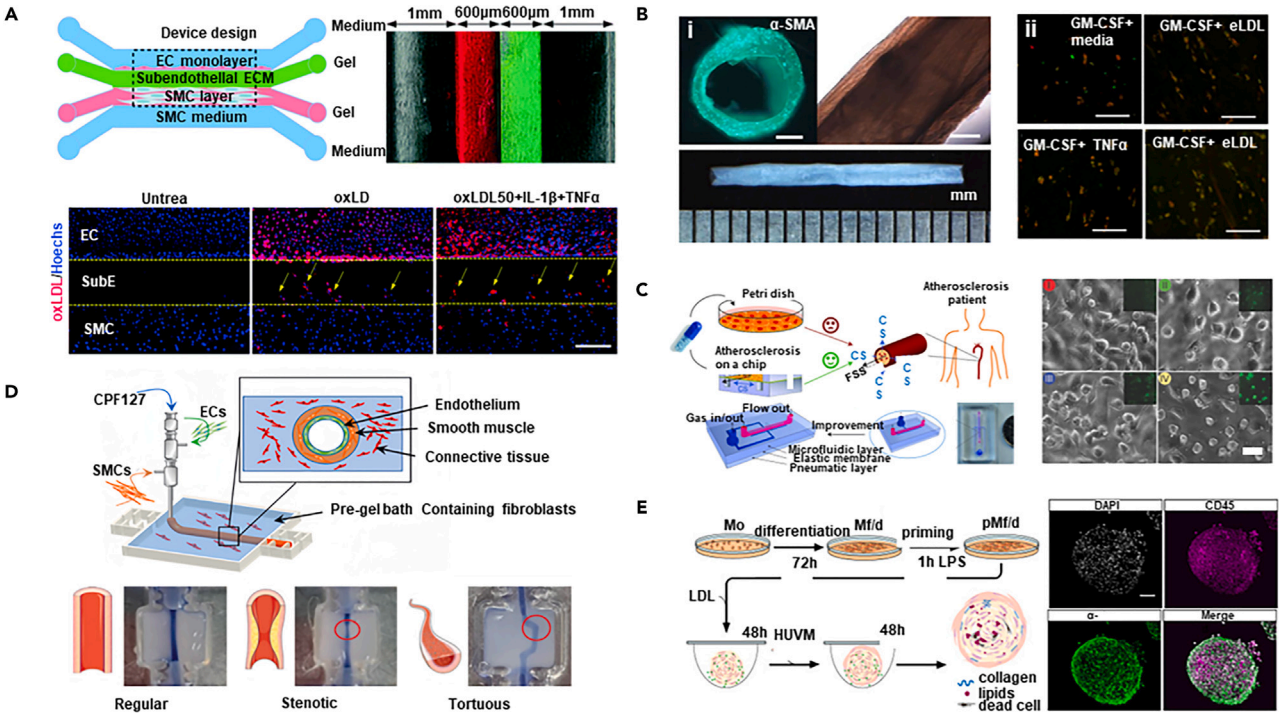

Figure 13. Representative examples that show *in vitro* model of AS

(A) The micro-engineered arterial wall device on a chip and the migration of SMCs under hyperlipidemic conditions (scale bar 500 μm). Copyright 2021, Royal Society of Chemistry, Reproduced with permission.[229]

(B) Bright-field views of TEBVs, along with macrophage polarization within these vessels following exposure to eLDL and/or TNF-α (scale bar i: 200 μm, ii: 100 μm). Copyright 2020, Springer Nature, Reproduced with permission.[105]

(C) The structure of the early-stage AS model and the actual model, as well as the morphology of HUVECs under different mechanical stimuli (scale bar 50 μm). Copyright 2016, Wiley-VCH, Reproduced with permission.[230]

(D) The schematic diagram illustrates the fabrication process of triple-layered AEs, resulting in arterial constructs with controlled geometries. Copyright 2021, Wiley-VCH, Reproduced with permission.[231]

(E) The schematic view depicts the assembly of ps-plaques with blood-derived cells and reveals the inner architecture of these ps-plaques (scale bar 100 μm). Copyright 2018, Elsevier Science, Reproduced with permission.[232]

In vitro thrombosis model

Thrombus formation is closely associated with changes in hemodynamics. The forces exerted by blood flow have a significant impact on thrombus size, growth rate, and the risk of embolization. Therefore, reconstructing the morphological characteristics of arteries at sites prone to thrombosis is crucial for exploring the mechanisms of thrombosis. Currently, a variety of technologies have enabled the creation of arterial models that include stenotic, convoluted, and branched structures. In one representative study, quantitative image analysis was utilized to reconstruct the thrombus formation process in an *in vitro* thrombosis model with controllable stenotic and cross-sectional profiles of the channel using partially cured PDMS (Figure 14A).[235] Through image analysis, this study reveals that physical flow has a significant impact on thrombus formation, with narrower channels accelerating the growth of the thrombus and increasing the risk of embolism. The starting point and growth characteristics of the thrombus are influenced by the way it forms, showing different growth rates and binding strengths. Combined with image analysis technology, the analysis of the thrombosis process was quantitatively analyzed, and the accuracy of the study of the thrombosis growth pattern was improved by dividing the image into multiple sub-parts.

Additionally, the *in vitro* models can also be utilized to investigate the relationship between thrombus structure and the formation of high shear stress as well as Von Willebrand factor (VWF) platelet strings.[198] By creating a stenotic artery model that replicates high shear flow conditions akin to atherosclerotic arteries, researchers used whole blood to induce macroscopic thrombi in a collagen-coated setup. The study demonstrated that the thrombus has a complex structure, which includes slender platelet aggregates (strings) that converge into a dense mass near the apex and abruptly end in the expansion region, forming a thrombus with microchannels that allow some blood flow through the main body of the thrombus. The findings of the study elucidate how VWF platelet strings rapidly form and bridge the vascular lumen under high shear stress, and how this structure can quickly create an occlusion or hemostasis while maintaining a certain porosity, offering the potential for the delivery of thrombolytic agents to the core of the thrombus.

Besides abnormal hemodynamics, thrombus formation involves complex interactions between cells, extracellular matrix (ECM), and biomolecules. Microfluidic chip technology provides a controlled platform to simulate these processes, accurately replicating blood flow and

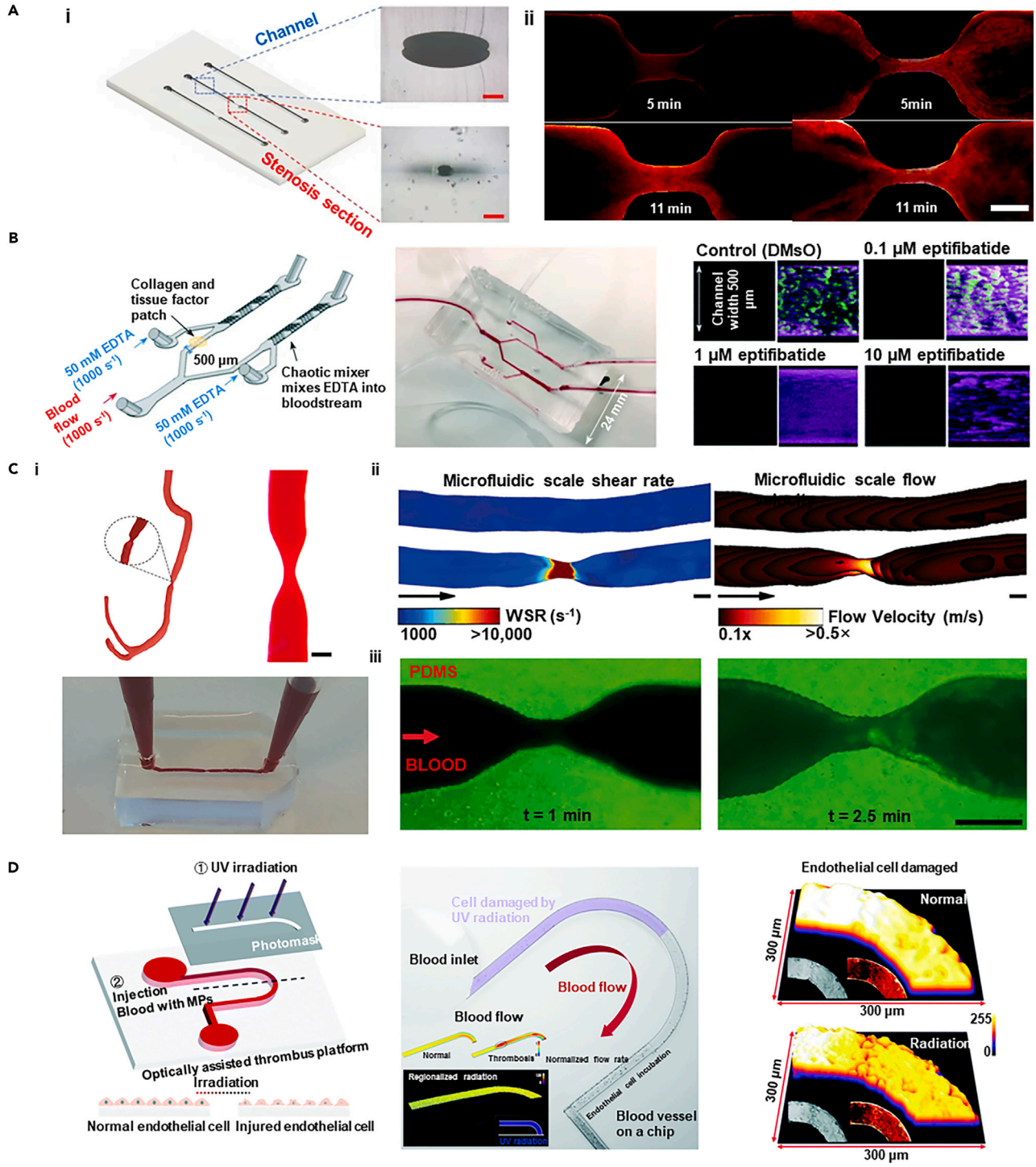

Figure 14. Representative examples that show *in vitro* model of thrombosis

(A) The 3D model and cross-section of a channel with an 83.73% stenosis, along with the observation of thrombus growth through image analysis (scale bar i: 100 μm, ii: 200 μm). Copyright 2022, Springer Nature, Reproduced with permission.[235]

(B) A schematic of a "single channel" and "pressure relief" device, alongside the development of an innovative "EDTA-quenched" device with a chaotic mixer, demonstrates the eptifibatide's concentration-dependent inhibition of platelet accumulation over time. Copyright 2021, Royal Society of Chemistry, Reproduced with permission.[203]

Figure 14. *Continued*

(C) Three-dimensional models of healthy and stenotic vessels, finite element analysis of rheological parameters in 67% occluded vessels, and microfluidic chips with endothelialised 3D geometries perfused with re-calcified citrated whole blood (scale bar i: 370 μm, ii,iii: 200 μm). Copyright 2017, Springer Nature, Reproduced with permission.[236]

(D) The optically assisted thrombus platform features a schematic diagram, finite element analysis of flow fields in normal and thrombus-forming conditions, regional radiation-induced ECs damage, light intensity distribution, and micrograph imaging of the damaged cells. Copyright 2022, Royal Society of Chemistry, Reproduced with permission.[199]

vascular structures. For instance, an "occlusive thrombosis-on-a-chip" device, using collagen and biochemical factors, initiates platelet activation and thrombus formation to assess antithrombotic drugs (Figure 14B).[203] This study highlights that distal coagulation in such devices may obscure drug effects, offering a valuable tool for the early-stage evaluation of antithrombotic drugs.

3D bioprinting technology, which allows for the fabrication of detailed three-dimensional structures, is playing an increasingly significant role in the development of *in vitro* thrombosis models.[237–241] It replicates vascular stenosis and branching while integrating ECM and cells to simulate thrombotic processes accurately. One innovative approach combines CT angiography (CTA) data, Stereolithography (SLA) 3D printing, and microfluidic technology to produce *in vitro* models of both healthy and stenotic arteries (Figure 14C).[236] SLA 3D printing is used to create molds for PDMS chips, facilitating Computational Fluid Dynamics (CFD) simulations to analyze flow patterns and shear rates. The ECs are cultured on microfluidic chips, and blood flow studies reveal how vascular geometry affects platelet aggregation. Additionally, a biomimetic thrombosis-on-a-chip model, developed through 3D sacrificial bioprinting, features microchannels embedded in GelMA hydrogel and lined with ECs.[242] This model induces thrombus formation and simulates thrombus dissolution with tPA perfusion, providing precise control over microchannel architecture and mimicking thrombus dynamics effectively.

While *in vitro* thrombosis models are crucial for understanding disease mechanisms and evaluating responses to drugs and medical devices, these devices are also helpful in observing and quantifying how environmental risks impact blood coagulation, platelet behavior, and thrombus stability. For instance, an *in vitro* model based on microfluidic technology has been developed to study the potential toxicity of microplastics (MPs) to the vascular system (Figure 14D).[199] This model uses an optically assisted thrombus platform to simulate thrombus formation due to localized tissue injury induced by photothermal irradiation. Key aspects include microfluidic chip fabrication, endothelial cell seeding, and precise endothelial damage via ultraviolet irradiation. The study integrates optofluidic techniques with microfluidic technology to visualize and record MP invasion into thrombi, revealing that MPs strongly bind to fibrinogen and platelets, reducing fibrin-platelet binding strength and increasing the risk of thrombus shedding.

In vitro aneurysm model

For aneurysms, hemodynamic studies are crucial due to their direct link with arterial bulge growth and rupture. As aneurysms develop, the complex and variable hemodynamic conditions within them, such as flow patterns, velocity, volume, wall pressure, and shear stress, change dynamically. Additionally, aneurysms exhibit unique shapes and structures in different patients, manifesting personalized features. CFD models are employed to simulate blood flow in designed microvessels or channels to explore circulatory system diseases.[243] An innovative approach involves 3D printing with water-soluble resin to create patient-specific cerebral artery phantom models (Figure 15A).[244] Using a desktop SLA 3D printer and low-cost resin, intricate sacrificial molds are produced and then cast in transparent silicone rubber (PDMS) to create high-resolution, full-scale cerebral arterial models. These water-soluble resin molds, which dissolve completely, allow for the creation of PDMS models with high transparency and adjustable elasticity, enhancing blood flow modeling and CFD simulation validation.

Frontier technologies, such as AI, are becoming crucial in developing predictive models for the effects of blood flow dynamics on aneurysms. Through advanced deep learning algorithms and computational fluid dynamics, AI can analyze complex blood flow patterns and predict their impact on aneurysm walls, leading to more accurate diagnostic and treatment strategies. A notable development in this field is the Artificial Intelligence Velocimetry (AIV) framework (Figure 15B).[245] This framework employs Physics-Informed Neural Networks to combine 2D image data from microfluidic experiments with the principles of fluid dynamics. It reconstructs three-dimensional blood flow fields without needing predefined boundary conditions by minimizing a loss function those accounts for data mismatches, physical law residuals, and boundary condition discrepancies. AIV technology addresses some challenges associated with traditional approaches to evaluating blood flow in intricate vascular networks. It serves as a beneficial diagnostic and monitoring aid for conditions such as diabetic retinopathy, particularly in scenarios where experimental data is limited.

Despite significant advancements in hemodynamic studies, the formation and progress of aneurysms also involve complex biological processes including inflammatory responses, cellular differentiation, and ECM degradation. Therefore, to fully explore the pathogenesis of aneurysms, it is crucial to develop *in vitro* models that not only reconstruct hemodynamics but also include functional vascular tissues. One study advanced this field by investigating cellular behavior under varying shear stress conditions, simulating hemodynamics using an enhanced liquid-assisted injection molding technique coupled with mechanically tuned GelMA hydrogel to reconstruct a 3D cerebral aneurysm model with clinically relevant dimensions (Figure 15C).[246] The model employed a catheter with a 2.7 mm diameter and a compliant balloon with a 10 mm diameter, with water volume controlled to adjust the neck width and bulge diameter of the aneurysm model. Within the GelMA hydrogel, ECs and SMCs were cultured to mimic the vascular endothelium. This setup, under physiologically relevant hemodynamics, allows for the simulation of ECs forming a monolayer on SMCs under physiological wall shear stress, and the permeation of large molecules in the bulge area due to the absence of an endothelial layer. It effectively demonstrates differential cellular behaviors in response to the dynamic conditions in both the simulated vessel and aneurysm bulge regions.

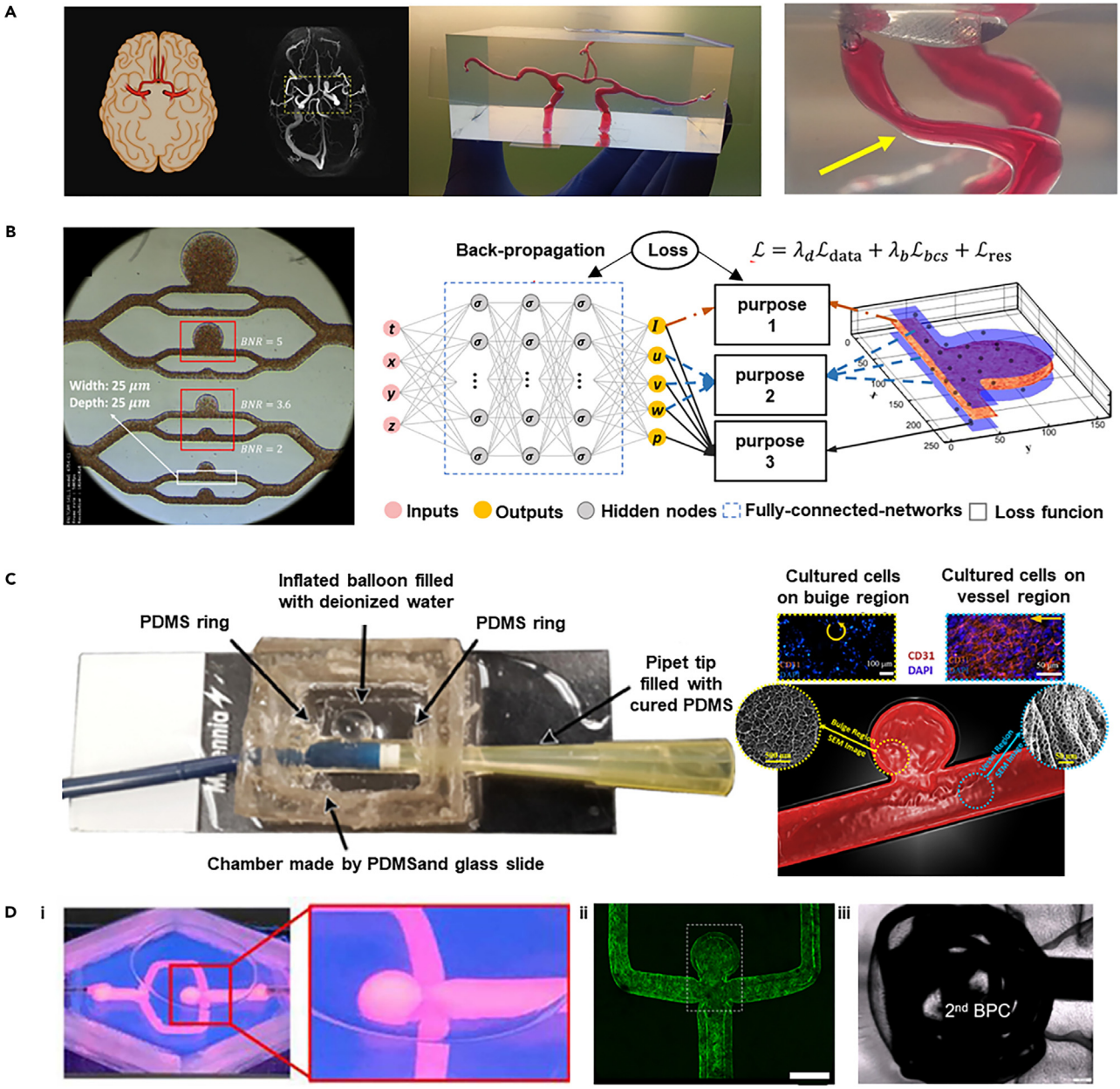

Figure 15. Representative examples that show *in vitro* model of aneurysm

(A) A full-scale PDMS phantom model replicates the anterior cerebral arterial network, with the model's surface capable of being depressed by a thumb to simulate effects on the vasculature. Copyright 2022, Nature Publishing Group, Reproduced with permission.[244]

(B) The schematic diagram of AIV, microscopic images from the microfluidic platform showing a microaneurysm on a chip, and 3D predictions of the AIV in the microaneurysm channel with a branching number ratio of 5 collectively illustrate the visual presentation of this study. Copyright 2021, National Academy of Sciences, Reproduced with permission.[245]

(C) An *in vitro* human IA model is fabricated using a modified liquid-assisted injection molding approach, resulting in cellularized IA models for study. Copyright 2021, Elsevier BV, Reproduced with permission.[246]

(D) The *in vitro* aneurysm vessel structure undergoes perfusion, followed by the endothelialization of the printed vessels containing aneurysms, and is monitored through brightfield micrographs during the insertion of bare platinum coil via an endovascular microcatheter (scale bar ii: 2 mm). Copyright 2019, John Wiley & Sons, Reproduced with permission.[247]

The complexity of aneurysms, characterized by their irregular shapes, varying wall thicknesses, and diverse hemodynamic features, presents challenges for traditional modeling methods, which struggle with intricate structures. To overcome these challenges, innovative biofabrication strategies are crucial for enhancing the morphological and structural similarity of models to that of their natural counterparts.

A pioneering study bioengineered an *in vitro* aneurysm model with intricate structures using 3D printing technology (Figure 15D).[247] This model employs a gelatin-fibrin hydrogel as the printing medium for supporting the subsequent formation of endothelium on the luminal wall, closely mimicking the physiological mechanical properties of blood vessel walls. Owing to the transparency of the 3D printing platform, the model facilitates the use of microcatheters to introduce detachable coils into the 3D-printed aneurysms, enabling the monitoring of static plasma clotting within the aneurysm sac and around the coils. This setup not only assesses the biocompatibility and hemostatic efficacy of embolic devices but also provides valuable insights into the risk of aneurysm rupture and hemodynamic responses post-treatment.

CONCLUSION AND FUTURE PERSPECTIVES

Bioengineered AEs have contributed to incremental advancements in the field of vascular graft development and have provided valuable insights into pathogenic mechanisms. These AEs mimic the mechanical properties of native arteries, emulate the physiological functions of vascular tissues, and recapitulate the pathological responses of cells. A variety of innovative technologies including electrospinning, 3D bioprinting, decellularization, and self-assembly have been applied to promote the performances of AEs in different ways, such as improving biocompatibility, reducing immune reaction, and refining the mechanical characteristics.

Beyond grafting, AEs have significantly contributed to the advancement of *in vitro* disease modeling, providing simulations of human arterial conditions with improved accuracy compared to traditional models. Technologies such as microfluidic chips and 3D bioprinting enable the development of disease models for atherosclerosis, thrombosis, and aneurysms, enhancing our understanding of these conditions and facilitating the testing of new treatments. These advancements not only deepen our understanding of arterial diseases but also support the development of more effective therapeutic strategies.

Looking forward, the sophistication of AEs is expected to increase, aiming to closely mimic the intricate structures of natural arteries, including features such as the tunica adventitia, elastic membranes, and microvessels. This enhancement is crucial for both practical applications *in vivo* and for more effective *in vitro* disease modeling. Advanced biomaterials and biofabrication techniques such as 3D bioprinting and electrospinning will play pivotal roles in creating AEs with tunable mechanical properties that closely match those of native arteries, thereby improving their durability, functionality, and integration with host tissues.

In terms of 3D bioprinting, although the deposition in yielding-stress suspension baths has emerged as an effective way to construct complex tissues by enhancing spatial fidelity,[248,249] such a methodology highly relies on the careful selection or formulation of the bath materials. Therefore, new innovative strategies remain required to fully unleash the potential of 3D bioprinting technique for constructing sophisticated tissue equivalents. For instance, microgravity or zero-gravity environment is envisioned to largely accelerate the development of tissue equivalents possessing more elaborate structures and functionalities, given that the levitation state of cells, materials, or bioinks helps to avoid the structure collapse and composition precipitation that usually occur under gravitational environment. Due to these advantages, 3D bioprinting in space has evoked increasing interest in tissue engineering and regenerative medicine.[250–253] More importantly, microgravity may cause diverse space diseases and health abnormality.[254–257] Thus, it is meaningful to understand the changes in structures and functions of proteins, cells, or tissues under microgravity conditions.[258–260] The exploitation of 3D bioprinted AEs and other tissue equivalents as *in vitro* models provides an attractive strategy to resolve these fundamental problems under simulated microgravity or in space,[261–263] enabling tackling unknown medical challenges and offering promising healthcare solutions for astronauts in space.

Personalized medicine stands at the forefront of modern healthcare innovations, and the development of personalized AEs aligns perfectly with this trend. By using patient-derived cells and genetic profiling, AEs can be tailored to individual patients, enhancing compatibility and effectiveness. This personalized approach not only promises greater success in implantations but also transforms AEs into powerful platforms for studying vascular diseases in a patient-specific manner.

The convergence of AEs with cutting-edge techniques such as smart materials, AI, and big data is set to revolutionize the field of precise medicine. Smart materials that respond to environmental stimuli can be integrated into AEs to provide dynamic control over their physiological properties and biological responses.[264–266] These advantages could endow the grafts with additional functions, such as tunable stem cell/drug delivery, dynamically defined mechanical properties, triggerable biodegradation, and promoted host cell integration, which might be meaningful to developing advanced regenerative strategies. AI and big data analytics can be used to analyze the vast amounts of data generated by *in vitro* models, identifying patterns and biomarkers that are indicative of disease progression and treatment efficacy. This integration will enable the development of accurately predictive *in vitro* arterial disease models, facilitating the discovery of new therapeutic targets and the evaluation of drug candidates.

In addition, despite these advancements, the clinical urgency for vascular grafts demands the development of readily available off-the-shelf AEs. To meet this need, advances in automation and scalability in AE production are essential. Techniques such as robotic-assisted 3D bioprinting could facilitate rapid, consistent manufacturing of AEs, ensuring timely availability for clinical use.[267,268] The development of standardized protocols for the storage and preservation of cell-laden AEs will also be crucial for maintaining their viability and functionality. For *in vitro* disease models, the demand for high-throughput testing is driving the need for scalable models that can be produced and analyzed in large numbers. This will be essential for drug screening, target identification, and the study of disease mechanisms, ultimately accelerating the pace of medical discovery and innovation.

ACKNOWLEDGMENTS

This work is supported by the National Natural Science Foundation of China (32201126, 32311540144), the Beijing Natural Science Foundation (7232344), the National Research Foundation of Korea (NRF) grant funded by the Korean Government (MSIT) (No2022R1A5A2027161), and Beijing Institute of Technology Teli Young Fellow Program (RCPT-20220029).

AUTHOR CONTRIBUTIONS

Xi Luo: Writing – original draft. **Zherui Pang:** Writing – original draft. **Jinhua Li:** Writing – review and editing. **Minjun Anh:** Data curation. **Byoung Soo Kim:** Writing – review and editing. **Ge Gao:** Supervision, funding acquisition, and conceptualization.

DECLARATION OF INTERESTS

The authors have no competing interests or financial ties to disclose.

REFERENCES

1. Pittman, R.N. (2013). Oxygen transport in the microcirculation and its regulation. Microcirculation *20*, 117–137. https://doi.org/10.1111/micc.12017.
2. Viles-Gonzalez, J.F., Fuster, V., and Badimon, J.J. (2004). Atherothrombosis: A widespread disease with unpredictable and life-threatening consequences. Eur. Heart J. *25*, 1197–1207. https://doi.org/10.1016/j.ehj.2004.03.011.
3. Matta, A.G., Yaacoub, N., Nader, V., Moussallem, N., Carrie, D., and Roncalli, J. (2021). Coronary artery aneurysm: A review. World J. Cardiol. *13*, 446–455. https://doi.org/10.4330/wjc.v13.i9.446.
4. Flora, G.D., and Nayak, M.K. (2019). A brief review of cardiovascular diseases, associated risk factors and current treatment regimes. Curr. Pharmaceut. Des. *25*, 4063–4084. https://doi.org/10.2174/1381612825666190925163827.
5. Jagannathan, R., Patel, S.A., Ali, M.K., and Narayan, K.M.V. (2019). Global updates on cardiovascular disease mortality trends and attribution of traditional risk factors. Curr. Diabetes Rep. *19*, 44. https://doi.org/10.1007/s11892-019-1161-2.
6. Naegeli, K.M., Kural, M.H., Li, Y., Wang, J., Hugentobler, E.A., and Niklason, L.E. (2022). Bioengineering human tissues and the future of vascular replacement. Circ. Res. *131*, 109–126. https://doi.org/10.1161/CIRCRESAHA.121.319984.
7. Boland, J., and Long, C. (2021). Update on the inflammatory hypothesis of coronary artery disease. Curr. Cardiol. Rep. *23*, 6. https://doi.org/10.1007/s11886-020-01439-2.
8. Li, M.-X., Wei, Q.-Q., Mo, H.-L., Ren, Y., Zhang, W., Lu, H.-J., and Joung, Y.K. (2023). Challenges and advances in materials and fabrication technologies of small-diameter vascular grafts. Biomater. Res. *27*, 58. https://doi.org/10.1186/s40824-023-00399-2.
9. L'Heureux, N., Dusserre, N., Marini, A., Garrido, S., de la Fuente, L., and McAllister, T. (2007). Technology insight: the evolution of tissue-engineered vascular grafts from research to clinical practice. Nat. Clin. Pract. Cardiovasc. Med. *4*, 389–395. https://doi.org/10.1038/ncpcardio0930.
10. Doh, G., Kim, B., Lee, D., Yoon, J., Lim, S., Han, Y.S., and Eo, S. (2021). Hemodynamic principles in free tissue transfer: vascular changes at the anastomosis site. Arch. Hand Microsurg. *26*, 285–292. https://doi.org/10.12790/ahm.21.0118.
11. Camasão, D.B., and Mantovani, D. (2021). The mechanical characterization of blood vessels and their substitutes in the continuous quest for physiological-relevant performances. A critical review. Mater. Today. Bio *10*, 100106. https://doi.org/10.1016/j.mtbio.2021.100106.
12. Weinberg, C.B., and Bell, E. (1986). A blood vessel model constructed from collagen and cultured vascular cells. Science *231*, 397–400. https://doi.org/10.1126/science.2934816.
13. Maina, R.M., Barahona, M.J., Finotti, M., Lysyy, T., Geibel, P., D'Amico, F., Mulligan, D., and Geibel, J.P. (2018). Generating vascular conduits: from tissue engineering to three-dimensional bioprinting. Innov. Surg. Sci. *3*, 203–213. https://doi.org/10.1515/iss-2018-0016.
14. Pashneh-Tala, S., MacNeil, S., and Claeyssens, F. (2016). The tissue-engineered vascular graft-past, present, and future. Tissue Eng., Part B *22*, 68–100. https://doi.org/10.1089/ten.teb.2015.0100.
15. Gao, G., Kim, H., Kim, B.S., Kong, J.S., Lee, J.Y., Park, B.W., Chae, S., Kim, J., Ban, K., Jang, J., et al. (2019). Tissue-engineering of vascular grafts containing endothelium and smooth-muscle using triple-coaxial cell printing. Appl. Phys. Rev. *6*, 041402. https://doi.org/10.1063/1.5099306.
16. Bosch-Rué, E., Delgado, L.M., Gil, F.J., and Perez, R.A. (2020). Direct extrusion of individually encapsulated endothelial and smooth muscle cells mimicking blood vessel structures and vascular native cell alignment. Biofabrication *13*, 015003. https://doi.org/10.1088/1758-5090/abbd27.
17. Zaragoza, C., Gomez-Guerrero, C., Martin-Ventura, J.L., Blanco-Colio, L., Lavin, B., Mallavia, B., Tarin, C., Mas, S., Ortiz, A., and Egido, J. (2011). Animal models of cardiovascular diseases. J. Biomed. Biotechnol. *2011*, 497841. https://doi.org/10.1155/2011/497841.
18. Kastora, S.L., Eley, J., Gannon, M., Melvin, R., Munro, E., and Makris, S.A. (2022). What went wrong with VEGF-A in peripheral arterial disease? A systematic review and biological insights on future therapeutics. J. Vasc. Res. *59*, 381–393. https://doi.org/10.1159/000527079.
19. Luna, D.J., R Pandian, N.K., Mathur, T., Bui, J., Gadangi, P., Kostousov, V.V., Hui, S.-K.R., Teruya, J., and Jain, A. (2020). Tortuosity-powered microfluidic device for assessment of thrombosis and antithrombotic therapy in whole blood. Sci. Rep. *10*, 5742. https://doi.org/10.1038/s41598-020-62768-4.
20. Park, W., Lee, J.-S., Gao, G., Kim, B.S., and Cho, D.-W. (2023). 3D bioprinted multilayered cerebrovascular conduits to study cancer extravasation mechanism related with vascular geometry. Nat. Commun. *14*, 7696. https://doi.org/10.1038/s41467-023-43586-4.
21. Humphrey, J.D., and Schwartz, M.A. (2021). Vascular mechanobiology: homeostasis, adaptation, and disease. Annu. Rev. Biomed. Eng. *23*, 1–27. https://doi.org/10.1146/annurev-bioeng-092419-060810.
22. Varzideh, F., Mone, P., and Santulli, G. (2022). Bioengineering strategies to create 3D cardiac constructs from human induced pluripotent stem cells. Bioengineering *9*, 168. https://doi.org/10.3390/bioengineering9040168.
23. Zhang, Y., Li, X.S., Guex, A.G., Liu, S.S., Müller, E., Malini, R.I., Zhao, H.J., Rottmar, M., Maniura-Weber, K., Rossi, R.M., and Spano, F. (2017). A compliant and biomimetic three-layered vascular graft for small blood vessels. Biofabrication *9*, 025010. https://doi.org/10.1088/1758-5090/aa6bae.
24. Eble, J.A., and Niland, S. (2009). The extracellular matrix of blood vessels. Curr. Pharmaceut. Des. *15*, 1385–1400. https://doi.org/10.2174/138161209787846757.
25. Jouda, H., Larrea Murillo, L., and Wang, T. (2022). Current progress in vascular engineering and its clinical applications. Cells *11*, 493. https://doi.org/10.3390/cells11030493.
26. Sumpio, B.E., Riley, J.T., and Dardik, A. (2002). Cells in focus: endothelial cell. Int. J. Biochem. Cell Biol. *34*, 1508–1512. https://doi.org/10.1016/S1357-2725(02)00075-4.
27. Zihni, C., Mills, C., Matter, K., and Balda, M.S. (2016). Tight junctions: from simple barriers to multifunctional molecular gates. Nat. Rev. Mol. Cell Biol. *17*, 564–580. https://doi.org/10.1038/nrm.2016.80.
28. Ross, R. (1993). The pathogenesis of atherosclerosis: a perspective for the 1990s. Nature *362*, 801–809. https://doi.org/10.1038/362801a0.
29. Aquino, J.B., Sierra, R., and Montaldo, L.A. (2021). Diverse cellular origins of adult blood vascular endothelial cells. Dev. Biol. *477*, 117–132. https://doi.org/10.1016/j.ydbio.2021.05.010.
30. Xu, Y., Yazbeck, R., and Duan, C. (2021). Anomalous mechanosensitive ion transport in nanoparticle-blocked nanopores. J. Chem. Phys. *154*, 224702. https://doi.org/10.1063/5.0046086.
31. Niklason, L., and Dai, G. (2018). Arterial venous differentiation for vascular bioengineering. Annu. Rev. Biomed. Eng. *20*, 431–447. https://doi.org/10.1146/annurev-bioeng-062117-121231.
32. Chan-Park, M.B., Shen, J.Y., Cao, Y., Xiong, Y., Liu, Y., Rayatpisheh, S., Kang, G.C.-W., and Greisler, H.P. (2009). Biomimetic control of vascular smooth muscle cell morphology and phenotype for functional tissue-engineered small-diameter blood vessels. J. Biomed. Mater. Res. *88*, 1104–1121. https://doi.org/10.1002/jbm.a.32318.
33. Brozovich, F.V., Nicholson, C.J., Degen, C.V., Gao, Y.Z., Aggarwal, M., and Morgan, K.G. (2016). Mechanisms of vascular smooth muscle contraction and the basis for pharmacologic treatment of smooth muscle disorders. Pharmacol. Rev. *68*, 476–532. https://doi.org/10.1124/pr.115.010652.
34. Shi, J., Yang, Y., Cheng, A., Xu, G., and He, F. (2020). Metabolism of vascular smooth muscle cells in vascular diseases. Am. J. Physiol. Heart Circ. Physiol. *319*, H613–H631.

https://doi.org/10.1152/ajpheart.00220.2020.
35. Sarelius, I., and Pohl, U. (2010). Control of muscle blood flow during exercise: local factors and integrative mechanisms. Acta Physiol. *199*, 349–365. https://doi.org/10.1111/j.1748-1716.2010.02129.x.
36. Palikuqi, B., Nguyen, D.H.T., Li, G., Schreiner, R., Pellegata, A.F., Liu, Y., Redmond, D., Geng, F., Lin, Y., Gómez-Salinero, J.M., et al. (2020). Adaptable haemodynamic endothelial cells for organogenesis and tumorigenesis. Nature *585*, 426–432. https://doi.org/10.1038/s41586-020-2712-z.
37. Frismantiene, A., Philippova, M., Erne, P., and Resink, T.J. (2018). Smooth muscle cell-driven vascular diseases and molecular mechanisms of VSMC plasticity. Cell. Signal. *52*, 48–64. https://doi.org/10.1016/j.cellsig.2018.08.019.
38. Synofzik, J., Heene, S., Jonczyk, R., and Blume, C. (2024). Ink-structing the future of vascular tissue engineering: a review of the physiological bioink design. Biodes. Manuf. *7*, 181–205. https://doi.org/10.1007/s42242-024-00270-w.
39. Nerem, R.M., and Seliktar, D. (2001). Vascular tissue engineering. Annu. Rev. Biomed. Eng. *3*, 225–243. https://doi.org/10.1146/annurev.bioeng.3.1.225.
40. Majesky, M.W. (2015). Adventitia and perivascular cells. Arterioscler. Thromb. Vasc. Biol. *35*, e31–e35. https://doi.org/10.1161/ATVBAHA.115.306088.
41. Xu, F., Ji, J., Li, L., Chen, R., and Hu, W. (2007). Activation of adventitial fibroblasts contributes to the early development of atherosclerosis: A novel hypothesis that complements the "Response-to-Injury Hypothesis" and the "Inflammation Hypothesis". Med. Hypotheses *69*, 908–912. https://doi.org/10.1016/j.mehy.2007.01.062.
42. Xu, F., Liu, Y., Shi, L., Liu, W., Zhang, L., Cai, H., Qi, J., Cui, Y., Wang, W., and Hu, Y. (2015). NADPH oxidase p47phox siRNA attenuates adventitial fibroblasts proliferation and migration in apoE(-/-) mouse. J. Transl. Med. *13*, 38. https://doi.org/10.1186/s12967-015-0407-2.
43. Cheng, J., Jia, Z., Guo, H., Nie, Z., and Li, T. (2019). Delayed burst of a gel balloon. J. Mech. Phys. Solid. *124*, 143–158. https://doi.org/10.1016/j.jmps.2018.10.010.
44. Ciszek, B., Cieślicki, K., Krajewski, P., and Piechnik, S.K. (2013). Critical pressure for arterial wall rupture in major human cerebral arteries. Stroke *44*, 3226–3228. https://doi.org/10.1161/STROKEAHA.113.002370.
45. Matsumoto, T., Sugita, S., and Nagayama, K. (2016). Tensile properties of smooth muscle cells, elastin, and collagen fibers. In Vascular Engineering: New Prospects of Vascular Medicine and Biology with a Multidiscipline Approach, K. Tanishita and K. Yamamoto, eds. (Springer Japan), pp. 127–140. https://doi.org/10.1007/978-4-431-54801-0_7.
46. Roussis, P.C., Giannakopoulos, A.E., Charalambous, H.P., Demetriou, D.C., and Georghiou, G.P. (2015). Dynamic behavior of suture-anastomosed arteries and implications to vascular surgery operations. Biomed. Eng. Online *14*, 1. https://doi.org/10.1186/1475-925X-14-1.
47. Lim, S.Y., Yeo, M.S.-W., Nicoli, F., Ciudad, P., Constantinides, J., Kiranantawat, K., Sapountzis, S., Ho, A.C.W., and Chen, H.-C. (2015). End-to-patch anastomosis for microvascular transfer of free flaps with small pedicle. J. Plast. Reconstr. Aesthetic Surg. *68*, 559–564. https://doi.org/10.1016/j.bjps.2014.11.020.
48. Wayne Causey, M., and Eichler, C. (2014). Infrainguinal bypass for critical limb ischemia: tips and tricks. Semin. Vasc. Surg. *27*, 59–67. https://doi.org/10.1053/j.semvascsurg.2014.11.001.
49. Seo, M.H., Kim, S.M., Myoung, H., and Lee, J.H. (2013). Influence of vascular twisting on the supermicroanastomosis of superficial inferior epigastric artery. J. Craniofac. Surg. *24*, 1772–1780. https://doi.org/10.1097/SCS.0b013e31829024bc.
50. Xue, L., Lu, Y., Qiu, W., Zhou, H., Zhang, G., Jin, Z., Lin, M., Chen, H., Rui, Z., and Zheng, Y. (2009). Surgical experience of refined 3-cuff technique for orthotopic small-bowel transplantation in rat: a report of 270 cases. Am. J. Surg. *198*, 110–121. https://doi.org/10.1016/j.amjsurg.2008.07.057.
51. Sonoda, H., Takamizawa, K., Nakayama, Y., Yasui, H., and Matsuda, T. (2001). Small-diameter compliant arterial graft prosthesis: Design concept of coaxial double tubular graft and its fabrication. J. Biomed. Mater. Res. *55*, 266–276. https://doi.org/10.1002/1097-4636(20010605)55:3<266::AID-JBM1014>3.0.CO;2-C.
52. El-Kurdi, M.S., Hong, Y., Stankus, J.J., Soletti, L., Wagner, W.R., and Vorp, D.A. (2008). Transient elastic support for vein grafts using a constricting microfibrillar polymer wrap. Biomaterials *29*, 3213–3220. https://doi.org/10.1016/j.biomaterials.2008.04.009.
53. Konig, G., McAllister, T.N., Dusserre, N., Garrido, S.A., Iyican, C., Marini, A., Fiorillo, A., Avila, H., Wystrychowski, W., Zagalski, K., et al. (2009). Mechanical properties of completely autologous human tissue engineered blood vessels compared to human saphenous vein and mammary artery. Biomaterials *30*, 1542–1550. https://doi.org/10.1016/j.biomaterials.2008.11.011.
54. Bikia, V., Rovas, G., Pagoulatou, S., and Stergiopulos, N. (2021). Determination of aortic characteristic impedance and total arterial compliance from regional pulse wave velocities using machine learning: an *in-silico* study. Front. Bioeng. Biotechnol. *9*, 649866. https://doi.org/10.3389/fbioe.2021.649866.
55. Mulvany, M.J. (2002). Small artery remodeling in hypertension. Curr. Hypertens. Rep. *4*, 49–55. https://doi.org/10.1007/s11906-002-0053-y.
56. Langille, B.L., and O'Donnell, F. (1986). Reductions in arterial diameter produced by chronic decreases in blood flow are endothelium-dependent. Science *231*, 405–407. https://doi.org/10.1126/science.3941904.
57. Huang, A.H., and Niklason, L.E. (2014). Engineering of arteries *in vitro*. Cell. Mol. Life Sci. *71*, 2103–2118. https://doi.org/10.1007/s00018-013-1546-3.
58. Gu, S.Z., Ahmed, M.E., Huang, Y., Hakim, D., Maynard, C., Cefalo, N.V., Coskun, A.U., Costopoulos, C., Maehara, A., Stone, G.W., et al. (2024). Comprehensive biomechanical and anatomical atherosclerotic plaque metrics predict major adverse cardiovascular events: A new tool for clinical decision making. Atherosclerosis *390*, 117449. https://doi.org/10.1016/j.atherosclerosis.2024.117449.
59. Francis, S.E., Tu, J., Qian, Y., and Avolio, A.P. (2013). A combination of genetic, molecular and haemodynamic risk factors contributes to the formation, enlargement and rupture of brain aneurysms. J. Clin. Neurosci. *20*, 912–918. https://doi.org/10.1016/j.jocn.2012.12.003.
60. Mohan, D., Munteanu, V., Coman, T., and Ciurea, A.V. (2015). Genetic factors involves in intracranial aneurysms-actualities. J. Med. Life *8*, 336–341. https://www.ncbi.nlm.nih.gov/pmc/articles/PMC4556916/.
61. Tsao, P.S., Lewis, N.P., Alpert, S., and Cooke, J.P. (1995). Exposure to shear stress alters endothelial adhesiveness. Circulation *92*, 3513–3519. https://doi.org/10.1161/01.CIR.92.12.3513.
62. Peiffer, V., Sherwin, S.J., and Weinberg, P.D. (2013). Does low and oscillatory wall shear stress correlate spatially with early atherosclerosis? A systematic review. Cardiovasc. Res. *99*, 242–250. https://doi.org/10.1093/cvr/cvt044.
63. Kono, K., Fujimoto, T., and Terada, T. (2014). Proximal stenosis may induce initiation of cerebral aneurysms by increasing wall shear stress and wall shear stress gradient. Int. J. Numer. Method. Biomed. Eng. *30*, 942–950. https://doi.org/10.1002/cnm.2637.
64. Chiu, J.-J., and Chien, S. (2011). Effects of disturbed flow on vascular endothelium: pathophysiological basis and clinical perspectives. Physiol. Rev. *91*, 327–387. https://doi.org/10.1152/physrev.00047.2009.
65. Dolan, J.M., Kolega, J., and Meng, H. (2013). High wall shear stress and spatial gradients in vascular pathology: a review. Ann. Biomed. Eng. *41*, 1411–1427. https://doi.org/10.1007/s10439-012-0695-0.
66. Gallo, G., Volpe, M., and Savoia, C. (2021). Endothelial dysfunction in hypertension: current concepts and clinical implications. Front. Med. *8*, 798958. https://doi.org/10.3389/fmed.2021.798958.
67. Ma, J., Li, Y., Yang, X., Liu, K., Zhang, X., Zuo, X., Ye, R., Wang, Z., Shi, R., Meng, Q., and Chen, X. (2023). Signaling pathways in vascular function and hypertension: molecular mechanisms and therapeutic interventions. Signal Transduct. Targeted Ther. *8*, 168. https://doi.org/10.1038/s41392-023-01430-7.
68. Climie, R.E., Alastruey, J., Mayer, C.C., Schwarz, A., Laucyte-Cibulskiene, A., Voicehovska, J., Bianchini, E., Bruno, R.M., Charlton, P.H., Grillo, A., et al. (2023). Vascular ageing: moving from bench towards bedside. Eur. J. Prev. Cardiol. *30*, 1101–1117. https://doi.org/10.1093/eurjpc/zwad028.
69. Kong, P., Cui, Z.-Y., Huang, X.-F., Zhang, D.-D., Guo, R.-J., and Han, M. (2022). Inflammation and atherosclerosis: signaling pathways and therapeutic intervention. Signal Transduct. Targeted Ther. *7*, 131. https://doi.org/10.1038/s41392-022-00955-7.
70. Libby, P. (2012). Inflammation in atherosclerosis. Arterioscler. Thromb. Vasc. Biol. *32*, 2045–2051. https://doi.org/10.1161/ATVBAHA.108.179705.
71. Fan, J., and Watanabe, T. (2022). Atherosclerosis: Known and unknown. Pathol. Int. *72*, 151–160. https://doi.org/10.1111/pin.13202.
72. Fan, J., and Watanabe, T. (2003). Inflammatory reactions in the pathogenesis of atherosclerosis. J. Atherosclerosis

Thromb. *10*, 63–71. https://doi.org/10.5551/jat.10.63.

73. Falk, E. (2006). Pathogenesis of atherosclerosis. J. Am. Coll. Cardiol. *47*, C7–C12. https://doi.org/10.1016/j.jacc.2005.09.068.
74. Bentzon, J.F., Otsuka, F., Virmani, R., and Falk, E. (2014). Mechanisms of plaque formation and rupture. Circ. Res. *114*, 1852–1866. https://doi.org/10.1161/CIRCRESAHA.114.302721.
75. Klouche, M., May, A.E., Hemmes, M., Meßner, M., Kanse, S.M., Preissner, K.T., and Bhakdi, S. (1999). Enzymatically modified, nonoxidized ldl induces selective adhesion and transmigration of monocytes and T-lymphocytes through human endothelial cell monolayers. Arterioscler. Thromb. Vasc. Biol. *19*, 784–793. https://doi.org/10.1161/01.ATV.19.3.784.
76. Tomaiuolo, M., Brass, L.F., and Stalker, T.J. (2017). Regulation of platelet activation and coagulation and its role in vascular injury and arterial thrombosis. Interv. Cardiol. Clin. *6*, 1–12. https://doi.org/10.1016/j.iccl.2016.08.001.
77. Bettiol, A., Galora, S., Argento, F.R., Fini, E., Emmi, G., Mattioli, I., Bagni, G., Fiorillo, C., and Becatti, M. (2022). Erythrocyte oxidative stress and thrombosis. Expet Rev. Mol. Med. *24*, e31. https://doi.org/10.1017/erm.2022.25.
78. Li, P., Ma, X., and Huang, G. (2024). Understanding thrombosis: the critical role of oxidative stress. Hematology *29*, 2301633. https://doi.org/10.1080/16078454.2023.2301633.
79. Lipp, S.N., Niedert, E.E., Cebull, H.L., Diorio, T.C., Ma, J.L., Rothenberger, S.M., Stevens Boster, K.A., and Goergen, C.J. (2020). Computational hemodynamic modeling of arterial aneurysms: a mini-review. Front. Physiol. *11*, 454. https://doi.org/10.3389/fphys.2020.00454.
80. Fennell, V.S., Kalani, M.Y.S., Atwal, G., Martirosyan, N.L., and Spetzler, R.F. (2016). Biology of saccular cerebral aneurysms: a review of current understanding and future directions. Front. Surg. *3*, 43. https://doi.org/10.3389/fsurg.2016.00043.
81. Starke, R.M., Chalouhi, N., Ding, D., Raper, D.M.S., McKisic, M.S., Owens, G.K., Hasan, D.M., Medel, R., and Dumont, A.S. (2014). Vascular smooth muscle cells in cerebral aneurysm pathogenesis. Transl. Stroke Res. *5*, 338–346. https://doi.org/10.1007/s12975-013-0290-1.
82. Frösen, J., Cebral, J., Robertson, A.M., and Aoki, T. (2019). Flow-induced, inflammation-mediated arterial wall remodeling in the formation and progression of intracranial aneurysms. Neurosurg. Focus *47*, E21. https://doi.org/10.3171/2019.5.FOCUS19234.
83. Hernandez-Sanchez, D., Comtois-Bona, M., Muñoz, M., Ruel, M., Suuronen, E.J., and Alarcon, E.I. (2024). Manufacturing and validation of small-diameter vascular grafts: A mini review. iScience *27*, 109845. https://doi.org/10.1016/j.isci.2024.109845.
84. Helms, F., Haverich, A., Böer, U., and Wilhelmi, M. (2021). Transluminal compression increases mechanical stability, stiffness and endothelialization capacity of fibrin-based bioartificial blood vessels. J. Mech. Behav. Biomed. Mater. *124*, 104835. https://doi.org/10.1016/j.jmbbm.2021.104835.
85. Al Kayal, T., Losi, P., Pierozzi, S., and Soldani, G. (2020). A new method for fibrin-based electrospun/sprayed scaffold fabrication. Sci. Rep. *10*, 5111. https://doi.org/10.1038/s41598-020-61933-z.
86. Kim, N.E., Park, S., Kim, S., Choi, J.H., Kim, S.E., Choe, S.H., Kang, T.w., Song, J.E., and Khang, G. (2023). Development of gelatin-based shape-memory polymer scaffolds with fast responsive performance and enhanced mechanical properties for tissue engineering applications. ACS Omega *8*, 6455–6462. https://doi.org/10.1021/acsomega.2c06730.
87. Lamprou, D., Zhdan, P., Labeed, F., and Lekakou, C. (2011). Gelatine and gelatine/elastin nanocomposites for vascular grafts: Processing and characterization. J. Biomater. Appl. *26*, 209–226. https://doi.org/10.1177/0885328210364429.
88. Zhou, L., Li, Y., Tu, Q., and Wang, J. (2023). A 3D printing mold method for rapid fabrication of artificial blood vessels. Colloids Surf. A Physicochem. Eng. Asp. *662*, 130952. https://doi.org/10.1016/j.colsurfa.2023.130952.
89. Syedain, Z.H., Meier, L.A., Bjork, J.W., Lee, A., and Tranquillo, R.T. (2011). Implantable arterial grafts from human fibroblasts and fibrin using a multi-graft pulsed flow-stretch bioreactor with noninvasive strength monitoring. Biomaterials *32*, 714–722. https://doi.org/10.1016/j.biomaterials.2010.09.019.
90. Pezzoli, D., Cauli, E., Chevallier, P., Farè, S., and Mantovani, D. (2017). Biomimetic coating of cross-linked gelatin to improve mechanical and biological properties of electrospun PET: A promising approach for small caliber vascular graft applications. J. Biomed. Mater. Res. *105*, 2405–2415. https://doi.org/10.1002/jbm.a.36098.
91. Madhavan, K., Belchenko, D., Motta, A., and Tan, W. (2010). Evaluation of composition and crosslinking effects on collagen-based composite constructs. Acta Biomater. *6*, 1413–1422. https://doi.org/10.1016/j.actbio.2009.09.028.
92. Xue, X., Hu, Y., Wang, S., Chen, X., Jiang, Y., and Su, J. (2022). Fabrication of physical and chemical crosslinked hydrogels for bone tissue engineering. Bioact. Mater. *12*, 327–339. https://doi.org/10.1016/j.bioactmat.2021.10.029.
93. Kanamori, T., Habu, T., Shinbo, T., and Sakai, K. (2000). Difference in solute diffusivity in crosslinked collagen gels prepared under various conditions. Mater. Sci. Eng. C *13*, 85–89. https://doi.org/10.1016/S0928-4931(00)00180-6.
94. Lee, C.-S., Hwang, H.S., Kim, S., Fan, J., Aghaloo, T., and Lee, M. (2020). Inspired by nature: facile design of nanoclay–organic hydrogel bone sealant with multifunctional properties for robust bone regeneration. Adv. Funct. Mater. *30*, 2003717. https://doi.org/10.1002/adfm.202003717.
95. Zafeiris, K., Brasinika, D., Karatza, A., Koumoulos, E., Karoussis, I.K., Kyriakidou, K., and Charitidis, C.A. (2021). Additive manufacturing of hydroxyapatite-chitosan-genipin composite scaffolds for bone tissue engineering applications. Mater. Sci. Eng., C *119*, 111639. https://doi.org/10.1016/j.msec.2020.111639.
96. Wang, Y., Li, L., Ma, Y., Tang, Y., Zhao, Y., Li, Z., Pu, W., Huang, B., Wen, X., Cao, X., et al. (2020). Multifunctional supramolecular hydrogel for prevention of epidural adhesion after laminectomy. ACS Nano *14*, 8202–8219. https://doi.org/10.1021/acsnano.0c01658.
97. Qiao, Y., Liu, X., Zhou, X., Zhang, H., Zhang, W., Xiao, W., Pan, G., Cui, W., Santos, H.A., and Shi, Q. (2020). Gelatin templated polypeptide co-cross-linked hydrogel for bone regeneration. Adv. Healthcare Mater. *9*, 1901239. https://doi.org/10.1002/adhm.201901239.
98. Piluso, S., Flores Gomez, D., Dokter, I., Moreira Texeira, L., Li, Y., Leijten, J., van Weeren, R., Vermonden, T., Karperien, M., and Malda, J. (2020). Rapid and cytocompatible cell-laden silk hydrogel formation via riboflavin-mediated crosslinking. J. Mater. Chem. B *8*, 9566–9575. https://doi.org/10.1039/D0TB01731K.
99. Girton, T.S., Oegema, T.R., and Tranquillo, R.T. (1999). Exploiting glycation to stiffen and strengthen tissue equivalents for tissue engineering. J. Biomed. Mater. Res. *46*, 87–92. https://doi.org/10.1002/(SICI)1097-4636(199907)46:1<87::AID-JBM10>3.0.CO;2-K.
100. Zhao, J., Griffin, M., Cai, J., Li, S., Bulter, P.E., and Kalaskar, D.M. (2016). Bioreactors for tissue engineering: An update. Biochem. Eng. J. *109*, 268–281. https://doi.org/10.1016/j.bej.2016.01.018.
101. Hoenig, E., Winkler, T., Mielke, G., Paetzold, H., Schuettler, D., Goepfert, C., Machens, H.-G., Morlock, M.M., and Schilling, A.F. (2011). High amplitude direct compressive strain enhances mechanical properties of scaffold-free tissue-engineered cartilage. Tissue Eng. *17*, 1401–1411. https://doi.org/10.1089/ten.tea.2010.0395.
102. Bravo-Olín, J., Martínez-Carreón, S.A., Francisco-Solano, E., Lara, A.R., and Beltran-Vargas, N.E. (2024). Analysis of the role of perfusion, mechanical, and electrical stimulation in bioreactors for cardiac tissue engineering. Bioproc. Biosyst. Eng. *47*, 767–839. https://doi.org/10.1007/s00449-024-03004-5.
103. Gemmiti, C.V., and Guldberg, R.E. (2006). Fluid flow increases type II collagen deposition and tensile mechanical properties in bioreactor-grown tissue-engineered cartilage. Tissue Eng. *12*, 469–479. https://doi.org/10.1089/ten.2006.12.469.
104. Lee, J.H., Chen, Z., He, S., Zhou, J., Tsai, A., Truskey, G., and Leong, K.W. (2021). Emulating early atherosclerosis in a vascular microphysiological system using branched tissue-engineered blood vessels. Adv. Biol. *5*, 2000428. https://doi.org/10.1002/adbi.202000428.
105. Zhang, X., Bishawi, M., Zhang, G., Prasad, V., Salmon, E., Breithaupt, J.J., Zhang, Q., and Truskey, G.A. (2020). Modeling early stage atherosclerosis in a primary human vascular microphysiological system. Nat. Commun. *11*, 5426. https://doi.org/10.1038/s41467-020-19197-8.
106. Li, W., Yin, Y., Zhou, H., Fan, Y., Yang, Y., Gao, Q., Li, P., Gao, G., and Li, J. (2024). Recent Advances in Electrospinning Techniques for Precise Medicine. Cyborg Bionic Syst. *5*, 0101. https://doi.org/10.34133/cbsystems.0101.
107. Zhang, M., Xu, S., Wang, R., Che, Y., Han, C., Feng, W., Wang, C., and Zhao, W. (2023). Electrospun nanofiber/hydrogel composite materials and their tissue engineering applications. J. Mater. Sci. Technol. *162*,

157–178. https://doi.org/10.1016/j.jmst.2023.04.015.
108. Yalcin Enis, I., and Gok Sadikoglu, T. (2018). Design parameters for electrospun biodegradable vascular grafts. J. Ind. Textil. *47*, 2205–2227. https://doi.org/10.1177/1528083716654470.
109. Wang, N., Peng, Y., Zheng, W., Tang, L., Cheng, S., Yang, J., Liu, S., Zhang, W., and Jiang, X. (2018). A strategy for rapid construction of blood vessel-like structures with complex cell alignments. Macromol. Biosci. *18*, 1700408. https://doi.org/10.1002/mabi.201700408.
110. Bagherzadeh, R., Najar, S.S., Latifi, M., Tehran, M.A., and Kong, L. (2013). A theoretical analysis and prediction of pore size and pore size distribution in electrospun multilayer nanofibrous materials. J. Biomed. Mater. Res. *101*, 2107–2117. https://doi.org/10.1002/jbm.a.34487.
111. Wu, H., Fan, J., Chu, C.-C., and Wu, J. (2010). Electrospinning of small diameter 3-D nanofibrous tubular scaffolds with controllable nanofiber orientations for vascular grafts. J. Mater. Sci. Mater. Med. *21*, 3207–3215. https://doi.org/10.1007/s10856-010-4164-8.
112. Hu, J.-J., Chao, W.-C., Lee, P.-Y., and Huang, C.-H. (2012). Construction and characterization of an electrospun tubular scaffold for small-diameter tissue-engineered vascular grafts: A scaffold membrane approach. J. Mech. Behav. Biomed. Mater. *13*, 140–155. https://doi.org/10.1016/j.jmbbm.2012.04.013.
113. Elliott, M.B., Ginn, B., Fukunishi, T., Bedja, D., Suresh, A., Chen, T., Inoue, T., Dietz, H.C., Santhanam, L., Mao, H.Q., et al. (2019). Regenerative and durable small-diameter graft as an arterial conduit. Proc. Natl. Acad. Sci. USA *116*, 12710–12719. https://doi.org/10.1073/pnas.1905966116.
114. Fahad, M.A.A., Lee, H.-Y., Park, S., Choi, M., Shanto, P.C., Park, M., Bae, S.H., and Lee, B.-T. (2024). Small-diameter vascular graft composing of core-shell structured micro-nanofibers loaded with heparin and VEGF for endothelialization and prevention of neointimal hyperplasia. Biomaterials *306*, 122507. https://doi.org/10.1016/j.biomaterials.2024.122507.
115. Weekes, A., Wehr, G., Pinto, N., Jenkins, J., Li, Z., Meinert, C., and Klein, T.J. (2023). Highly compliant biomimetic scaffolds for small diameter tissue-engineered vascular grafts (TEVGs) produced via melt electrowriting (MEW). Biofabrication *16*, 015017. https://doi.org/10.1088/1758-5090/ad0ee1.
116. Law, J.X., Liau, L.L., Saim, A., Yang, Y., and Idrus, R. (2017). Electrospun collagen nanofibers and their applications in skin tissue engineering. Tissue Eng. Regen. Med. *14*, 699–718. https://doi.org/10.1007/s13770-017-0075-9.
117. El-Seedi, H.R., Said, N.S., Yosri, N., Hawash, H.B., El-Sherif, D.M., Abouzid, M., Abdel-Daim, M.M., Yaseen, M., Omar, H., Shou, Q., et al. (2023). Gelatin nanofibers: Recent insights in synthesis, bio-medical applications and limitations. Heliyon *9*, e16228. https://doi.org/10.1016/j.heliyon.2023.e16228.
118. McManus, M.C., Boland, E.D., Koo, H.P., Barnes, C.P., Pawlowski, K.J., Wnek, G.E., Simpson, D.G., and Bowlin, G.L. (2006). Mechanical properties of electrospun fibrinogen structures. Acta Biomater. *2*, 19–28. https://doi.org/10.1016/j.actbio.2005.09.008.
119. Wang, S., Ju, J., Wu, S., Lin, M., Sui, K., Xia, Y., and Tan, Y. (2020). Electrospinning of biocompatible alginate-based nanofiber membranes via tailoring chain flexibility. Carbohydr. Polym. *230*, 115665. https://doi.org/10.1016/j.carbpol.2019.115665.
120. Vaz, C.M., van Tuijl, S., Bouten, C.V.C., and Baaijens, F.P.T. (2005). Design of scaffolds for blood vessel tissue engineering using a multi-layering electrospinning technique. Acta Biomater. *1*, 575–582. https://doi.org/10.1016/j.actbio.2005.06.006.
121. Sukchanta, A., Kummanee, P., and Nuansing, W. (2021). Development and study on mechanical properties of small diameter artificial blood vessel by using electrospinning and 3d printing. J. Phys, Conf. Ser. *2145*, 012037. https://doi.org/10.1088/1742-6596/2145/1/012037.
122. Abdullah, T., Saeed, U., Memic, A., Gauthaman, K., Hussain, M.A., and Al-Turaif, H. (2019). Electrospun cellulose nano fibril reinforced PLA/PBS composite scaffold for vascular tissue engineering. J. Polym. Res. *26*, 110. https://doi.org/10.1007/s10965-019-1772-y.
123. Banitaba, S.N., Gharehaghaji, A.A., and Jeddi, A.A.A. (2021). Fabrication and characterization of hollow electrospun PLA structure through a modified electrospinning method applicable as vascular graft. Bull. Mater. Sci. *44*, 158. https://doi.org/10.1007/s12034-021-02463-w.
124. Jin, Q., Fu, Y., Zhang, G., Xu, L., Jin, G., Tang, L., Ju, J., Zhao, W., and Hou, R. (2022). Nanofiber electrospinning combined with rotary bioprinting for fabricating small-diameter vessels with endothelium and smooth muscle. Compos. B Eng. *234*, 109691. https://doi.org/10.1016/j.compositesb.2022.109691.
125. Rickel, A.P., Deng, X., Engebretson, D., and Hong, Z. (2021). Electrospun nanofiber scaffold for vascular tissue engineering. Mater. Sci. Eng., C *129*, 112373. https://doi.org/10.1016/j.msec.2021.112373.
126. Zhao, W., Li, J., Jin, K., Liu, W., Qiu, X., and Li, C. (2016). Fabrication of functional PLGA-based electrospun scaffolds and their applications in biomedical engineering. Mater. Sci. Eng., C *59*, 1181–1194. https://doi.org/10.1016/j.msec.2015.11.026.
127. Wang, S., and Zhang, Y. (2012). Preparation, structure, and *in vitro* degradation behavior of the electrospun poly(lactide-co-glycolide) ultrafine fibrous vascular scaffold. Fibers Polym. *13*, 754–761. https://doi.org/10.1007/s12221-012-0754-z.
128. Xie, X., Chen, Y., Wang, X., Xu, X., Shen, Y., Aldalbahi, A., Fetz, A.E., Bowlin, G.L., El-Newehy, M., and Mo, X. (2020). Electrospinning nanofiber scaffolds for soft and hard tissue regeneration. J. Mater. Sci. Technol. *59*, 243–261. https://doi.org/10.1016/j.jmst.2020.04.037.
129. Schiller, T., and Scheibel, T. (2024). Bioinspired and biomimetic protein-based fibers and their applications. Commun. Mater. *5*, 56. https://doi.org/10.1038/s43246-024-00488-2.
130. Montoya, Y., Cardenas, J., Bustamante, J., and Valencia, R. (2021). Effect of sequential electrospinning and co-electrospinning on morphological and fluid mechanical wall properties of polycaprolactone and bovine gelatin scaffolds, for potential use in small diameter vascular grafts. Biomater. Res. *25*, 38. https://doi.org/10.1186/s40824-021-00240-8.
131. Mndlovu, H., Kumar, P., du Toit, L.C., and Choonara, Y.E. (2024). A review of biomaterial degradation assessment approaches employed in the biomedical field. npj Mater. Degrad. *8*, 66. https://doi.org/10.1038/s41529-024-00487-1.
132. Elsawy, M.A., Kim, K.-H., Park, J.-W., and Deep, A. (2017). Hydrolytic degradation of polylactic acid (PLA) and its composites. Renew. Sustain. Energy Rev. *79*, 1346–1352. https://doi.org/10.1016/j.rser.2017.05.143.
133. Weston, M.W., Rhee, K., and Tarbell, J.M. (1996). Compliance and diameter mismatch affect the wall shear rate distribution near an end-to-end anastomosis. J. Biomech. *29*, 187–198. https://doi.org/10.1016/0021-9290(95)00028-3.
134. Salacinski, H.J., Goldner, S., Giudiceandrea, A., Hamilton, G., Seifalian, A.M., Edwards, A., and Carson, R.J. (2001). The mechanical behavior of vascular grafts: a review. J. Biomater. Appl. *15*, 241–278. https://doi.org/10.1106/NA5T-J57A-JTDD-FD04.
135. Quint, C., Kondo, Y., Manson, R.J., Lawson, J.H., Dardik, A., and Niklason, L.E. (2011). Decellularized tissue-engineered blood vessel as an arterial conduit. Proc. Natl. Acad. Sci. USA *108*, 9214–9219. https://doi.org/10.1073/pnas.1019506108.
136. Jiang, S., Zhuang, Y., Cai, M., Wang, X., and Lin, K. (2023). Decellularized extracellular matrix: A promising strategy for skin repair and regeneration. Engineered Regeneration *4*, 357–374. https://doi.org/10.1016/j.engreg.2023.05.001.
137. Ott, H.C., Matthiesen, T.S., Goh, S.-K., Black, L.D., Kren, S.M., Netoff, T.I., and Taylor, D.A. (2008). Perfusion-decellularized matrix: Using nature's platform to engineer a bioartificial heart. Nat. Med. *14*, 213–221. https://doi.org/10.1038/nm1684.
138. Petrella, F., and Spaggiari, L. (2018). Artificial lung. J. Thorac. Dis. *10*, S2329–S2332. https://doi.org/10.21037/jtd.2017.12.89.
139. Uygun, B.E., Soto-Gutierrez, A., Yagi, H., Izamis, M.L., Guzzardi, M.A., Shulman, C., Milwid, J., Kobayashi, N., Tilles, A., Berthiaume, F., et al. (2010). Organ reengineering through development of a transplantable recellularized liver graft using decellularized liver matrix. Nat. Med. *16*, 814–820. https://doi.org/10.1038/nm.2170.
140. de Haan, M.J., Witjas, F.M., Engelse, M.A., and Rabelink, T.J. (2021). Have we hit a wall with whole kidney decellularization and recellularization: A review. Current Opinion in Biomedical Engineering *20*, 100335. https://doi.org/10.1016/j.cobme.2021.100335.
141. Nishimura, Y. (2023). Current status and future prospects of decellularized kidney tissue. J. Artif. Organs *26*, 171–175. https://doi.org/10.1007/s10047-022-01366-9.
142. Crapo, P.M., Gilbert, T.W., and Badylak, S.F. (2011). An overview of tissue and whole organ decellularization processes. Biomaterials *32*, 3233–3243. https://doi.org/10.1016/j.biomaterials.2011.01.057.
143. Fang, S., Riber, S.S., Hussein, K., Ahlmann, A.H., Harvald, E.B., Khan, F., Beck, H.C., Weile, L.K.K., Sørensen, J.A., Sheikh, S.P., et al. (2020). Decellularized human umbilical artery: Biocompatibility and *in vivo* functionality in sheep carotid bypass model. Mater. Sci. Eng., C *112*, 110955. https://doi.org/10.1016/j.msec.2020.110955.

144. Dahl, S.L.M., Kypson, A.P., Lawson, J.H., Blum, J.L., Strader, J.T., Li, Y., Manson, R.J., Tente, W.E., DiBernardo, L., Hensley, M.T., et al. (2011). Readily available tissue-engineered vascular grafts. Sci. Transl. Med. *3*, 68ra9. https://doi.org/10.1126/scitranslmed.3001426.
145. Schaner, P.J., Martin, N.D., Tulenko, T.N., Shapiro, I.M., Tarola, N.A., Leichter, R.F., Carabasi, R.A., and DiMuzio, P.J. (2004). Decellularized vein as a potential scaffold for vascular tissue engineering. J. Vasc. Surg. *40*, 146–153. https://doi.org/10.1016/j.jvs.2004.03.033.
146. Jarrett, F., and Mahood, B.A. (1994). Long-term results of femoropopliteal bypass with stabilized human umbilical vein. Am. J. Surg. *168*, 111–114. https://doi.org/10.1016/S0002-9610(94)80047-2.
147. Wilshaw, S.-P., Rooney, P., Berry, H., Kearney, J.N., Homer-Vanniasinkam, S., Fisher, J., and Ingham, E. (2012). Development and characterization of acellular allogeneic arterial matrices. Tissue Eng. *18*, 471–483. https://doi.org/10.1089/ten.tea.2011.0287.
148. Ma, X., He, Z., Li, L., Liu, G., Li, Q., Yang, D., Zhang, Y., and Li, N. (2017). Development and *in vivo* validation of tissue-engineered, small-diameter vascular grafts from decellularized aortae of fetal pigs and canine vascular endothelial cells. J. Cardiothorac. Surg. *12*, 101. https://doi.org/10.1186/s13019-017-0661-x.
149. Daugs, A., Hutzler, B., Meinke, M., Schmitz, C., Lehmann, N., Markhoff, A., and Bloch, O. (2017). Detergent-based decellularization of bovine carotid arteries for vascular tissue engineering. Ann. Biomed. Eng. *45*, 2683–2692. https://doi.org/10.1007/s10439-017-1892-7.
150. Omid, H., Abdollahi, S., Bonakdar, S., Haghighipour, N., Shokrgozar, M.A., and Mohammadi, J. (2023). Biomimetic vascular tissue engineering by decellularized scaffold and concurrent cyclic tensile and shear stresses. J. Mater. Sci. Mater. Med. *34*, 12. https://doi.org/10.1007/s10856-023-06716-4.
151. Gilbert, T.W., Sellaro, T.L., and Badylak, S.F. (2006). Decellularization of tissues and organs. Biomaterials *27*, 3675–3683. https://doi.org/10.1016/j.biomaterials.2006.02.014.
152. Zhang, X., Chen, X., Hong, H., Hu, R., Liu, J., and Liu, C. (2022). Decellularized extracellular matrix scaffolds: Recent trends and emerging strategies in tissue engineering. Bioact. Mater. *10*, 15–31. https://doi.org/10.1016/j.bioactmat.2021.09.014.
153. Fernández-Pérez, J., and Ahearne, M. (2019). The impact of decellularization methods on extracellular matrix derived hydrogels. Sci. Rep. *9*, 14933. https://doi.org/10.1038/s41598-019-49575-2.
154. Luo, Z., Bian, Y., Su, W., Shi, L., Li, S., Song, Y., Zheng, G., Xie, A., and Xue, J. (2019). Comparison of various reagents for preparing a decellularized porcine cartilage scaffold. Am. J. Transl. Res. *11*, 1417–1427. https://www.ncbi.nlm.nih.gov/pmc/articles/PMC6456528/.
155. Gao, G., Lee, J.H., Jang, J., Lee, D.H., Kong, J., Kim, B.S., Choi, Y., Jang, W.B., Hong, Y.J., Kwon, S., and Cho, D. (2017). Tissue engineered bio-blood-vessels constructed using a tissue-specific bioink and 3D coaxial cell printing technique: A novel therapy for ischemic disease. Adv. Funct. Mater. *27*, 1700798. https://doi.org/10.1002/adfm.201700798.
156. Gao, G., Park, J.Y., Kim, B.S., Jang, J., and Cho, D.-W. (2018). Coaxial cell printing of freestanding, perfusable, and functional *in vitro* vascular models for recapitulation of native vascular endothelium pathophysiology. Adv. Healthcare Mater. *7*, 1801102. https://doi.org/10.1002/adhm.201801102.
157. Hou, Y.-C., Cui, X., Qin, Z., Su, C., Zhang, G., Tang, J.-N., Li, J.-A., and Zhang, J.-Y. (2023). Three-dimensional bioprinting of artificial blood vessel: process, bioinks, and challenges. Int. J. Bioprint. *9*, 740. https://doi.org/10.18063/ijb.740.
158. Zhu, J., Wang, X., Lin, L., and Zeng, W. (2023). 3D bioprinting for vascular grafts and microvasculature. Int. J. Bioprint. *9*, 0012. https://doi.org/10.36922/ijb.0012.
159. Kim, S.-J., Kim, M.-G., Kim, J., Jeon, J.S., Park, J., and Yi, H.-G. (2023). Bioprinting methods for fabricating *in vitro* tubular blood vessel models. Cyborg Bionic Syst. *4*, 0043. https://doi.org/10.34133/cbsystems.0043.
160. Gold, K.A., Saha, B., Rajeeva Pandian, N.K., Walther, B.K., Palma, J.A., Jo, J., Cooke, J.P., Jain, A., and Gaharwar, A.K. (2021). 3D bioprinted multicellular vascular models. Adv. Healthcare Mater. *10*, 2101141. https://doi.org/10.1002/adhm.202101141.
161. Vrana, N.E., Gupta, S., Mitra, K., Rizvanov, A.A., Solovyeva, V.V., Antmen, E., Salehi, M., Ehterami, A., Pourchet, L., Barthes, J., et al. (2022). From 3D printing to 3D bioprinting: the material properties of polymeric material and its derived bioink for achieving tissue specific architectures. Cell Tissue Bank. *23*, 417–440. https://doi.org/10.1007/s10561-021-09975-z.
162. Hinton, T.J., Jallerat, Q., Palchesko, R.N., Park, J.H., Grodzicki, M.S., Shue, H.-J., Ramadan, M.H., Hudson, A.R., and Feinberg, A.W. (2015). Three-dimensional printing of complex biological structures by freeform reversible embedding of suspended hydrogels. Sci. Adv. *1*, e1500758. https://doi.org/10.1126/sciadv.1500758.
163. Fang, Y., Guo, Y., Wu, B., Liu, Z., Ye, M., Xu, Y., Ji, M., Chen, L., Lu, B., Nie, K., et al. (2023). Expanding embedded 3D bioprinting capability for engineering complex organs with freeform vascular networks. Adv. Mater. *35*, 2205082. https://doi.org/10.1002/adma.202205082.
164. Lee, A., Hudson, A.R., Shiwarski, D.J., Tashman, J.W., Hinton, T.J., Yerneni, S., Bliley, J.M., Campbell, P.G., and Feinberg, A.W. (2019). 3D bioprinting of collagen to rebuild components of the human heart. Science *365*, 482–487. https://doi.org/10.1126/science.aav9051.
165. Ouyang, L., Armstrong, J.P.K., Lin, Y., Wojciechowski, J.P., Lee-Reeves, C., Hachim, D., Zhou, K., Burdick, J.A., and Stevens, M.M. (2020). Expanding and optimizing 3D bioprinting capabilities using complementary network bioinks. Sci. Adv. *6*, eabc5529. https://doi.org/10.1126/sciadv.abc5529.
166. Budharaju, H., Sundaramurthi, D., and Sethuraman, S. (2024). Embedded 3D bioprinting-an emerging strategy to fabricate biomimetic & large vascularized tissue constructs. Bioact. Mater. *32*, 356–384. https://doi.org/10.1016/j.bioactmat.2023.10.012.
167. Kjar, A., McFarland, B., Mecham, K., Harward, N., and Huang, Y. (2021). Engineering of tissue constructs using coaxial bioprinting. Bioact. Mater. *6*, 460–471. https://doi.org/10.1016/j.bioactmat.2020.08.020.
168. Watanabe, T., Kanda, K., Yamanami, M., Ishibashi-Ueda, H., Yaku, H., and Nakayama, Y. (2011). Long-term animal implantation study of biotube-autologous small-caliber vascular graft fabricated by in-body tissue architecture. J. Biomed. Mater. Res. B Appl. Biomater. *98*, 120–126. https://doi.org/10.1002/jbm.b.31841.
169. Nakayama, Y., Furukoshi, M., Terazawa, T., and Iwai, R. (2018). Development of long *in vivo* tissue-engineered "Biotube" vascular grafts. Biomaterials *185*, 232–239. https://doi.org/10.1016/j.biomaterials.2018.09.032.
170. Zhi, D., Cheng, Q., Midgley, A.C., Zhang, Q., Wei, T., Li, Y., Wang, T., Ma, T., Rafique, M., Xia, S., et al. (2022). Mechanically reinforced biotubes for arterial replacement and arteriovenous grafting inspired by architectural engineering. Sci. Adv. *8*, eabl3888. https://doi.org/10.1126/sciadv.abl3888.
171. De Pieri, A., Rochev, Y., and Zeugolis, D.I. (2021). Scaffold-free cell-based tissue engineering therapies: advances, shortfalls and forecast. NPJ Regen. Med. *6*, 18. https://doi.org/10.1038/s41536-021-00133-3.
172. Narita, T., Shintani, Y., Ikebe, C., Kaneko, M., Campbell, N.G., Coppen, S.R., Uppal, R., Sawa, Y., Yashiro, K., and Suzuki, K. (2013). The use of scaffold-free cell sheet technique to refine mesenchymal stromal cell-based therapy for heart failure. Mol. Ther. *21*, 860–867. https://doi.org/10.1038/mt.2013.9.
173. Prestigiacomo, V., Weston, A., and Suter-Dick, L. (2020). Rat multicellular 3D liver microtissues to explore TGF-β1 induced effects. J. Pharmacol. Toxicol. Methods *101*, 106650. https://doi.org/10.1016/j.vascn.2019.106650.
174. Kim, G., Jung, Y., Cho, K., Lee, H.J., and Koh, W.-G. (2020). Thermoresponsive poly(*N*-isopropylacrylamide) hydrogel substrates micropatterned with poly(ethylene glycol) hydrogel for adipose mesenchymal stem cell spheroid formation and retrieval. Mater. Sci. Eng., C *115*, 111128. https://doi.org/10.1016/j.msec.2020.111128.
175. Kamoya, T., Anada, T., Shiwaku, Y., Takano-Yamamoto, T., and Suzuki, O. (2016). An oxygen-permeable spheroid culture chip (Oxy chip) promotes osteoblastic differentiation of mesenchymal stem cells. Sensor. Actuator. B Chem. *232*, 75–83. https://doi.org/10.1016/j.snb.2016.03.107.
176. Hidalgo San Jose, L., Stephens, P., Song, B., and Barrow, D. (2018). Microfluidic encapsulation supports stem cell viability, proliferation, and neuronal differentiation. Tissue Eng. C Methods *24*, 158–170. https://doi.org/10.1089/ten.tec.2017.0368.
177. Kelm, J.M., Lorber, V., Snedeker, J.G., Schmidt, D., Broggini-Tenzer, A., Weisstanner, M., Odermatt, B., Mol, A., Zünd, G., and Hoerstrup, S.P. (2010). A novel concept for scaffold-free vessel tissue engineering: Self-assembly of microtissue building blocks. J. Biotechnol. *148*, 46–55. https://doi.org/10.1016/j.jbiotec.2010.03.002.
178. Mattix, B.M., Olsen, T.R., Casco, M., Reese, L., Poole, J.T., Zhang, J., Visconti, R.P.,

Simionescu, A., Simionescu, D.T., and Alexis, F. (2014). Janus magnetic cellular spheroids for vascular tissue engineering. Biomaterials *35*, 949–960. https://doi.org/10.1016/j.biomaterials.2013.10.036.

179. Norotte, C., Marga, F.S., Niklason, L.E., and Forgacs, G. (2009). Scaffold-free vascular tissue engineering using bioprinting. Biomaterials *30*, 5910–5917. https://doi.org/10.1016/j.biomaterials.2009.06.034.
180. Itoh, M., Nakayama, K., Noguchi, R., Kamohara, K., Furukawa, K., Uchihashi, K., Toda, S., Oyama, J.-i., Node, K., and Morita, S. (2015). Scaffold-free tubular tissues created by a bio-3D printer undergo remodeling and endothelialization when implanted in rat aortae. PLoS One *10*, e0136681. https://doi.org/10.1371/journal.pone.0136681.
181. Banerjee, D., Singh, Y.P., Datta, P., Ozbolat, V., O'Donnell, A., Yeo, M., and Ozbolat, I.T. (2022). Strategies for 3D bioprinting of spheroids: A comprehensive review. Biomaterials *291*, 121881. https://doi.org/10.1016/j.biomaterials.2022.121881.
182. Lee, H. (2023). Engineering *in vitro* models: bioprinting of organoids with artificial intelligence. Cyborg Bionic Syst. *4*, 0018. https://doi.org/10.34133/cbsystems.0018.
183. Itoh, M., Mukae, Y., Kitsuka, T., Arai, K., Nakamura, A., Uchihashi, K., Toda, S., Matsubayashi, K., Oyama, J.I., Node, K., et al. (2019). Development of an immunodeficient pig model allowing long-term accommodation of artificial human vascular tubes. Nat. Commun. *10*, 2244. https://doi.org/10.1038/s41467-019-10107-1.
184. Matsuda, N., Shimizu, T., Yamato, M., and Okano, T. (2007). Tissue engineering based on cell sheet technology. Adv. Mater. *19*, 3089–3099. https://doi.org/10.1002/adma.200701978.
185. Silva, A.S., Santos, L.F., Mendes, M.C., and Mano, J.F. (2020). Multi-layer pre-vascularized magnetic cell sheets for bone regeneration. Biomaterials *231*, 119664. https://doi.org/10.1016/j.biomaterials.2019.119664.
186. Sakaguchi, K., Akimoto, K., Takaira, M., Tanaka, R.-i., Shimizu, T., and Umezu, S. (2022). Cell-based microfluidic device utilizing cell sheet technology. Cyborg Bionic Syst. *2022*, 9758187. https://doi.org/10.34133/2022/9758187.
187. L'Heureux, N., Pâquet, S., Labbé, R., Germain, L., and Auger, F.A. (1998). A completely biological tissue-engineered human blood vessel. Faseb. J. *12*, 47–56. https://doi.org/10.1096/fsb2fasebj.12.1.47.
188. L'Heureux, N., Dusserre, N., Konig, G., Victor, B., Keire, P., Wight, T.N., Chronos, N.A.F., Kyles, A.E., Gregory, C.R., Hoyt, G., et al. (2006). Human tissue-engineered blood vessels for adult arterial revascularization. Nat. Med. *12*, 361–365. https://doi.org/10.1038/nm1364.
189. Tang, H., Wang, X., Zheng, J., Long, Y.-Z., Xu, T., Li, D., Guo, X., and Zhang, Y. (2023). Formation of low-density electrospun fibrous network integrated mesenchymal stem cell sheet. J. Mater. Chem. B *11*, 389–402. https://doi.org/10.1039/D2TB02029G.
190. Falconnet, D., Csucs, G., Grandin, H.M., and Textor, M. (2006). Surface engineering approaches to micropattern surfaces for cell-based assays. Biomaterials *27*, 3044–3063. https://doi.org/10.1016/j.biomaterials.2005.12.024.
191. Yuan, B., Jin, Y., Sun, Y., Wang, D., Sun, J., Wang, Z., Zhang, W., and Jiang, X. (2012). A strategy for depositing different types of cells in three dimensions to mimic tubular structures in tissues. Adv. Mater. *24*, 890–896. https://doi.org/10.1002/adma.201104589.
192. Jung, Y., Ji, H., Chen, Z., Fai Chan, H., Atchison, L., Klitzman, B., Truskey, G., and Leong, K.W. (2015). Scaffold-free, human mesenchymal stem cell-based tissue engineered blood vessels. Sci. Rep. *5*, 15116. https://doi.org/10.1038/srep15116.
193. Wystrychowski, W., McAllister, T.N., Zagalski, K., Dusserre, N., Cierpka, L., and L'Heureux, N. (2014). First human use of an allogeneic tissue-engineered vascular graft for hemodialysis access. J. Vasc. Surg. *60*, 1353–1357. https://doi.org/10.1016/j.jvs.2013.08.018.
194. Hu, D., Li, X., Li, J., Tong, P., Li, Z., Lin, G., Sun, Y., and Wang, J. (2023). The preclinical and clinical progress of cell sheet engineering in regenerative medicine. Stem Cell Res. Ther. *14*, 112. https://doi.org/10.1186/s13287-023-03340-5.
195. Shahin-Shamsabadi, A., and Cappuccitti, J. (2024). Anchored cell sheet engineering: a novel scaffold-free platform for *in vitro* modeling. Adv. Funct. Mater. *34*, 2308552. https://doi.org/10.1002/adfm.202308552.
196. Chandra Sekar, N., Khoshmanesh, K., and Baratchi, S. (2024). Bioengineered models of cardiovascular diseases. Atherosclerosis *393*, 117565. https://doi.org/10.1016/j.atherosclerosis.2024.117565.
197. Kim, S., Kim, W., Lim, S., and Jeon, J.S. (2017). Vasculature-on-a-chip for *in vitro* disease models. Bioengineering *4*, 8. https://doi.org/10.3390/bioengineering4010008.
198. Kim, D.A., and Ku, D.N. (2022). Structure of shear-induced platelet aggregated clot formed in an *in vitro* arterial thrombosis model. Blood Adv. *6*, 2872–2883. https://doi.org/10.1182/bloodadvances.2021006248.
199. Chen, L., Zheng, Y., Liu, Y., Tian, P., Yu, L., Bai, L., Zhou, F., Yang, Y., Cheng, Y., Wang, F., et al. (2022). Microfluidic-based *in vitro* thrombosis model for studying microplastics toxicity. Lab Chip *22*, 1344–1353. https://doi.org/10.1039/D1LC00989C.
200. Xu, Y., Deng, P., Yu, G., Ke, X., Lin, Y., Shu, X., Xie, Y., Zhang, S., Nie, R., and Wu, Z. (2021). Thrombogenicity of microfluidic chip surface manipulation: Facile, one-step, none-protein technique for extreme wettability contrast micropatterning. Sensor. Actuator. B Chem. *343*, 130085. https://doi.org/10.1016/j.snb.2021.130085.
201. Yeom, E., Park, J.H., Kang, Y.J., and Lee, S.J. (2016). Microfluidics for simultaneous quantification of platelet adhesion and blood viscosity. Sci. Rep. *6*, 24994. https://doi.org/10.1038/srep24994.
202. Wang, H.C., Zhao, M.M., and Wu, L.Q. (2018). Fabrication of sandwich-like microfluidic chip with circular cross-section micro-channels. Int. J. Mod. Phys. B *32*, 1850288. https://doi.org/10.1142/S0217979218502880.
203. Berry, J., Peaudecerf, F.J., Masters, N.A., Neeves, K.B., Goldstein, R.E., and Harper, M.T. (2021). An "occlusive thrombosis-on-a-chip" microfluidic device for investigating the effect of anti-thrombotic drugs. Lab Chip *21*, 4104–4117. https://doi.org/10.1039/D1LC00347J.
204. Dellaquila, A., Le Bao, C., Letourneur, D., and Simon-Yarza, T. (2021). *In vitro* strategies to vascularize 3D physiologically relevant models. Adv. Sci. *8*, 2100798. https://doi.org/10.1002/advs.202100798.
205. Kolesky, D.B., Homan, K.A., Skylar-Scott, M.A., and Lewis, J.A. (2016). Three-dimensional bioprinting of thick vascularized tissues. Proc. Natl. Acad. Sci. USA *113*, 3179–3184. https://doi.org/10.1073/pnas.1521342113.
206. Haase, K., and Kamm, R.D. (2017). Advances in on-chip vascularization. Regen. Med. *12*, 285–302. https://doi.org/10.2217/rme-2016-0152.
207. Vila Cuenca, M., Cochrane, A., van den Hil, F.E., de Vries, A.A.F., Lesnik Oberstein, S.A.J., Mummery, C.L., and Orlova, V.V. (2021). Engineered 3D vessel-on-chip using hiPSC-derived endothelial- and vascular smooth muscle cells. Stem Cell Rep. *16*, 2159–2168. https://doi.org/10.1016/j.stemcr.2021.08.003.
208. Shakeri, A., Wang, Y., Zhao, Y., Landau, S., Perera, K., Lee, J., and Radisic, M. (2023). Engineering organ-on-a-chip systems for vascular diseases. Arterioscler. Thromb. Vasc. Biol. *43*, 2241–2255. https://doi.org/10.1161/ATVBAHA.123.318233.
209. Jin, Q., Bhatta, A., Pagaduan, J.V., Chen, X., West-Foyle, H., Liu, J., Hou, A., Berkowitz, D., Kuo, S.C., Askin, F.B., et al. (2020). Biomimetic human small muscular pulmonary arteries. Sci. Adv. *6*, eaaz2598. https://doi.org/10.1126/sciadv.aaz2598.
210. Ching, T., Vasudevan, J., Chang, S.-Y., Tan, H.Y., Sargur Ranganath, A., Lim, C.T., Fernandez, J.G., Ng, J.J., Toh, Y.-C., and Hashimoto, M. (2022). Biomimetic vasculatures by 3D-printed porous molds. Small *18*, 2203426. https://doi.org/10.1002/smll.202203426.
211. Pan, C., Xu, J., Gao, Q., Li, W., Sun, T., Lu, J., Shi, Q., Han, Y., Gao, G., and Li, J. (2023). Sequentially suspended 3D bioprinting of multiple-layered vascular models with tunable geometries for *in vitro* modeling of arterial disorders initiation. Biofabrication *15*, 045017. https://doi.org/10.1088/1758-5090/aceffa.
212. Gu, X., Xie, S., Hong, D., and Ding, Y. (2019). An *in vitro* model of foam cell formation induced by a stretchable microfluidic device. Sci. Rep. *9*, 7461. https://doi.org/10.1038/s41598-019-43902-3.
213. Hong, S., Song, Y., Choi, J., and Hwang, C. (2022). Bonding of flexible membranes for perfusable vascularized networks patch. Tissue Eng. Regen. Med. *19*, 363–375. https://doi.org/10.1007/s13770-021-00409-1.
214. Zheng, W., Jiang, B., Wang, D., Zhang, W., Wang, Z., and Jiang, X. (2012). A microfluidic flow-stretch chip for investigating blood vessel biomechanics. Lab Chip *12*, 3441–3450. https://doi.org/10.1039/C2LC40173H.
215. Niklason, L.E., and Lawson, J.H. (2020). Bioengineered human blood vessels. Science *370*, eaaw8682. https://doi.org/10.1126/science.aaw8682.
216. Chan, A.H.P., Tan, R.P., Michael, P.L., Lee, B.S.L., Vanags, L.Z., Ng, M.K.C., Bursill, C.A., and Wise, S.G. (2017). Evaluation of synthetic vascular grafts in a mouse carotid grafting model. PLoS One *12*, e0174773. https://doi.org/10.1371/journal.pone.0174773.

217. Zhu, T., Gu, H., Ma, W., Zhang, Q., Du, J., Chen, S., Wang, L., and Zhang, W. (2021). A fabric reinforced small diameter tubular graft for rabbits' carotid artery defect. Compos. B Eng. *225*, 109274. https://doi.org/10.1016/j.compositesb.2021.109274.
218. Fang, Z., Xiao, Y., Geng, X., Jia, L., Xing, Y., Ye, L., Gu, Y., Zhang, A.-y., and Feng, Z.-g. (2022). Fabrication of heparinized small diameter TPU/PCL bi-layered artificial blood vessels and *in vivo* assessment in a rabbit carotid artery replacement model. Biomater. Adv. *133*, 112628. https://doi.org/10.1016/j.msec.2021.112628.
219. Mahara, A., Somekawa, S., Kobayashi, N., Hirano, Y., Kimura, Y., Fujisato, T., and Yamaoka, T. (2015). Tissue-engineered acellular small diameter long-bypass grafts with neointima-inducing activity. Biomaterials *58*, 54–62. https://doi.org/10.1016/j.biomaterials.2015.04.031.
220. Shin'oka, T., Imai, Y., and Ikada, Y. (2001). Transplantation of a tissue-engineered pulmonary artery. N. Engl. J. Med. Overseas. Ed. *344*, 532–533. https://doi.org/10.1056/NEJM200102153440717.
221. L'Heureux, N., McAllister, T.N., and De La Fuente, L.M. (2007). Tissue-engineered blood vessel for adult arterial revascularization. N. Engl. J. Med. Overseas. Ed. *357*, 1451–1453. https://doi.org/10.1056/NEJMc071536.
222. Sokolov, O., Shaprynskyi, V., Skupyy, O., Stanko, O., Yurets, S., Yurkova, Y., and Niklason, L.E. (2023). Use of bioengineered human acellular vessels to treat traumatic injuries in the Ukraine–Russia conflict. Lancet Reg. Health. Eur. *29*, 100650. https://doi.org/10.1016/j.lanepe.2023.100650.
223. Kirkton, R.D., Santiago-Maysonet, M., Lawson, J.H., Tente, W.E., Dahl, S.L.M., Niklason, L.E., and Prichard, H.L. (2019). Bioengineered human acellular vessels recellularize and evolve into living blood vessels after human implantation. Sci. Transl. Med. *11*, eaau6934. https://doi.org/10.1126/scitranslmed.aau6934.
224. Jakimowicz, T., Przywara, S., Turek, J., Pilgrim, A., Macech, M., Zapotoczny, N., Zubilewicz, T., Lawson, J.H., and Niklason, L.E. (2022). Five year outcomes in patients with end stage renal disease who received a bioengineered human acellular vessel for dialysis access. EJVES Vasc. Forum *54*, 58–63. https://doi.org/10.1016/j.ejvsvf.2022.01.003.
225. Nickerson, M.C., Thamba, A., Rao, V., Peterson, D.B., Peterson, D.A., and Cuddy, D.S. (2023). Expanded utility of human acellular vessel in hemodialysis access surgery and arterial aneurysm repair. Cureus *15*, e46325. https://doi.org/10.7759/cureus.46325.
226. Loewa, A., Feng, J.J., and Hedtrich, S. (2023). Human disease models in drug development. Nat. Rev. Bioeng. *1*, 1–15. https://doi.org/10.1038/s44222-023-00063-3.
227. Leung, C.M., de Haan, P., Ronaldson-Bouchard, K., Kim, G.A., Ko, J., Rho, H.S., Chen, Z., Habibovic, P., Jeon, N.L., Takayama, S., et al. (2022). A guide to the organ-on-a-chip. Nat. Rev. Methods Primers *2*, 33. https://doi.org/10.1038/s43586-022-00118-6.
228. Hofer, M., and Lutolf, M.P. (2021). Engineering organoids. Nat. Rev. Mater. *6*, 402–420. https://doi.org/10.1038/s41578-021-00279-y.
229. Su, C., Menon, N.V., Xu, X., Teo, Y.R., Cao, H., Dalan, R., Tay, C.Y., and Hou, H.W. (2021). A novel human arterial wall-on-a-chip to study endothelial inflammation and vascular smooth muscle cell migration in early atherosclerosis. Lab Chip *21*, 2359–2371. https://doi.org/10.1039/D1LC00131K.
230. Zheng, W., Huang, R., Jiang, B., Zhao, Y., Zhang, W., and Jiang, X. (2016). An early-stage atherosclerosis research model based on microfluidics. Small *12*, 2022–2034. https://doi.org/10.1002/smll.201503241.
231. Gao, G., Park, W., Kim, B.S., Ahn, M., Chae, S., Cho, W.-W., Kim, J., Lee, J.Y., Jang, J., and Cho, D.-W. (2021). Construction of a novel *in vitro* atherosclerotic model from geometry-tunable artery equivalents engineered *via* in-bath coaxial cell printing. Adv. Funct. Mater. *31*, 2008878. https://doi.org/10.1002/adfm.202008878.
232. Mallone, A., Stenger, C., Von Eckardstein, A., Hoerstrup, S.P., and Weber, B. (2018). Biofabricating atherosclerotic plaques: *In vitro* engineering of a three-dimensional human fibroatheroma model. Biomaterials *150*, 49–59. https://doi.org/10.1016/j.biomaterials.2017.09.034.
233. Bhakdi, S., Dorweiler, B., Kirchmann, R., Torzewski, J., Weise, E., Tranum-Jensen, J., Walev, I., and Wieland, E. (1995). On the pathogenesis of atherosclerosis: enzymatic transformation of human low density lipoprotein to an atherogenic moiety. J. Exp. Med. *182*, 1959–1971. https://doi.org/10.1084/jem.182.6.1959.
234. Chellan, B., Reardon, C.A., Getz, G.S., and Hofmann Bowman, M.A. (2016). Enzymatically modified low-density lipoprotein promotes foam cell formation in smooth muscle cells via macropinocytosis and enhances receptor-mediated uptake of oxidized low-density lipoprotein. Arterioscler. Thromb. Vasc. Biol. *36*, 1101–1113. https://doi.org/10.1161/ATVBAHA.116.307306.
235. Choi, J.-S., Ham, D.-H., Kim, J.-H., Marcial, H.B.F., Jeong, P.-H., Choi, J.-H., and Park, W.-T. (2022). Quantitative image analysis of thrombus formation in microfluidic *in-vitro* models. Micro and Nano Syst. Lett. *10*, 23. https://doi.org/10.1186/s40486-022-00166-3.
236. Costa, P.F., Albers, H.J., Linssen, J.E.A., Middelkamp, H.H.T., van der Hout, L., Passier, R., van den Berg, A., Malda, J., and van der Meer, A.D. (2017). Mimicking arterial thrombosis in a 3D-printed microfluidic *in vitro* vascular model based on computed tomography angiography data. Lab Chip *17*, 2785–2792. https://doi.org/10.1039/C7LC00202E.
237. Murphy, S.V., and Atala, A. (2014). 3D bioprinting of tissues and organs. Nat. Biotechnol. *32*, 773–785. https://doi.org/10.1038/nbt.2958.
238. Lee, V.K., Kim, D.Y., Ngo, H., Lee, Y., Seo, L., Yoo, S.-S., Vincent, P.A., and Dai, G. (2014). Creating perfused functional vascular channels using 3D bio-printing technology. Biomaterials *35*, 8092–8102. https://doi.org/10.1016/j.biomaterials.2014.05.083.
239. Kolesky, D.B., Truby, R.L., Gladman, A.S., Busbee, T.A., Homan, K.A., and Lewis, J.A. (2014). 3D bioprinting of vascularized, heterogeneous cell-laden tissue constructs. Adv. Mater. *26*, 3124–3130. https://doi.org/10.1002/adma.201305506.
240. Bertassoni, L.E., Cecconi, M., Manoharan, V., Nikkhah, M., Hjortnaes, J., Cristino, A.L., Barabaschi, G., Demarchi, D., Dokmeci, M.R., Yang, Y., and Khademhosseini, A. (2014). Hydrogel bioprinted microchannel networks for vascularization of tissue engineering constructs. Lab Chip *14*, 2202–2211. https://doi.org/10.1039/C4LC00030G.
241. Miller, J.S., Stevens, K.R., Yang, M.T., Baker, B.M., Nguyen, D.H.T., Cohen, D.M., Toro, E., Chen, A.A., Galie, P.A., Yu, X., et al. (2012). Rapid casting of patterned vascular networks for perfusable engineered three-dimensional tissues. Nat. Mater. *11*, 768–774. https://doi.org/10.1038/nmat3357.
242. Zhang, Y.S., Davoudi, F., Walch, P., Manbachi, A., Luo, X., Dell'Erba, V., Miri, A.K., Albadawi, H., Arneri, A., Li, X., et al. (2016). Bioprinted thrombosis-on-a-chip. Lab Chip *16*, 4097–4105. https://doi.org/10.1039/C6LC00380J.
243. Gompper, G., and Fedosov, D.A. (2016). Modeling microcirculatory blood flow: current state and future perspectives. WIREs Systems Biology and Medicine *8*, 157–168. https://doi.org/10.1002/wsbm.1326.
244. Nilsson, D.P.G., Holmgren, M., Holmlund, P., Wåhlin, A., Eklund, A., Dahlberg, T., Wiklund, K., and Andersson, M. (2022). Patient-specific brain arteries molded as a flexible phantom model using 3D printed water-soluble resin. Sci. Rep. *12*, 10172. https://doi.org/10.1038/s41598-022-14279-7.
245. Cai, S., Li, H., Zheng, F., Kong, F., Dao, M., Karniadakis, G.E., and Suresh, S. (2021). Artificial intelligence velocimetry and microaneurysm-on-a-chip for three-dimensional analysis of blood flow in physiology and disease. Proc. Natl. Acad. Sci. USA *118*, e2100697118. https://doi.org/10.1073/pnas.2100697118.
246. Yong, K.W., Janmaleki, M., Pachenari, M., Mitha, A.P., Sanati-Nezhad, A., and Sen, A. (2021). Engineering a 3D human intracranial aneurysm model using liquid-assisted injection molding and tuned hydrogels. Acta Biomater. *136*, 266–278. https://doi.org/10.1016/j.actbio.2021.09.022.
247. Jang, L.K., Alvarado, J.A., Pepona, M., Wasson, E.M., Nash, L.D., Ortega, J.M., Randles, A., Maitland, D.J., Moya, M.L., and Hynes, W.F. (2020). Three-dimensional bioprinting of aneurysm-bearing tissue structure for endovascular deployment of embolization coils. Biofabrication *13*, 015006. https://doi.org/10.1088/1758-5090/abbb9b.
248. McCormack, A., Highley, C.B., Leslie, N.R., and Melchels, F.P.W. (2020). 3D printing in suspension baths: keeping the promises of bioprinting afloat. Trends Biotechnol. *38*, 584–593. https://doi.org/10.1016/j.tibtech.2019.12.020.
249. Daly, A.C., Prendergast, M.E., Hughes, A.J., and Burdick, J.A. (2021). Bioprinting for the biologist. Cell *184*, 18–32. https://doi.org/10.1016/j.cell.2020.12.002.
250. Van Ombergen, A., Chalupa-Gantner, F., Chansoria, P., Colosimo, B.M., Costantini, M., Domingos, M., Dufour, A., De Maria, C., Groll, J., Jungst, T., et al. (2023). 3D bioprinting in microgravity: Opportunities, challenges, and possible applications in space. Adv. Healthcare Mater. *12*, 2300443. https://doi.org/10.1002/adhm.202300443.
251. Windisch, J., Reinhardt, O., Duin, S., Schütz, K., Rodriguez, N.J.N., Liu, S., Lode, A., and Gelinsky, M. (2023). Bioinks for space missions: The influence of long-term storage

of alginate-methylcellulose-based bioinks on printability as well as cell viability and function. Adv. Healthcare Mater. *12*, 2300436. https://doi.org/10.1002/adhm.202300436.

252. Sun, W., Starly, B., Daly, A.C., Burdick, J.A., Groll, J., Skeldon, G., Shu, W., Sakai, Y., Shinohara, M., Nishikawa, M., et al. (2020). The bioprinting roadmap. Biofabrication *12*, 022002. https://doi.org/10.1088/1758-5090/ab5158.
253. Mo, X., Zhang, Y., Wang, Z., Zhou, X., Zhang, Z., Fang, Y., Fan, Z., Guo, Y., Zhang, T., and Xiong, Z. (2024). Satellite-based on-orbit printing of 3D tumor models. Adv. Mater. *36*, 2309618. https://doi.org/10.1002/adma.202309618.
254. Afshinnekoo, E., Scott, R.T., MacKay, M.J., Pariset, E., Cekanaviciute, E., Barker, R., Gilroy, S., Hassane, D., Smith, S.M., Zwart, S.R., et al. (2020). Fundamental biological features of spaceflight: Advancing the field to enable deep-space exploration. Cell *183*, 1162–1184. https://doi.org/10.1016/j.cell.2020.10.050.
255. Mao, W., Huai, Y., An, L., Wang, X., Ru, K., Patil, S., Zhang, W., Ran, F., Chen, Z., and Qian, A. (2024). Microgravity inhibits cell proliferation and promotes senescence and apoptosis in embryonic stem cells. Space. Sci. Technol. *4*, 0104. https://doi.org/10.34133/space.0104.
256. Paulsen, K., Thiel, C., Timm, J., Schmidt, P.M., Huber, K., Tauber, S., Hemmersbach, R., Seibt, D., Kroll, H., Grote, K.H., et al. (2010). Microgravity-induced alterations in signal transduction in cells of the immune system. Acta Astronaut. *67*, 1116–1125. https://doi.org/10.1016/j.actaastro.2010.06.053.
257. Yan, R., Zhang, Y., Li, Y., Wang, J., Bibi, H., Deng, Y.-L., and Li, Y. (2023). Dragon's blood protect rat blood-brain barrier dysfunction induced by simulated microgravity effect. Space. Sci. Technol. *3*, 0071. https://doi.org/10.34133/space.0071.
258. Blaber, E., Marçal, H., and Burns, B.P. (2010). Bioastronautics: The influence of microgravity on astronaut health. Astrobiology *10*, 463–473. https://doi.org/10.1089/ast.2009.0415.
259. Li, Y., Huang, L., Iqbal, J., and Deng, Y. (2021). Investigation on P-glycoprotein function and its interacting proteins under simulated microgravity. Space. Sci. Technol. *2021*, 9835728. https://doi.org/10.34133/2021/9835728.
260. Juhl, O.J., Buettmann, E.G., Friedman, M.A., DeNapoli, R.C., Hoppock, G.A., and Donahue, H.J. (2021). Update on the effects of microgravity on the musculoskeletal system. npj Microgravity *7*, 28. https://doi.org/10.1038/s41526-021-00158-4.
261. Moroni, L., Tabury, K., Stenuit, H., Grimm, D., Baatout, S., and Mironov, V. (2022). What can biofabrication do for space and what can space do for biofabrication? Trends Biotechnol. *40*, 398–411. https://doi.org/10.1016/j.tibtech.2021.08.008.
262. Ren, Z., Harriot, A.D., Mair, D.B., Chung, M.K., Lee, P.H.U., and Kim, D.-H. (2023). Biomanufacturing of 3D tissue constructs in microgravity and their applications in human pathophysiological studies. Adv. Healthcare Mater. *12*, 2300157. https://doi.org/10.1002/adhm.202300157.
263. Cubo-Mateo, N., Podhajsky, S., Knickmann, D., Slenzka, K., Ghidini, T., and Gelinsky, M. (2020). Can 3D bioprinting be a key for exploratory missions and human settlements on the Moon and Mars? Biofabrication *12*, 043001. https://doi.org/10.1088/1758-5090/abb53a.
264. Armstrong, J.P.K., and Stevens, M.M. (2020). Using remote fields for complex tissue engineering. Trends Biotechnol. *38*, 254–263. https://doi.org/10.1016/j.tibtech.2019.07.005.
265. Zhou, H., Dong, G., Gao, G., Du, R., Tang, X., Ma, Y., and Li, J. (2022). Hydrogel-based stimuli-responsive micromotors for biomedicine. Cyborg Bionic Syst. *2022*, 9852853. https://doi.org/10.34133/2022/9852853.
266. Koetting, M.C., Peters, J.T., Steichen, S.D., and Peppas, N.A. (2015). Stimulus-responsive hydrogels: Theory, modern advances, and applications. Mater. Sci. Eng. R Rep. *93*, 1–49. https://doi.org/10.1016/j.mser.2015.04.001.
267. Wang, Y., Pereira, R.F., Peach, C., Huang, B., Vyas, C., and Bartolo, P. (2023). Robotic *in situ* bioprinting for cartilage tissue engineering. Int. J. Extrem. Manuf. *5*, 032004. https://doi.org/10.1088/2631-7990/acda67.
268. Dong, H., Hu, B., Zhang, W., Xie, W., Mo, J., Sun, H., and Shang, J. (2023). Robotic-assisted automated *in situ* bioprinting. Int. J. Bioprint. *9*, 629. https://doi.org/10.18063/ijb.v9i1.629.